Multi-objective Optimization of Fenestration Design in Residential spaces.

The case of MKB Greenhouse, Malmö, Sweden

Iason Bournas, Ludvig Haav

Master thesis in Energy-efficient and Environmental Buildings
Faculty of Engineering | Lund University

Lund University

Lund University, with eight faculties and a number of research centres and specialized institutes, is the largest establishment for research and higher education in Scandinavia. The main part of the University is situated in the small city of Lund which has about 112 000 inhabitants. A number of departments for research and education are, however, located in Malmö. Lund University was founded in 1666 and has today a total staff of 6 000 employees and 47 000 students attending 280 degree programmes and 2 300 subject courses offered by 63 departments.

Master Programme in Energy-efficient and Environmental Building Design

This international programme provides knowledge, skills and competencies within the area of energy-efficient and environmental building design in cold climates. The goal is to train highly skilled professionals, who will significantly contribute to and influence the design, building or renovation of energy-efficient buildings, taking into consideration the architecture and environment, the inhabitants' behaviour and needs, their health and comfort as well as the overall economy.

The degree project is the final part of the master programme leading to a Master of Science (120 credits) in Energy-efficient and Environmental Buildings.

Keywords: Fenestration, optimization, daylighting, heating, overheating time, residential

Thesis: EEBD - # / 2016

Abstract

This thesis investigates the optimization of fenestration design for multi-family apartments, considering the heating demand, daylight autonomy as well as overheating. A literature review was conducted to situate the thesis focus within the broader academic field of façade optimization, and a specific apartment located in the city of Malmö was chosen as the study object. The results presented are the outcome of climate-based daylight modelling (CBDM) simulations and dynamic thermal modelling (DTM) simulations, all of which were integrated in a single script definition within the visual programming environment of Grasshopper (2016). A significant part of the study involved the use of an optimization algorithm, to assess multiple fenestration designs based on their daylighting and heating performance. The optimum window position, size and shape were assessed as a function of the achieved daylight levels, the energy required for heating, the impact of solar gains and the amount of overheating time for the studied spaces. Overall, it was shown that the objectives of heating and daylighting are in conflict in the Swedish context, when the aim is to satisfy both luminous and thermal needs. In addition, it was shown that the window-to-wall ratio is not sufficient as information regarding the building performance, as different geometrical aspects of windows and their position can lead to different results for the same glazing area.

Acknowledgements

This thesis would not have reached to its present level and form if it were not for Marie-Claude Dubois. The authors would like to thank her for her constant consultation, support, guidance and encouragement.

The authors are also grateful to the *Division of Energy and Building Design* of Lund University, and especially to Maria Wall, for providing the computer hardware without which the simulations conducted would not have been possible on time.

The authors are indebted to the people in the Grasshopper forums, who addressed critical issues of this thesis during the modelling stage. Especially Mostapha Sadeghipour for answering multiple questions on the fenestration design definition, David Rutten for clarifying details on data management and Chris Mackey who devoted time to clarify aspects of the Honeybee energy model.

Finally yet importantly, the authors would like to thank Odysseas Bournas for his contribution in bypassing issues regarding the upload of deployable *.json files for the presentation of this thesis.

Contribution

Due to the integrated nature of the simulation model used for this thesis, most of the work was conducted by both authors as a joint team. Nevertheless, specific parts were studied by each author more in detail. Ludvig Haav undertook the daylight modelling, its validation, and the dynamic grasshopper definition to generate different fenestration designs. Iason Bournas was responsible for the energy model, its validation and the structuring of the literature review. Both authors contributed in the investigation of the optimization algorithm internal settings, the measurement grid study for the daylight model and the writing of this thesis.

Table of contents

Nomenclature

A_f	Window frame area (m^2)
A_g	Glazing area (m^2)
cp_{water}	Specific heat capacity of water (J/kg·K)
E	Illuminance (lx)
L_g	Glazing perimeter (m)
$\dot{m}$	Mass flow rate (Kg/s)
q	Heat power (W) or (kW)
R	Thermal resistance (m^2·K/W)
R_{si}	Thermal resistance of indoor surface (m^2·K/W)
R_{so}	Thermal resistance of outdoor surface (m^2·K/W)
t	time / s or step (-)
U_f	Window frame U-Value (W/m^2·K)
U_g	Glazing U-Value (W/m^2·K)
U_{win}	Window U-Value (W/m^2·K)
$\dot{V}$	Volume flow rate (m^3/s)
ΔT	Temperature difference (K)

λ	Thermal conductivity (W/m·K)
ρ_{water}	Density of water (Kg/m³)
Ψ	Glazing/frame linear thermal bridge (W/m·K)

Abbreviations

General

ADDT	Annual deficient daylight time
BBR	Boverkets byggregler (National Board of Housing, Building and Planning)
BELOK	Beställargrupper Lokaler (Organization of Swedish non-residential real estate owners)
BREEAM	Building Research Establishment Environmental Method
CAV	Constant air volume
CLA	Classroom
COM	Commercial
DHW	Domestic hot water
DTM	Dynamic thermal modelling
FEBY	Forum för energieffektiva byggnader (Forum for Energy Efficient Buildings)
GA	Genetic algorithm
HVAC	Heating, ventilation and air-conditioning
IESNA	Illuminating engineering society of Northern America
IGU	Insulated glazed unit
LEED	Leadership in Energy and Environmental Design
LUB	Lund Universitets Bibliotek (Lund University Library)
MIPS	Millions of instructions per second
MKB	Malmö Kommunala Bostads (Malmö Municipal Housing Companies)
NS	Not specified
NURBS	Non-uniform rational basis spline
OA	Optimization algorithm

OFF	Office
RAI	Railway station
RES	Residential
SAD	Seasonal affective disorder
WGR	Window-to-floor ratio
WWR	Window-to-wall ratio
ΔDA	Average daylight autonomy difference
ΔV	Volumetric difference

Daylight

aa	Ambient accuracy
ab	Ambient bounces
ad	Ambient division
ADA	Acceptably daylit area
ar	Ambient resolution
as	Ambient sampling
CBDM	Climate-based daylight modeling
DA	Daylight Autonomy
DAV	Daylight availability
DF	Daylight Factor
DGP	Daylight glare probability
LD	Light dependency
LM	Lighting measurements
NDA	Non daylit area
UDI	Useful daylight illuminance
UR	Daylight factor uniformity ratio

Definitions

Heating

Specific energy use: Annual energy required for heating, cooling, domestic hot water and property electricity, divided by the zone floor area (annual kWh/m^2).

Overheating time: Amount of hours when the operative temperature is higher than a user-set threshold. These hours are counted only during the time that a studied space is occupied.

Daylight

Daylight Autonomy (DA): "Percentage of the occupied hours of the year when the minimum illuminance threshold is met by daylight alone" (Reinhart & Walkenhorst, 2001).

Light Dependency (LD): Inverse of DA and is equal to 100 % - DA. It represents the percentage of the occupied hours of the year when electrical light sources are required to maintain a minimum illuminance threshold when it cannot be met by daylight alone.

Daylight Factor (DF): Ratio of the daylight illuminance on a given surface to the simultaneous illuminance, expressed as a percentage, under an unobstructed CIE Standard Overcast Sky (Tregenza & Wilson, 2011).

DF Uniformity Ratio (UR): Ratio of the minimum DF to the average DF of all points of a given daylight measurement grid. By definition, uniformity of daylight levels is calculated as the uniformity of absolute illuminance E across the measurement points of a given grid.

Useful Daylight Illuminance (UDI): Percentage of the occupied hours of the year when illuminance lies within one of the three illumination ranges: 0-100 lx, 100-2000 lx, and over 2000 lx (Nabil & Mardaljevic, 2006). It provides information not only on useful daylight levels, but also on excessive levels that could be the cause of glare or unwanted solar gains.

Overlit Area (OA): Percentage of area that is considered overlit. It is based on the *Daylight Availability* (DAV), a metric proposed in 2010 that is meant to combine DA and Useful Daylight Illuminance (UDI) into a single figure (Reinhart & Wienold, 2011). Daylight Availability measures the percentage of occupied time in a year when the illuminance is ten times higher than a user-set threshold. The intension is to detect areas with oversupply of light that could be the cause of discomfort glare or overheating. A warning is invoked when DAV exceeds 5 % of the occupied time. From there, the Overlit Area is defined as the quotient of the number of sensor points with a warning, divided by the total number of sensor points in the room under study.

“*Let there be more light*”

A Saucerful of Secrets
Pink Floyd

1 Introduction

This thesis assesses the trade-offs between heating and daylighting when considering fenestration solutions for residential spaces. Of all the parameters affecting heating, cooling and lighting of buildings, fenestration is the most freely controlled by the architectural team. The decision on a specific design must be made during the early design stage, as it can shape the overall building performance dramatically.

In 1929 the prominent architect Le Corbusier said: "The history of architectural material… has been the endless struggle for light… in other words, the history of windows." Today, architects should consider not only the amount of light that can be admitted through the façade, but also the amount of heat that will subsequently exit the building, as windows constitute the weakest thermal barrier between the indoor and outdoor environment. Taking heat into consideration is an absolute necessity in countries like Sweden, where the outdoor air temperature remains beneath the comfort zone most of the time.

This conflict between heating and daylight objectives has been mentioned by researchers in the context of energy codes and certification system requirements. Mardaljevic, Heschong and Lee (2009) argued in a seminal paper that practitioners encounter recommendations for target daylight factor (DF) values that result in over-glazed buildings with excessive solar gain and/or heat loss. The Heschong Mahone Group (2003) monitored six building spaces that did not achieve the LEED criteria of an average DF of 2 % and found that even with high transmission glass, the window area would need to have been increased to such an extent that the spaces would not pass the energy code performance requirements.

Due to the geometrical complexity involved in fenestration studies, many researchers have utilized evolutionary-based optimization algorithms to find solutions that can satisfy both energy and daylighting goals. This type of facade optimization has been investigated numerous times and in general, the related work has shown that thermal and luminous needs can be satisfied with more than one facade solutions. Following this logic, this thesis provides architects the tools to select designs from a range of solutions. The intention is to guide design choices based on simulation results processing and evaluation, rather than on architectural intuition or conventional wisdom.

1.1 Goal definition

The aim of this thesis is to assess: a) the trade-offs between heating and daylighting due to different fenestration choices, and b) the inter-dependence between daylight performance indicators used today, and their possible benchmark values in residential buildings. To facilitate this goal, a case study was chosen: the MKB Green House project in Augustenborg, Malmö.

Achieving both objectives simultaneously requires a time-consuming amount of iterations between different fenestration solutions. The use of an optimization algorithm lies at the core of this study as a form-generative tool. The amount of result data of such sophisticated optimization tools can be significant and difficult to assess. This study is also focusing on reducing simulation time and design iterations by making proper simplifications without compromising the validity of results.

1.2 Background

Design optimization problems of window size and position on the facade have been investigated in the past, with regard to energy and visual comfort criteria (Torres & Sakamoto, 2007; Zemella, et al., 2011; Ochoa, et al., 2012; Shan, 2013; Manzan & Padovan, 2015). The interdependence between heating and daylighting has received much attention during the last ten years, as the computational power has increased and the recent simulation software developments paved the way to unprecedented possibilities for designers and architects.

1.2.1 The importance of efficient fenestration design

The window-to-wall ratio (WWR), the properties of glazing and the way windows are arranged on the facade are variables of fenestration design. These variables can have a significant effect on different functions of windows.

Among the different functions of windows, daylight admission is the most appreciated, especially in regions where the overcast sky is the dominant sky condition. Acosta et al. (2013) investigated different window geometries and positions under overcast sky conditions. They concluded that windows located higher up result in deeper penetration of daylight in space. They also compared the daylight conditions with using horizontal or vertical windows of the same glazing area, and concluded that the horizontal ones have a higher potential in increasing the average daylight factor.

At the same time daylight is related to health aspects and has been associated with reduction of absenteeism and fatigue, decrease of Seasonal Affective Disorder (SAD) and other depressive symptoms, and it can improve human skin conditions and vision (Aries, et al., 2015). It is therefore necessary to increase daylight to a certain extent, to ensure the occupants well-being.

Fenestration design also serves the necessity for a view towards the external environment. In a post-occupancy evaluation for 20 office buildings in Denmark, Christoffersen et al. (1999) stated that when asked to choose the three things they liked more about windows, the occupants reported the possibility to look out, the ability to know the weather, and the advantage of letting in fresh air. All pre mentioned advantages are dependent on the position and size of windows.

Electrical lighting use is likely to decrease with a wise fenestration design. Past studies have shown that ensuring the penetration of daylight throughout the interior of buildings can keep the energy use for lighting to a minimum (Gago, et al., 2015). Du et al. (2014) investigated the impact of window-to-floor ratio (WGR) on Swedish and French houses and concluded that daylight utilization could result in a reduction of one third of the electric lighting demand.

There is also a potential to decrease heating and cooling energy, by exploiting passive solar gains through the optimum position and orientation of the façade openings. Relevant research showed that daylight utilization has the potential to decrease the cooling demand of spaces, without increasing the heating demand and that orientation, shading, glazing size and the U-Value are the most important parameters during the heating season (Bülow-Hübe, 2001; Gunnlaug, et al., 2016). Persson et al. (2006) showed that for highly insulated houses in Sweden, relatively small windows should be placed in a south orientation while it is possible to use larger windows towards north as overheating is the main parameter influencing design.

1.2.2 Multi-objective optimization for fenestration design

In fenestration design schemes, multiple variables need to be considered in order to satisfy the often conflicting functional requirements of the façade. The range of possible solutions given to a specific problem plotted in a Cartesian space is called the *solution space.* Bader and Zitzler (2008) stated that the simulation time increases exponentially with respect to the number of variables considered. Figure 1 exemplifies this growth for six variables of a five-step range each. The increase of complexity indicates that it is difficult to map the entire solution space using conventional methods.

Therefore, when faced with a large number of iterations, simplifications are traditionally made. However, dividing the solution space into regions by introducing parameters in a stepwise manner, the designer runs the risk of not exploring the total solution space. Parameters in façade design have a high degree of interaction, emphasizing this problem. As stated by Caldas and Norford, (2002) the process of iteratively evaluating large solution spaces is slow and typically only a limited number of solutions are examined and therefore alternative methods are required.

In recent years, the use of optimization algorithms (OA) have become increasingly popular in various disciplines dealing with optimization. OAs can find minimum values of mathematical functions, for instance, the minimum WWR to achieve a given daylight level. Genetic algorithms (GA) are one subtype of optimization algorithms that were outlined for the first time by Turing (1950). According to Zemella et al. (2011), GAs have been proved to facilitate performance based façade design optimization efficiently. During a GA process, a set of initial solutions (a generation) is calculated based upon randomly generated variables. These solutions are assigned a "fitness value" representing performance with respect to an evaluated objective. The most successful solutions are then used to produce a subsequent set of solutions. This process continues until a solution, or set of solutions are found that match the user-defined criteria. This way, the algorithm can provide not only the best solution but also a range of sufficient and diverse solutions for the designer to select among them based on specific requirements that cannot be quantified.

Dynamic thermal and daylighting simulations are computationally intensive tasks. GAs can accelerate the optimization process but they require a substantial amount of iterations to yield conclusive results. State-of-the-art programming environments can automate multiple iterations, which has recently led architects to explore the field of GAs. This widespread adoption coincides with the increase in computational power, commonly measured in MIPS (millions of instructions per second). Figure 2 shows the evolution of computational power (Wikipedia, 2016) and the amount and date of relevant publications that were investigated for this thesis.

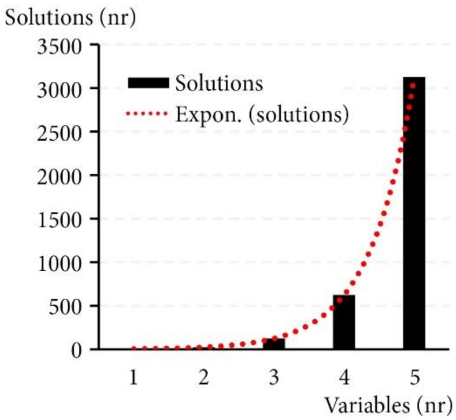

Figure 1: The exponential growth of solutions as a function of the variables.

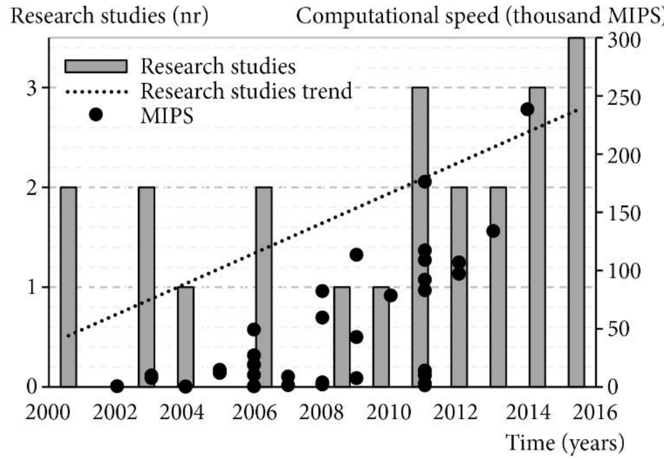

Figure 2: Computational power increase and amount and date of publications reviewed in this thesis.

As pre mentioned in section 1.1, studies that use GAs extract a large number of output data. A common practice is to use a Pareto front to facilitate the processing and presentation of results. A Pareto front allows one to understand the trade-offs between conflicting objectives of design solutions that are said to be "Pareto optimal solutions" (Burke & Kendall, 2005). A solution is called Pareto optimal (or non-dominated), if none of the objectives can be improved, without degrading the other objective. Futrell et al. (2015) have utilized Pareto fronts to evaluate the trade-offs between thermal and daylighting objectives for a single classroom in Charlotte, North Carolina, while varying windows size and glazing properties. They stated that the Pareto front indicates the amount of conflict between the objectives. For their case, the north among all orientations proved to have the largest conflict between heating and daylight.

1.2.3 Literature review

The following literature review was conducted prior to studying the fenestration design alternatives for the MKB Greenhouse in Augustenborg, Malmö, to situate the thesis focus within the broader academic field of façade optimization. A total of 22 relevant journal articles and conference papers were tracked by utilizing the *LUBsearch* engine, provided by Lund University library domain (Lund University, 2016). *LUBsearch* is a collective entry point to all academic joint resources that includes journal articles, conference publications, doctoral theses and books.

To establish the research framework, specific keywords were used to track the aforementioned publications, which included "optimization" or "multi-objective optimization" and "fenestration" or "façade" or "windows". The selection included only articles and papers that were published after 2000, to focus more on the state-of-the-art studies. All of these cases used simulation software to carry out their work, and no field measurements were reported.

An organizational pattern of the reviewed publications is presented in Table 1. In brief, it shows the study object of each of the 22 publications and the extent to which they included: *i*) different optimization objectives, *ii*) different daylight metrics, *iii*) usage of an optimization algorithm, *iv*) usage of Pareto fronts, *v*) different fenestration parameters (window position or distribution, WWR, orientation and glazing properties).

Table 1: Organizational pattern based on the publications extent of research.

Author, year	Study object	Objectives	Daylight metrics	Optimization algorithm	Pareto front	Fenestration variables			
						Position Distribution	WWR	Orientation	Glazing properties
Gagne & Andersen, 2012	NS	D	E, DGP	✓	✓	✓	✓	✓	✓
Hou et al., 2014	RAI	$, H, C, D	UDI	✓	✓	✓	✓	✓	-
Caldas, 2007	NS	$, L, H, C, D	E	✓	✓	✓	✓	✓	-
Futrell et al., 2015	CLA	H, D	UDI	✓	✓	-	✓	✓	✓
Konis et al., 2015	OFF	L, H, C, D	UDI	✓	✓	-	✓	✓	-
Torres & Sakamoto, 2007	NS	D	DGP	✓	-	✓	✓	-	✓
Mangkuto et al., 2016	OFF	L, D	DF, UR, DA, UDI, DGP	-	✓	-	✓	✓	-
Caldas & Norford, 2002	NS	L, H, C, D	E	✓	-	-	✓	✓	-
Wright & Mourshed, 2009	COM	L, H, C	-	✓	-	✓	✓	-	-
Shen & Tzempelikos, 2011	OFF	L, H, C, D	DA, UDI	-	-	-	✓	✓	✓
Znouda et al., 2005	NS	$, H, C	-	✓	-	-	✓	✓	-
Zemella et al., 2011	OFF	L, C, D	E	✓	✓	-	-	-	✓
Lartique et al., 2014	RES	H, C, D	E	✓	✓	-	✓	-	✓
Hu & Olbina, 2014	NS	H, C, D	UDI	-	-	-	✓	-	✓
Ochoa et al., 2012	OFF	L, H, C, D	E, DGI, UDI	-	-	-	✓	✓	-
Ghisi & Tinker, 2004	NS	L, H, C, D	DF	-	-	-	✓	✓	-
Shan, 2013	OFF	L, H, C, D	E	✓	-	-	✓	-	-
Manzan & Padovan, 2015	OFF	H, C, D	UDI	✓	✓	-	-	-	-
Rakha & Nassar, 2011	NS	D	UR	✓	-	-	-	-	-
Wang et al., 2004	OFF	$, Env	-	✓	✓	-	-	-	-
Tuhus-Bubrow & Krarti, 2009	RES	$, H, C	-	✓	-	-	-	-	-
Wright et al., 2002	HVAC	$, H, C	-	✓	✓	-	-	-	-

Study object - NS: Not specified RAI: Railway station CLA: Classroom OFF: Office COM: Commercial RES: Residential
Objectives - D: Daylight H: Heating C: Cooling L: Lighting $: Cost
Daylight metrics - E: Illuminance DGP: Daylight glare probability UDI: Useful daylight illuminance DF: Daylight factor
UR: DF Uniformity ratio DA: Daylight autonomy

The latter five studies did not include window variables, but were useful for this thesis in terms of developing an optimization algorithm. The studies that varied fenestration parameters were 17 in total. The following can be concluded by examining all studies in Table 1:

1. Among the studies that iterated fenestration variables, 71% used an optimization algorithm to generate the different design solutions.
2. Among the studies that used optimization algorithms, 63% used Pareto fronts to illustrate the solution space.
3. Most of the studies were conducted for office space characteristics and requirements.
4. Among the fenestration variables, WWR was the most commonly used when iterating between window alternatives (94% of studies).

5. The least used fenestration variable was the window position (five of 17 fenestration studies).
6. Most of the studies included one or two daylight metrics for the optimization process.
7. Illuminance (E), was used as a daylight metric in 47% of the cases, and UDI was used in 41% of the studies.
8. DA was used in only two out of the seventeen studies that varied fenestration parameters.
9. The objectives of heating, cooling and lighting were coupled with a daylight objective in a similar frequency.
10. Conflicting daylight metrics were not assessed by means of an optimization algorithm, except for one study.

The aforementioned points defined partly the thesis workflow. It was observed that optimization algorithms were used by studies where multiple objectives and/or multiple fenestration variables were considered. The presentation of results was facilitated in these cases by the use of Pareto fronts to illustrate the trade-offs between different objectives for a large number of solutions.

By examining the scope of each study, it was possible to define the research gap that this thesis addresses. Past studies have mainly analyzed office spaces, which makes it interesting in this case, since the daylight utilization is directly connected to the electricity used for lighting. Residential spaces require different daylight criteria to be fulfilled, and their inhabitants can occupy different rooms during different hours throughout the day. This was not examined in the reviewed studies. The vast majority of the studies used the WWR as a variable, and only a few examined the impact of the window position. This variable was used in this thesis, as it can allow for different daylight penetration depths for a constant WWR.

The interdependence between different daylight metrics was assessed comprehensively only in one recent study (Mangkuto, et al., 2016). The common practice among most studies was to analyze the illuminance and/or the UDI levels for the studied object. While choosing the UDI seems an efficient way to proceed with the optimization, Reinhart & Weissman (2012) argued that the DA metric could correlate more with the architects' assessment of daylight availability in space. In their study, they compared the amount of daylit area (m^2) of a one-story studio space calculated in two ways: a) simulated using different daylight metrics and b) calculated by 60 architectural students using their intuition upon observing the space. The results of the two ways converged more when daylight autonomy was used as the daylight metric. Nevertheless using as many daylight metrics as possible can ensure that daylight availability and visual comfort are studied more thoroughly.

Fenestration design optimization has received more attention in the past six years, when it comes to deploying GAs in the process. The literature review showed that an optimization algorithm to provide solutions for residential facades and to assess more daylight metrics is something that is missing from the research field. Although form finding has been the subject of numerous publications, previous attempts did not concern the fenestration of complete residential spaces, where the required illuminance is a function of time, as different rooms are occupied during different times of the day and have a different orientation. Nevertheless, there were examples of work that dealt with the same issues addressed in this thesis.

The following subsections elaborate more on six of these studies. They were selected based on their relevance with the thesis goals as they were defined in section 1.1.

1.2.3.1 Heating and daylighting optimization related work

Futrell et al. (2015) presented a bi-objective optimization method to solve the problem of the conflicting objectives of daylighting and heating for a classroom in North Carolina, USA. Their main objective was to maximize daylighting while retaining the energy performance of the building, for different configurations of windows in different orientations. They chose to use UDI as a daylight metric because unlike other metrics it has a defined illuminance range, which makes it possible to consider both daylight availability and discomfort glare potential. UDI was then optimized against the thermal load of the classroom, which was defined as the required heat transfer to the room air, in order to keep the air temperature at a setpoint temperature. This load considered internal gains of occupants, equipment and lighting, infiltration and ventilation, and the convected heat transfer from the classroom surfaces.

Optimization was conducted for three scenarios. One for maximizing daylighting, one for minimizing the thermal load and one for both. Among their findings, the amount of glazing for different orientations was shown to depend on the objective of optimization. When maximizing UDI, the east windows were larger than the south ones. When minimizing the thermal load, the south windows had to be the largest ones, showing that it was the only orientation exploiting passive solar gains during winter. The north orientation resulted the largest amount of conflict between the objectives, which showed that achieving UDI through northern windows could have severe consequences on the thermal load and vice versa.

Latrique et al. (2014) investigated the optimization of a dormitory room in Pittsburgh, USA, with respect to the objectives of heating, cooling and daylighting. The room had one exposed façade, for which the WWR was iterated in steps of 1% starting from 10% up to 60%. For each WWR, a set of 13 different window constructions was assigned, leading to 663 different cases. Two of the objectives were set as a) the annual heating demand in kWh and b) the annual cooling demand in kWh. The third objective, daylight, was formulated according to the authors as the Annual Deficient Daylight Time (ADDT). ADDT is the sum of all hours during one year when the illuminance is lower than 300lx, meaning the hours when electric lighting is needed to sustain the desired illuminance level of 300lx. The optimum cases were the ones that could minimize all three objectives.

The results of this study defined the range of WWR where each window type could achieve an optimum trade-off between the objectives. The window type with the lowest U-Value (0.71 $W/m^2 \cdot K$) could reach an optimum trade-off for a wide range of WWR. A high range of WWR was also achieved by the window type with the highest U-Value (2.89 $W/m^2 \cdot K$). This was because of its high visual transmittance that increased the daylight levels. Other window types were optimal only for one WWR, which is useful information if a specific WWR already exists and the window type is to be selected, as in renovation projects.

The authors provided a range of solutions that allowed reaching the optimum trade-off between heating, cooling and daylight. This is useful in the sense that it allows a decision maker to have a set of efficient alternatives, and to choose amongst them based on his/her personal considerations, geometrical constraints or cost parameters.

1.2.3.2 Studies related to the interdependence between daylight metrics

In a recent study that considered the optimization of fenestration for office buildings in the tropical climate, Mangkuto et al. (2016) investigated the influence of WWR, wall reflectance and window orientation on different daylight metrics. Each of these variables was given a range of discrete values, which generated a large number of configurations that were assessed in terms of DF, UR, DA, UDI and DGP. The daylight metrics were investigated in pairs, to assess their interdependence. Through a sensitivity analysis, Mangkuto et al. concluded that the WWR is highly influential on all daylight metrics except the UR, which is mostly affected by the interior surface reflectance. In addition, surface reflectance had the highest relative impact on the electrical lighting use. Orientation significantly affected only the DGP. Considering the freedom of occupant position in residential spaces, the DGP was not considered in this thesis.

Plotting pairs of daylight metrics in diagrams, the study concluded on the following findings: The DF was proven proportional to the DGP. In the cases of south and north orientation, DGP would increase slower as a function of DF, than in the west and east. South and north were orientations where DGP could be lower than the maximum benchmark set by the study, which was 50% of the time with a DGP over 0.35[1]. DA was also proportional to DGP and south and north orientations were the best choices to avoid discomfort glare. Comparing UDI with DF it was shown that higher UDI-accept values could be achieved when the DF was low. Among limitations and future work, Mangkuto et al. noted that different window configurations of equal WWR could lead to different daylight performance. The latter is assessed in the present thesis.

Gagne & Andersen (2012) presented a GA-based optimization tool that generates fenestration designs considering two objectives: a) the illuminance levels and b) the glare probability. The tool

[1] The probability of discomfort glare appearance in daylit spaces (Wienold & Christoffersen, 2006).

creates solutions based on criteria set by the user, and generates 3D-models with the purpose to be used as a starting point in the design process. The user inputs an initial massing geometry and specifies the areas where illuminance and glare sensors are placed. From there, the user inputs a desired illuminance range across the corresponding sensors, and a range of glare tolerance. The latter two are the values corresponding to the objectives of the optimization algorithms. The tool generates windows, overhangs and vertical fins to create a large amount of solutions, which are assessed in the final stage based on the optimum trade-offs between the objectives.

Gagne & Andersen formulated an optimization algorithm that considered all fenestration variables shown in Table 1 of section 1.2.3. They went one step further by solving for an entire building, meaning that facades of all orientations were optimized. Due to this aspect, they included the additional constraint that all facades should have a uniform aesthetic (windows head height, sill height etc.).

Among the different results, the shading fins and window areas present a correlation with the architectural methods commonly used in façade design. East and west oriented facades were generated by the algorithm with vertical fins beside the windows to avoid glare. The researchers also stated that designs with larger window areas and horizontal overhangs present a higher risk for glare, especially on east and west orientations. The illuminance objective was satisfied with larger windows, whereas the glare objective was met with smaller and more numerous windows. Overall, this tool has the advantage of informing the designer on possible façade designs that will perform better than other alternatives, already in the initial design stage.

1.2.3.3 Genetic Algorithm considerations

Hou et al. (2014) presented a three-objective optimization study to minimize the energy use and façade capital cost while maximizing the UDI for a railway station located in northern China. They iterated window configurations for the east and west façades of the building, as well as skylight configurations for the flat roof. The facades and roofs were divided into a grid, which constituted possible positions for the openings. That way, the algorithm could assess different WWRs but also different window positions for equal WWRs.

This study was of particular interest, since it deployed a methodology similar to the one used in this thesis. The researchers mostly investigated the optimization algorithm settings, which provided useful information for this thesis.

The study reported that *elitism* should be used to save the promising solutions during the optimizations process. Elitism defines which part of the solutions is sustained in the process. It was also stated that the most important operators dictating the algorithm logics are the *mutation rate* and the *crossover rate*. Mutation means searching the solution space as much as possible, whereas crossover controls the convergence of the objectives on the better solution. If the mutation rate is low, iterations between possible window design scenarios will not be generated to a full extent, posing a risk for the algorithm to converge to a local optimum solution. If the crossover rate is low, then designs will be generated but no convergence towards optimum solutions will be applied, which can reach to resulting diagrams of no particular indication as to which designs are the optimum ones.

1.2.3.4 Summary

The reviewed studies helped situate this thesis focus within the broader academic field of façade optimization. It was shown that different fenestration solutions satisfy different needs, and that optimization approaches can yield conclusive yet sufficiently diverse designs, based on the objectives under optimization.

The interdependence between optimization objectives was shown to vary based on window size, type, position and façade orientation. This led to specific decisions regarding the structure of the methodology. Most importantly, the selection of the variables and objectives under study. A geometric aspect of fenestration that was missing was the window position, and was therefore included in the parameters investigated in the present thesis (window head height, sill height and distance from the end of the façade).

The literature review also outlined the existing simulation tools to develop an optimization algorithm. This thesis borrows interesting approaches on how to combine different simulation engines to an overall platform, and how to process data in communicative ways for the reader. The latter is achieved by plotting the Pareto optimal solutions in different diagrams, to monitor the performance of these solutions on other variables such as the average DF or the uniformity ratio UR.

Finally, all the aforementioned studies helped shape the thesis hypothesis and specific research question: Can we define fenestration solutions that admit the highest possible daylight and yield the lowest possible heating demand at the initial design stage? It seems that the question has been investigated thoroughly in the past, but the answer is dependent on specific variables. What remains now, is to select the specific building type, the important fenestration parameters and the necessary optimization objectives.

1.3 Scope and limitations

Prior to reading this thesis, the following should be considered:

1. No field measurements were conducted in the studied spaces. All results are outcome of simulations.
2. Only two apartments were studied, more specifically, the west and east facing apartments located on the 12th floor.
3. No energy declaration or simulation results were available for information on each room of the studied apartments or on each apartment. NCC (2014) provided a preliminary documentation regarding the energy performance, which includes the overall building.
4. Each apartment geometry was simplified by using a reduced amount of surfaces, to yield shorter simulation times and to create convex zones. The latter was a necessity of the energy model, described further down.
5. No surroundings were considered for the daylight model. The studied apartments are located 36 m above ground level, with no obstructing objects in the field of view. Nevertheless part of the horizon is actually obstructed, but the obstructions were not modelled, as they would have a high impact on simulation time.
6. No vegetation was considered in the areas of the closed and open balconies.
7. No shading devices were included in the study.
8. The spectral properties of light were not considered. All opaque surfaces of the daylight study were considered *grey*, i.e. with the same RGB value and consisting of totally diffuse materials.
9. No detailed HVAC components were designed in the energy model (Heating/cooling coils, fans, heat pumps, ducts etc.).
10. The optimization algorithm was set to use discrete values for window parameters, which leads to a non-continuous solution space.
11. Optimization was performed in the time constraints of this thesis. Further optimization could potentially yield better performing solutions.

2 Methodology

The present study investigates fenestration solutions for two apartments located in the Greenhouse project in Augustenborg, Malmö, Sweden (latitude=55,60°, longitude=13,00°). Fenestration designs were generated to evaluate the trade-offs between the objectives of daylighting and heating. In order to achieve this, *climate-based daylight modelling* (CBDM) and *dynamic thermal modelling* (DTM) tools were combined into a single simulation set-up. The following sections describe the daylight and energy models of this set-up. Finally, the necessity for a high number of fenestration alternatives led to the use of a *genetic algorithm*, which is described further down.

2.1 Studied apartments

The Greenhouse apartments are located in the eco-city Augustenborg. In 1998, the City of Malmö initiated an urban renovation process in the Augustenborg neighborhood under the name of the Eco-city project. This area from the fifties was transformed during the past 15 years into a sustainable district at the forefront of the climate change adaptation and environmental movement. The Eco-city approach aimed at regenerating the formerly degraded area by transforming it into a living space of ecological, social and economic sustainability.

Augustenborg now condenses MKB, Malmö municipal housing companies, with a cutting-edge project to reduce the climate impact. The so-called Greenhouse apartments are part of this endeavor. In the project, it was decided to combine Green Building classification "gold" with FEBY (2012), the Swedish passive house standard. This type of apartments provide a representative case study, illustrating how different requirements may contradict each other in the design process. Figure 3*(a)* shows a rendering of the apartments. The two investigated apartments 1 and 2 are located on the 12th floor, as shown in Figure 3*(b)*. Figure 4 shows the plans of the apartments.

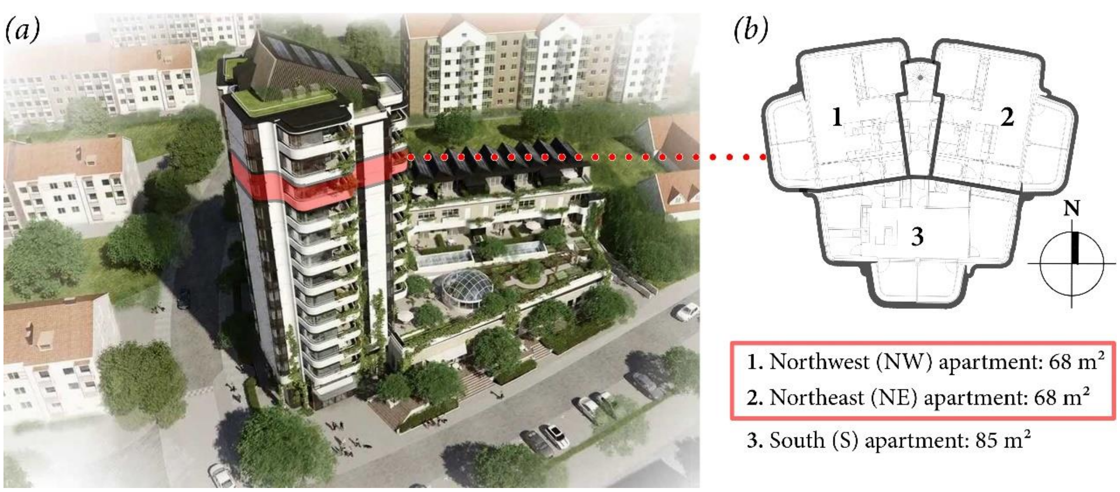

Figure 3: *(a)* Rendering of the Greenhouse apartments (*Image: Jaenecke Arkitekter AB*), *(b)* The studied floor division in apartments.

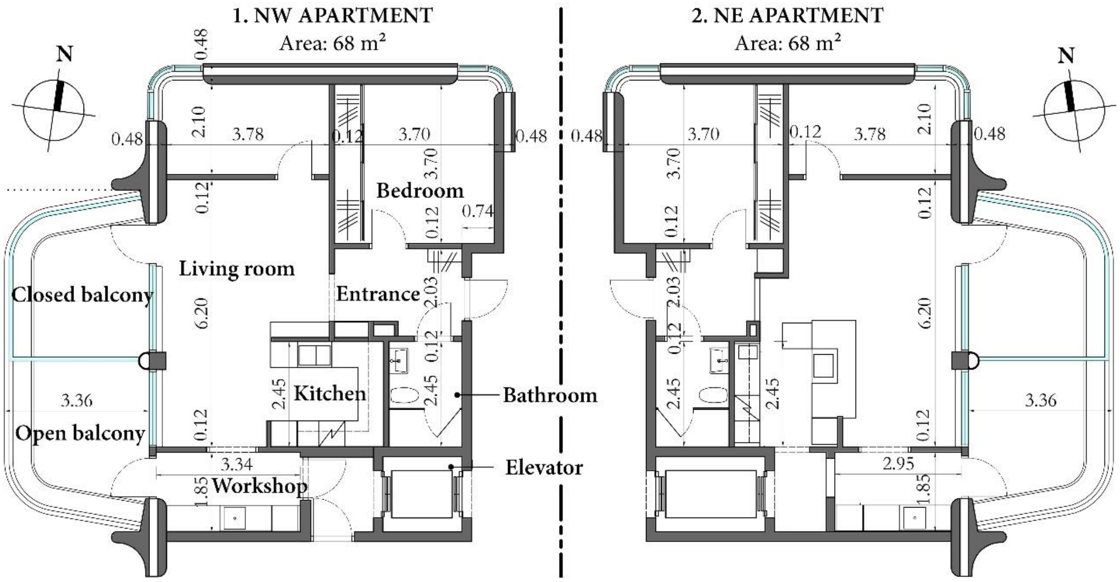

Figure 4: Plan layout of northwest (NW) apartment 1 and northeast (NE) apartment 2.

The two apartments have an equal area of 68 m² each and almost identical plan layouts. Minor differences include the kitchen layout and the elevator size. The study considered a single simplified layout for both apartments, as described under the following sections, where apartment 2 is a mirror of apartment 1. The only difference accounted for this study is the orientation. The south apartment was not included in this study, as it has a completely different room distribution.

2.2 Daylight dependent variables

This section gives the definitions of the daylight dependent variables used in this thesis. Light Dependency was used as an objective during the bi-objective optimization between daylight and heating. The rest of the variables were monitored to investigate their correlation. This correlation was examined after the bi-objective optimization process.

- **Daylight Autonomy (DA)**: Daylight Autonomy is the percentage of the occupied hours of the year when the minimum illuminance threshold is met by daylight alone" (Reinhart & Walkenhorst, 2001). For this thesis, the average daylight autonomy was calculated for a threshold of 150 lx (DA150lx) for the Living Room zone and a threshold of 50 lx (DA50lx) for the Bedroom zone. The Illuminating Engineering Society of Northern America (IESNA) suggests horizontal illuminance thresholds depending on specific applications/tasks (IESNA, 2011). Using these recommended illuminance levels for different tasks conducted in the Living Room and Bedroom zones, the aforementioned thresholds were set as an average requirement (see *APPENDIX A* for details on recommended illuminance levels). The DA schedule was identical to the occupancy schedule described further down, only not including the sleeping hours for the Bedroom zone.

- **Light Dependency (LD)**: Light Dependency is the inverse of DA and is equal to 100 % - DA. It represents the percentage of the occupied hours of the year when electrical light sources are required to maintain a minimum illuminance threshold when it cannot be met by daylight alone. This metric is used in the genetic algorithm, since the algorithms' architecture is programmed to converge towards solutions with minimum objective values. In other words, the genetic algorithm tries to minimize the objective under question, in this case, the Light Dependency. In short, the genetic algorithm is working on increasing the Daylight Autonomy by minimizing Light Dependency.

- **Daylight Factor (DF)**: The Daylight Factor is the ratio of the daylight illuminance on a given surface to the simultaneous illuminance from the whole sky, expressed as a percentage, under an unobstructed Standard CIE Overcast Sky (Tregenza & Wilson, 2011). It therefore does not consider the sun position, meaning that it cannot detect differences in daylight between orientations or between different points in time, which was required for this thesis topic. Nevertheless, the overcast sky condition in Sweden is very common and thus dictated that this metric should be considered as well. Furthermore, at the time of writing this thesis, certification systems such as Miljöbyggnad (2016), BREEAM (2014) and LEED (2016) proposed set criteria based on this metric.

- **DF Uniformity Ratio (UR)**: The UR is the ratio of the minimum to average DF of all points of a given measurement grid. This ratio can be used in addition to the DF, to assess whether there are unevenly daylit areas across the studied space or not. Normally in literature, the method to define uniformity of daylight levels in space is to calculate the ratio of the minimum to average absolute illuminance E (lx), and not DF. Nevertheless, the results of the two methods are identical. High UR normally avoids large contrasts and glare but complete uniformity should be avoided as it can create dull lighting conditions.

- **Useful Daylight Illuminance (UDI)**: Percentage of the occupied hours of the year when illuminance lies within one of the three illumination ranges: 0-100 lx, 100-2000 lx, and over 2000 lx (Nabil & Mardaljevic, 2006). It provides information not only on useful daylight levels, but also on excessive levels that could be the cause of glare or unwanted solar gains.

- **Overlit Area (OA)**: This variable indicates the percentage of area that is considered overlit. It is based on the *Daylight Availability* (DAV), a metric proposed by Reinhart & Wienold (2011) that is meant to combine DA and Useful Daylight Illuminance (UDI) into a single figure. Daylight Availability measures the percentage of occupied time in a year when the illuminance is ten times higher than a user-set threshold. The intension is to detect areas with oversupply of light that could be the cause of discomfort glare or overheating. A DAV exceeding 5 % of the occupied time is considered unacceptable. From there, the Overlit Area is defined as the quotient of the number of sensor points with unacceptable levels, divided by the total number of sensor points in the room under study.

2.3 Energy dependent variables

This section describes the energy dependent variables of the study, and the energy standards used to evaluate the performance of different fenestration designs. Two dependent variables were studied:

- **Specific energy use (annual kWh/m²)**: It is the annual energy required for heating, cooling, domestic hot water and property electricity, divided by the zone floor area.
- **Overheating time (hours)**: The amount of hours when the operative temperature is higher than a given threshold. These hours are counted only during the time for which the studied spaces are occupied.

2.4 Software

Due to the complexity of the parameters under study, different simulation engines were combined under the same platform. This way, a single simulation run was possible to provide result data regarding multiple objectives, including daylighting, heating and electrical lighting. The simulation model was created in the Grasshopper™ environment, which is a visual programming language integrated in the Rhino3D™ modeler (Grasshopper, 2016; Rhinoceros, 2016). Below is a brief description of the different software and simulation engines used in this thesis:

- **Grasshopper**: Grasshopper (2016) is a visual programming editor that operates as a plug-in for Rhino3D. Combined with Rhino3D, Grasshopper provides the capability to have precise parametric control over geometrical models. In addition, different simulation engines and plugins can be integrated in the Grasshopper platform, serving as a link between geometries and daylight-, energy- or lighting simulation tools. (see *APPENDIX F* for plugins used). The use of Grasshopper lies at the core of this thesis.
- **Rhino3D**: Rhino3D is a free form surface modeler that utilizes the non-uniform rational basis spline (NURBS) mathematical model (Wikipedia, 2016). By creating NURBS curves and surfaces, the user can have great control over shapes that can be recognized by different CBDM and DTM software as input geometry.
- **Radiance**: Radiance is a suite of programs for the analysis and visualization of lighting in design (Fritz & McNeil, 2016). It uses a hybrid Monte Carlo and deterministic ray-tracing approach and is one of the most advanced daylight/lighting simulation engines. Radiance has been validated to a high extent (Jarvis & Donn, 1997; Aizlewood, et al., 1998; Ubbelohde & Humann, 1998; Mardaljevic, 1999; Iversen, et al., 2013). Dubois (2001) documented work on Radiance rendering settings in her PhD thesis that was useful for setting the model for accurate and time-efficient daylight simulations.
- **EnergyPlus**: EnergyPlus is a whole-building energy simulation program that can calculate heating, cooling, ventilation, lighting, plug and process loads and water use in buildings

(U.S. Department of Energy, 2015). EnergyPlus is used as a simulation engine for different DTM tools, and has been fully validated (Chantrasrisalai, et al., 2003; Tabares-Velasco, et al., 2012; Pereira, et al., 2014).

- **Daysim**: Daysim is a validated, Radiance-based daylighting analysis software that models the annual amount of daylight in and around buildings. It is the first CBDM simulation engine created, and it uses the daylight coefficient approach (Mardaljevic, 1999) combined with the Perez Sky model (Perez, et al., 1993) in order to provide annual daylight performance evaluations. DAYSIM also generates hourly schedules for occupancy, electric lighting loads and shading device status, which can be directly coupled with thermal simulation engines such as EnergyPlus (Reinhart, 2016).

- **Honeybee**: Honeybee is an open source plugin for Grasshopper and Rhino3D that helps explore and evaluate environmental performance. Honeybee connects the visual programming environment of Grasshopper to four validated simulation engines - specifically, EnergyPlus, Radiance, Daysim and OpenStudio - which evaluate building energy consumption, comfort, and daylighting (Sadeghipour Roudsari & Pak, 2013). This plugin enables a dynamic coupling between the flexible, component-based, visual programming interface of Grasshopper and the validated environmental data sets and simulation engines (Sadeghipour Roudsari & Pak, 2013). Honeybee is used in this case to conduct the daylight, electric light and energy simulations.

- **Ladybug**: Ladybug is an open source plugin for Grasshopper and Rhino3D that connects Grasshopper with the same simulation engines as Honeybee does. Ladybug imports standard EnergyPlus weather files (*.epw) into Grasshopper and provides a variety of 3D interactive graphics to support the decision-making process during the initial stages of design (Sadeghipour Roudsari & Pak, 2013). Ladybug was only used complementary to Honeybee. It was required in order to import standard epw weather files and to read EnergyPlus surface results.

- **Octopus**: Octopus is a multi-objective evolutionary algorithm that operates in the Grasshopper environment. It is a plug-in for applying evolutionary principles to parametric design and problem solving. It allows the search for many goals at once, producing a range of optimized trade-off solutions between the extremes of each goal (Vierlinger, et al., 2016). The octopus-explicit plug-in was utilized for setting up the genetic algorithm.

A graphical representation of the interconnection between the aforementioned software is shown in Figure 5. The workflow included the design of the initial geometry within Rhino3D, importing it into Grasshopper and from there, connecting all simulation engines via Honeybee to form a single simulation script. Part of this script was the octopus genetic algorithm to produce and evaluate different fenestration designs in terms of the objectives of low heating demand and low light dependency.

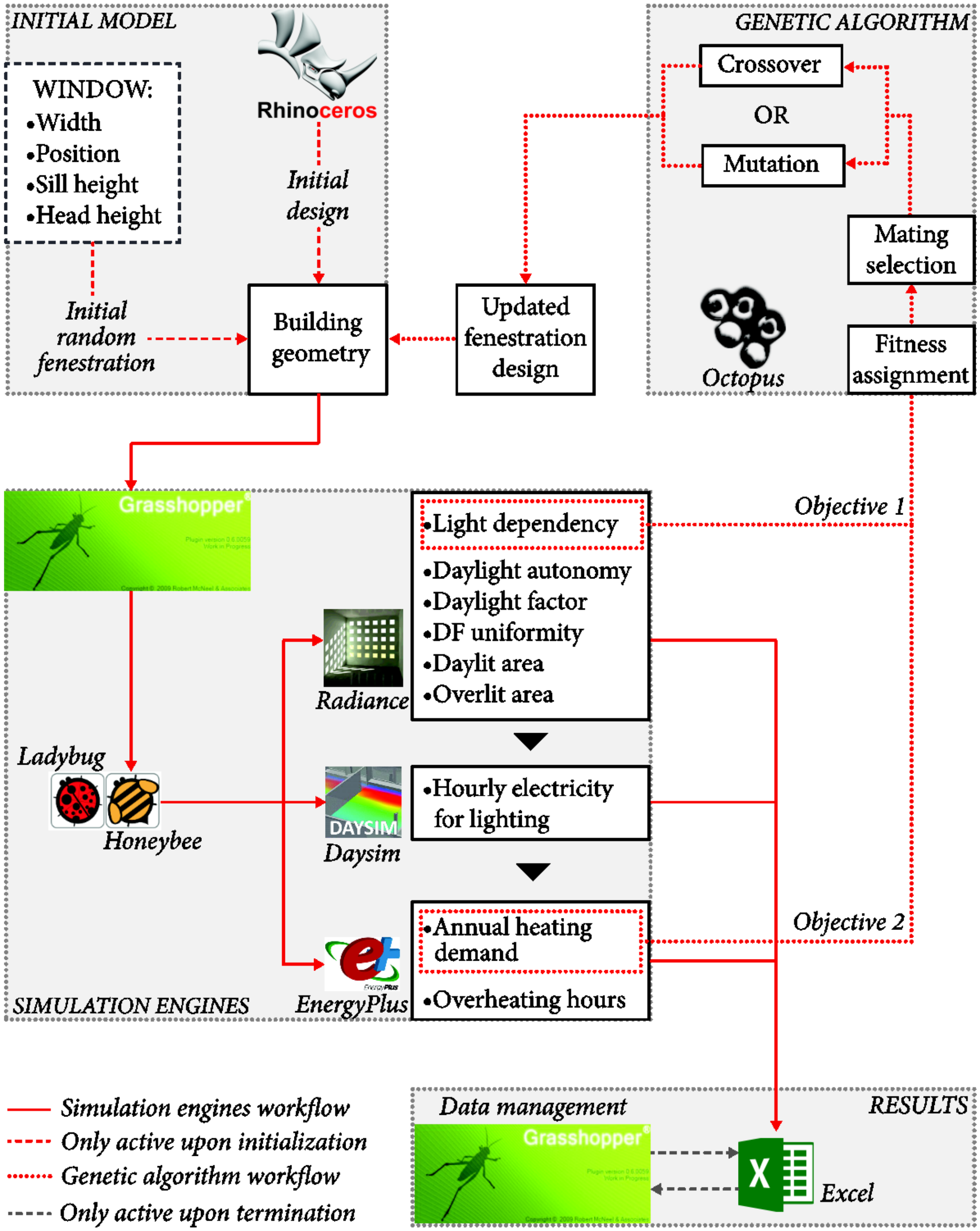

Figure 5: Optimization algorithm workflow.

The apartment geometry with an initial fenestration design were input in Grasshopper. Using Honeybee components inside Grasshopper, the simulation engines of Radiance, Daysim and EnergyPlus were connected to the geometry, assigning different zones and surface properties. The different dependent variables calculated by each simulation engine are described in the following sections of this thesis. During the operation of the algorithm, each simulation was followed by another one with an altered fenestration design. Prior to proceeding to the next simulation, the genetic algorithm provided by Octopus-explicit was used to generate a subsequent fenestration design for assessment. This was based on two optimization objectives (Lighting dependency and annual heating demand). Details about the interior architecture and the logics of the genetic algorithm are presented further down. After each simulation, results were recorded in Excel sheets. In the end, the resulting data was processed by reading these Excel sheets and managing their information using Grasshopper components.

2.5 Daylight model

The daylight study was conducted for the parts of the apartments that have external walls, where a fenestration design was investigated. Daylight measurement grids were therefore placed in the bedroom and living room of apartments 1 and 2. This section only presents the settings for apartment 1. The settings for apartment 2 were the same, only for the different orientation, as it was shown in Figure 4 of the previous section.

The apartment geometry and the different surface types used as input for the Radiance calculations are shown in Figure 6. Geometry simplifications compared to Figure 4 include the corners of the balcony and external walls, the extension of the living room to the area located between points DEFG and the exclusion of furniture from the model, with the exception of the bedroom wardrobe and the workshop door to the living room. The bedroom area is located between points ABCD.

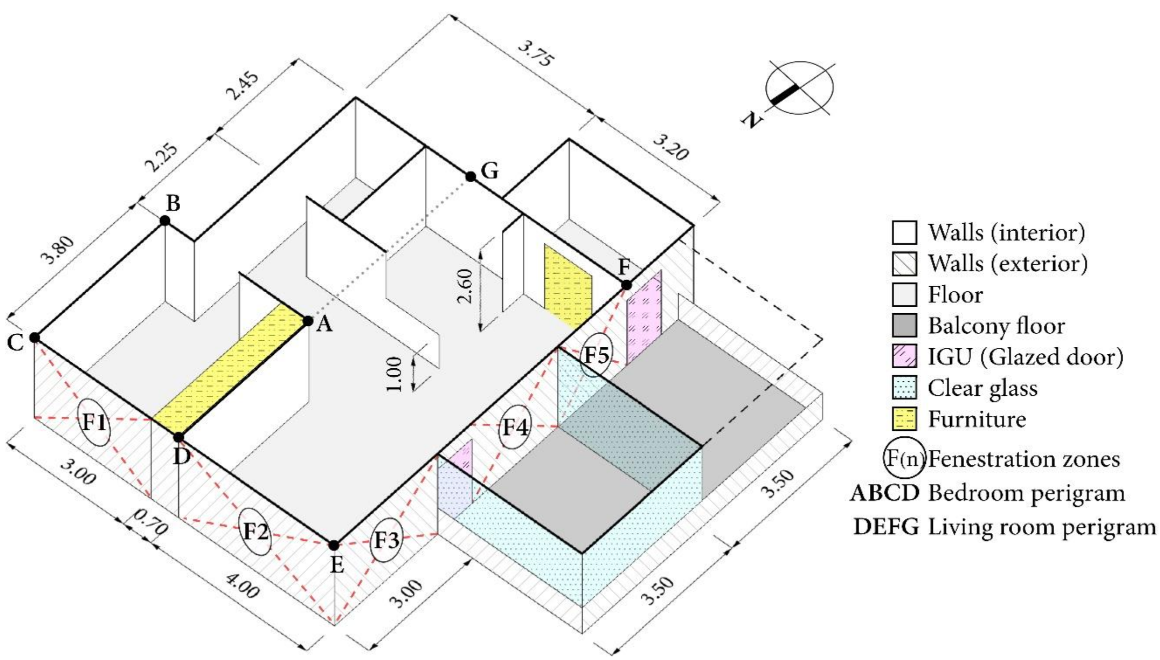

Figure 6: Apartment 1 model geometry and surface types used in Radiance simulations.

Different fenestration designs were generated by placing a single window in each of the five fenestration zones (F1, F2, F3, F4 and F5). The generation scheme and geometric rules for each window are described further down. The possibility for the absence of a window was also considered. Initially, the fenestration for the bedroom (F1) was optimized, not considering the luminous conditions or the heating intensity for the rest of the apartment. A selection was made among optimum solutions for the bedroom. The finally selected bedroom window was used as a constant input when varying the fenestration in zones F2, F3, F4 and F5 for the living room study.

Table 2 shows the rendering option settings for Radiance. Due to the necessity for reduced simulation times, the selected settings correspond to *medium accuracy* settings (Ward Larson & Shakespeare, 1998; Ward Larson, 1996). In the case of the *ambient bounces (ab)*, a parametric study was conducted to assess the optimum number of bounces, regarding accuracy and simulation time. The intention was that a comparative study would be conducted between different fenestration alternatives, and not a pursuit of absolute daylight levels in the studied apartments.

Table 2: Radiance rendering options settings.

Ambient bounces (ab)	Ambient division (ad)	Ambient sampling (as)	Ambient resolution (ar)	Ambient accuracy (aa)
5	512	128	128	0,15

The surface properties are shown in Table 3. All opaque surfaces were considered *grey*, i.e. with the same RGB value, consisting of totally *diffuse plastic* materials. A *plastic* material in Radiance has uncoloured highlights and no transmitted component. If a surface roughness is zero then a ray is traced in or near the mirror direction. The selected reflectance values are recommended for adequate light distribution and for avoiding discomfort glare according to Christoffersen (1995).

Table 3: Radiance surface properties.

	Material	Reflectance*	Transmissivity	Specularity	Roughness
Walls (interior)	Plastic	0,70	-	0	0
Walls (exterior)	Plastic	0,50	-	0	0
Triple pane (IGU)	Glass	-	0,64	-	-
Single pane (clear glass)	Glass	-	0,98	-	-
Frame	Plastic	0,70	-	0	0
Ceiling	Plastic	0,80	-	0	0
Balcony ceiling	Plastic	0,20	-	0	0
Floor	Plastic	0,30	-	0	0
Balcony floor	Plastic	0,20	-	0	0
Furniture	Plastic	0,65	-	0	0

**Average red, green and blue reflectance*

2.5.1 Measurement grid study

As Radiance annual simulations can be time-consuming, a parametric study was performed to select the optimum measurement grid for the daylight distribution. The requirements set were a) the possibility to deduct accurate results and b) acceptable simulation time. In the case of the bedroom, the measurement grid was set to nine points, located as shown in Figure 7a. Reducing this number was not a necessity, since the fenestration study for the bedroom consisted of only iterating a single window opening. The grid parametric study was conducted for the living room area DEFG, for which four windows were investigated, leading to an amount of approximately 7,5 million different fenestration designs with corresponding times for the DA simulations.

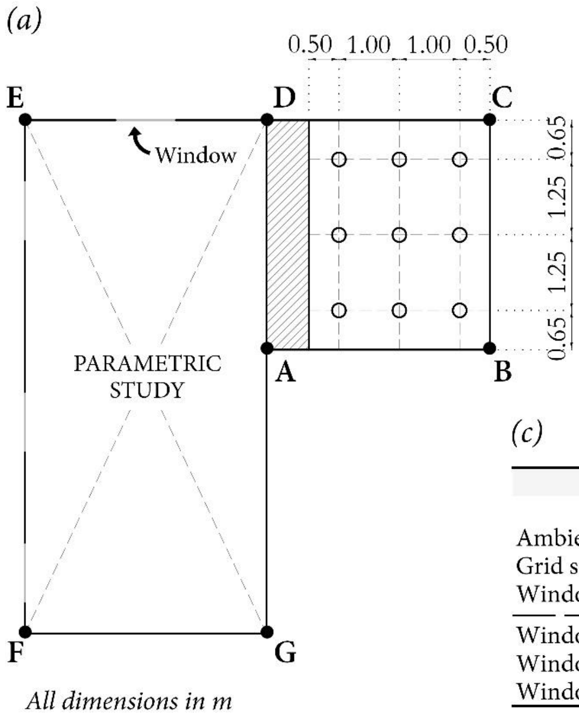

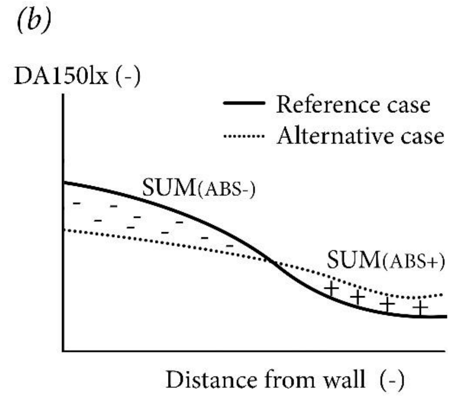

(c)

PARAMETRIC STUDY VARIABLES			
	Step	Range	
Ambient bounces	1	[2-5]	
Grid size	0,25 m	[0,50-2,50 m]	
Window configuration	-	[Low, Medium, High]	
Window position	Low	Medium	High
Window sill height	0,55 m	1,05 m	1,55 m
Window height	1,00 m	1,00 m	1,00 m

Figure 7: *a)* Areas where the measurement grids were applied, *b)* illustration of the differences between the reference and alternative grid cases and *c)* the variables in the grid parametric study.

A Reference case was set with a grid density of 0,25 m and 6 ab, regarded as an accurate but time-consuming setup. Every other case was set according to Figure 7c. One window was placed in each fenestration zone as shown in Figure 7a, and it was iterated for three positions on the vertical axis, to investigate the sensitivity of the measurements. The grid density was also iterated ranging from 0,5 m to 2,5 m, with a 0,25 m step. Two key resulting values were examined in order to compare each alternative with the reference case:

i) The average daylight autonomy for a desired illuminance of 150 lx (DA150lx).
ii) The sum of all interpolated DA150lx differences between the Reference and each alternative case (Figure 7b).

As it is illustrated in Figure 7b, each alternative case had a different DA150lx distribution across the living room area, due to the use of different ambient bounces and distances between measurement points. Using native Grasshopper components, a three dimensional mesh was generated for each case. This mesh represented the DA150lx distribution across space, and it was intersecting with the Reference case mesh in various points. $SUM_{(ABS-)}$ is the absolute value of the sum of differences when an alternative case result is lower than the reference case. $SUM_{(ABS+)}$ is the sum of all differences where the alternative case measures higher values than the Reference case. The volumetric difference was therefore defined as in Equation 1:

$$\Delta V = SUM_{(ABS-)} + SUM_{(ABS+)} \qquad [1]$$

The DA150lx of the Reference case was compared to the DA150lx of each alternative case, as an absolute difference ΔDA150lx. Both ΔV and ΔDA150lx should be minimized in order to avoid inaccuracy in both average values and distribution of daylight across space. The final criterion for the selection between accurate settings was the amount of simulation time.

2.5.2 Daylight standard requirements

The daylight conditions in the studied apartments were evaluated based on certification systems and relevant research. The evaluation of DF and UR was based on the Building Research Establishment Environmental Method (BREEAM, 2014). BREEAM is a widespread certification system that assesses sustainability of master-planning projects, infrastructure and buildings. It sets thorough daylight criteria for different types of spaces, including residential spaces. The BREEAM criteria utilized to evaluate different fenestration solutions was the average DF of 2,1 %, which corresponds to 3 credits according to the certification system.

Miljöbyggnad utilizes a point DF measurement that is set according to the SS 914201 standard (1987). It is placed one meter away from the center of the darkest wall in the room, at an elevation of 0,8 m. It must achieve a value of 1,2% or above in order to reach the Silver or Gold standards. For this thesis, the Miljöbyggnad point DF criteria was only used in the bedroom as what constitutes the darkest wall stays constant in that room. This wall is the one through which the bedroom is entered.

The aforementioned methods do not regard climate-based performance indicators, such as the DA. For the climate-based evaluation of the different fenestration solutions, the benchmark values stated in the previous sections were used.

2.6 Electrical lighting model

Moving past the daylight simulation, the workflow of the created algorithm continues with the electrical lighting simulation. The Radiance simulation that preceded this step provides the hourly illuminance values for each point on the grid. Following that, the simulation engine of Daysim utilizes these values to create a list of hourly electrical lighting power values. A unique feature of Daysim is the *manual lighting control model*, the use of which mimics how occupants switch electric lighting on or off, as documented in the Lightswitch study (Reinhart, 2004).

A “simple model” of Daysim was used, where the software assumes an *'ideal lighting system'*. In this case, it is the daylight in space that is modeled, and not the electric lighting system itself. The user only needs to input the installed lighting power per zone, the target illuminance and the type of control for the light sources. It is assumed that the lighting system will deliver the missing illuminance when fully switched on (Reinhart, 2016). Table 5 shows the utilized input data for Daysim.

Table 5: Utilized Daysim settings.

Lighting load	3 $W/m^2 \cdot lx$
Lighting target illuminance	150 lx
Lighting control	Manual*

**As in the Lightswitch study* (Reinhart, 2004)

The lighting load of 3 $W/m^2 \cdot lx$ corresponds to an electrical lighting system of compact fluorescent lamps that can provide 150 lx in the studied zones. Relevant research on key values for electrical lighting intensity when simulating residential spaces in Sweden do not exist yet. One report (Bladh, 2008) provides measured data on the annual electrical light use of Swedish houses. In this thesis, the lighting load value of 3 $W/m^2 \cdot lx$ was validated by calculating the annual electricity use of the whole apartment for a lighting schedule that follows the set occupancy schedule, as it is described further down. It was concluded that 3 $W/m^2 \cdot lx$ was a reasonable value, as it lead to an annual electricity use of approximately 700 kWh, which is equal to the average measured electric lighting use in Swedish households stated in the aforementioned report.

The *manual* lighting control corresponds to a lighting schedule where the lights are turned on or off during occupancy time, with a probability function that determines whether or not users will turn lighting on or off. This probability was set according to the statistical analysis of the *Lightswitch* study (Reinhart, 2004), which is integrated into the Daysim simulation engine, when selecting the *manual* control. The Lightswitch study was carried out for office spaces, but it was the only available that proposed a methodology that mimics human behavior in controlling electrical light switches. This statistical probability may differ in residential spaces, which is a limitation of the present thesis.

2.7 Energy model

After the Daysim simulation, the EnergyPlus engine is initiated to calculate the annual heating energy intensity, the amount of solar gains and the overheating time. The electrical lighting use had to precede the energy simulation, in order to provide the sensible heat load generated by the light sources. This load profile is integrated in the EnergyPlus simulation, as it affects the heating load of the studied space throughout the year.

This section describes the different simplifications and settings used for the energy modelling. It also defines the energy standard requirements that were used to evaluate different fenestration solutions. Finally, it includes a validation study that was conducted by comparing results from Honeybee and Designbuilder™ (2015), to create a robust energy model.

2.7.1 Construction

The energy zones and different construction types assumed in EnergyPlus are shown in Figure 8. All zones are conditioned spaces, apart from the *Closed* and *Open Balcony*. All zones were designed as convex shapes, in order to use the "Full interior and exterior" solar option in EnergyPlus (U.S. Department of Energy, 2015). This option is taking into account the effect of exterior shadowing surfaces and window shading devices. This was a necessity due to the existence of the *Closed Balcony* zone, in order to accurately estimate the solar gains reaching the *Living room* zone.

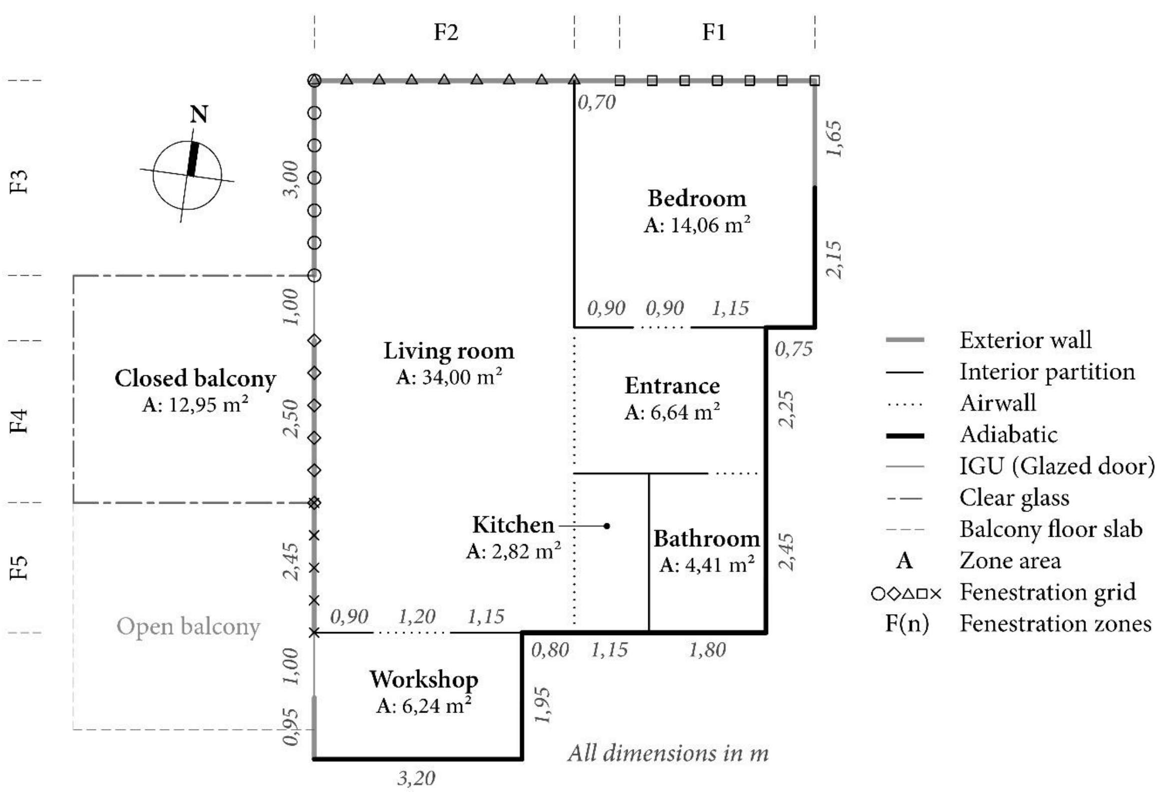

Figure 8: The different energy zones assigned in EnergyPlus and the surface constructions.

In reality, the *Closed balcony* is not conditioned, but it has a microclimate, due to its glazed envelope, which affects the *Living room* space. The *Airwall* constructions are assumed by EnergyPlus as surfaces that allow a constant airflow between zones, in other words, the air is mixed between two zones separated by an *Airwall*. This surface is not meant to model inter-zone buoyancy-driven flow, but to estimate a constant airflow. The adiabatic surfaces are the ones in contact with the storeys' common areas (Hallway, staircase). For reasons of simplicity and calculation time, no heat transfer was assumed between the apartment and these common spaces. Two different window types were modelled: One single pane clear glass mounted on the *Closed Balcony* walls that was not iterated in the fenestration study and one triple pane insulated glazed unit (IGU), that was used in the balcony doors and in every opening iterated during the optimization of fenestration zones F1, F2, F3, F4 and F5. Table 6 shows the construction properties of the different EnergyPlus surfaces. Detailed constructions including material layers can be found in *APPENDIX B*.

Table 6: EnergyPlus construction properties.

	U-Value (W/m²·K)	g-value (-)
Exterior wall	0,15	-
Interior partition	-	-
Airwall	-	100%
Floor & Ceiling slabs	Adiabatic	-
IGU (Glazed door)	0,80	53%
Clear glass	5,75	89%
IGU (Windows)	Variable*	53%

** Calculated as shown in section 2.8.1*

2.7.2 HVAC

The Heating, Ventilation and Air Conditioning (HVAC) system used for this thesis is the "Ideal Air Loads" system embedded in EnergyPlus (U.S. Department of Energy, 2015). In brief, this system is a demand control all-air system, where both ventilation and space heating are provided by air supplied to the zone to meet set requirements by the user. These were set as a heating setpoint and setback of 21 °C and 19 °C respectively. The heat recovery on the ventilation system was set to 80 %. The actual ventilation system in the Greenhouse apartments is a constant air volume (CAV) system, while the "Ideal Air Loads" is occupancy driven. By disabling the ventilation flow per person and calculating an average flow (per person + per area) to input as a constant flow, the system was modelled as a CAV system. No cooling was assumed for the apartments, as it is actually the case, but overheating time was calculated in this study. No other HVAC components were designed in the model (Heating/cooling coils, fans, heat pumps, ducts etc.). Table 7 shows the HVAC utilized settings.

Table 7: HVAC input data.

Heating*	
Setpoint	21 °C
Setback	19 °C
Schedule	Always ON
Cooling	NO
Mechanical ventilation	
Type	CAV
Fresh air per m^2	0,52 l/s
Heat recovery	80%
Schedule	Always ON

** After Ideal Air Loads System (US Department of Energy, 2015)*

2.7.3 Internal Loads

Internal loads in the form of sensible or latent heat are generated within the apartment by different sources. The ones considered in this thesis were as follows:

a) The occupants metabolic rate ($W/m^2 \cdot person$).
b) The electric equipment use (W/m^2).
c) The electric lighting use ($W/m^2 \cdot lx$).

The electric lighting calculation is described under section 2.6. The metabolic rate of the occupants depends on the occupant activity level (met) and clothing level (clo), among other parameters. Data on metabolic rate can be found in the American Society of Heating, Refrigerating and Air-Conditioning Engineers (ASHRAE) Handbook of Fundamentals, (ASHRAE, 2013). A constant clothing level of 1 clo was used for all studied thermal zones of the energy model. The activity level was selected according to the assumed activity conducted in each zone, as shown in Table 8, which led to the metabolic rate values shown in the table.

Table 8: Activity and electric equipment types and loads per zone.

Zone / (Name)	Activity / (Type)	Metabolic rate / ($W/person \cdot m^2$)	Equipment / (Type)	Equipment load / (W/m^2)
Bedroom	Sleeping	70	Various	0,65
Living room	Seated	100	TV, Stereo, Video	12,53
Kitchen	Cooking/eating	145	Fridge, Kitchen stoves, Dishwasher	218,79
Workshop	Workshop	250	Various	0,66
Bathroom	Bath	130	Various	0,66

The electric equipment load was calculated for each zone based on the assumed nominal power of each electric device. The wattage of each electric device was calculated so that the annual electricity use (kWh) would coincide with the measured values reported by Zimmermann (2009). In this way, the annual electricity use of the apartment equipment was set according to the statistics for Swedish houses, at 2300 kWh annually. The values for the equipment load shown in Table 8 correspond to the sum of the nominal powers of all zone electric devices, divided by the zone floor area. The types of devices correspond to the types described in the study of Zimmermann.

The heat generated due to the metabolic rate is dependent on the occupancy level in each zone. In other words, it is dependent on the number of occupants inside each room for every hour of the year. The occupancy schedule was assumed differently for weekends and weekdays, as shown in Table 9. These values represent the fraction of total occupancy including in this case two adults. The metabolic rate is thus multiplied by these values for every hour of the year.

Table 9: Fractional occupancy schedule per zone.

	Weekday occupancy / fraction					Weekend occupancy / fraction				
	L*	K*	B*	W*	Ba*	L*	K*	B*	W*	Ba*
00:00 - 07:00	0	0	1	0	0	0	0	1	0	0
07:00 - 08:00	0	0,7	0	0	0,3	0	0	1	0	0
08:00 - 09:00	0	0	0	0	0	0	0	1	0	0
09:00 - 10:00	0	0	0	0	0	0	0,5	0	0	0,5
10:00 - 11:00	0	0	0	0	0	0,8	0	0	0,1	0,1
11:00 - 18:00	0	0	0	0	0	0	0	0	0	0
18:00 - 19:00	0,1	0,8	0	0	0,1	0,1	0,8	0	0	0,1
19:00 - 20:00	0,8	0	0	0,1	0,1	0,8	0	0	0,1	0,1
20:00 - 21:00	0,8	0	0	0,1	0,1	0,8	0	0	0,1	0,1
21:00 - 22:00	0,5	0	0	0	0,5	0,9	0	0	0	0,1
22:00 - 23:00	0	0	1	0	0	0	0	0,5	0	0,5
23:00 - 24:00	0	0	1	0	0	0	0	1	0	0

Fraction of two people

** L: Living room, K: Kitchen, B: Bedroom, W: Workshop, Ba: Bathroom*

The heat generated by the electric equipment is dependent on the amount of devices turned on, and the duration of use. Both the amount and duration were set hourly, in a way that the equipment use per zone is in accordance with the occupancy of the zone. For example, when the kitchen is occupied, the stoves or the dishwasher can be turned on. Other devices such as the fridge or extra devices (Table 8) were assumed constantly on, at standby mode. Table 10 shows the equipment use schedule per zone, and the fraction of the equipment load used per hour.

Table 10: Fractional electric equipment schedule per zone.

	Weekday equipment load / Fraction					Weekend equipment load / Fraction				
	L*	K*	B*	W*	Ba*	L*	K*	B*	W*	Ba*
00:00 - 07:00	0,07	0,13	1	1	1	0,07	0,13	1	1	1
07:00 - 08:00	0,07	1,00	1	1	1	0,07	0,13	1	1	1
08:00 - 09:00	0,07	0,13	1	1	1	0,07	0,13	1	1	1
09:00 - 10:00	0,07	0,13	1	1	1	0,07	0,13	1	1	1
10:00 - 11:00	0,07	0,13	1	1	1	1,00	1,00	1	1	1
11:00 - 18:00	0,07	0,13	1	1	1	0,07	0,13	1	1	1
18:00 - 19:00	0,47	1,00	1	1	1	0,47	1,00	1	1	1
19:00 - 20:00	1,00	0,13	1	1	1	1,00	0,13	1	1	1
20:00 - 21:00	1,00	0,67	1	1	1	1,00	0,67	1	1	1
21:00 - 22:00	1,00	0,13	1	1	1	1,00	0,13	1	1	1
22:00 - 23:00	0,07	0,13	1	1	1	0,07	0,13	1	1	1
23:00 - 24:00	0,07	0,13	1	1	1	0,07	0,13	1	1	1

Fraction of equipment load shown in Table 8

** L: Living room, K: Kitchen, B: Bedroom, W: Workshop, Ba: Bathroom*

2.7.4 Energy standard requirements

The Swedish National Board of Housing, Building and Planning (Boverket) is responsible for the requirements set for the energy performance of Swedish houses. Boverket publishes the Swedish building code, Boverkets' Building Regulations (BBR) that sets the mandatory standards for new constructions and renovations. The BBR version applicable while this thesis was written was BBR22 (2015). In addition, voluntary criteria for zero-energy houses, passive houses and low-energy houses were developed by a group of experts appointed by the Forum for Energy Efficient Buildings (FEBY). At the time of writing this thesis, the FEBY12 was in application, which is divided into separate documents for residential and commercial buildings (FEBY12, 2012). Both BBR22 and FEBY12 criteria are defined in terms of specific energy use.

During the optimization process, only the energy used for space heating was weighted against the daylight levels. For the comparison of the different fenestration solutions based on the aforementioned standards, the energy use of DHW and property electricity were added to the space heating energy after the simulations, to provide the specific energy use. The property electricity was set to 7,40 kWh/m^2 annually according to the preliminary documentation regarding the energy performance of the apartments (NCC, 2014). According to the same report, the energy for the DHW was set to 20 kWh/m^2 annually. Table 11 shows the requirements on specific energy use for the corresponding climatic zone of Malmö.

Table 11: BBR22 and FEBY12 requirements for the apartment specific energy use.

	BBR22 (2015)	FEBY12 (2012)
Maximum specific energy use / (kWh/m²·year)	80*	50

*Non-electrically heated apartments in climatic zone IV

The operative temperature is often used to assess indoor thermal comfort, as it combines the room air temperature with the radiant temperatures of the room surfaces. So far, there is no requirement that dictates an acceptable amount of overheating time for residential spaces. Nevertheless, studies have shown that occupants prefer specific operative temperature levels, depending on their activity and clothing level, as well as the outdoor ambient air temperature (ISO7730, 2015). For Swedish workplaces, there is a requirement for different *temperature classes*, proposed by the "Beställargruppen Lokaler" project method (BELOK, 2008). According to FEBY, the resulting operative temperatures should fulfill any of the BELOK classes T_B= 24 °C, 25 °C, 26 °C. The value of the selected class should not be exceeded for more than 80 hours between April and September. This thesis follows this method in that it sorts results according to BELOK classes, but no specific requirements are set for the operative temperature of the apartment. The operative temperature was monitored both for the living room and the bedroom, and it was assumed that fenestration designs leading to shorter overheating periods are more desirable.

2.7.5 Validation

In order to create a robust energy model, a simple geometry was designed and simulated for a number of different input data, using two different software: the Designbuilder energy simulation tool and the Honeybee plugin for Grasshopper. The latter was the tool used in this study and the one under validation. Both software utilize the EnergyPlus simulation engine for the energy calculations, meaning that input and output data can be thoroughly compared under the same platform.

The simple model used for the validation represents the living room area. It was designed in a way that all possible model aspects of this thesis would be included and therefore tested prior to modelling the complete apartment. These include construction, internal loads and HVAC settings. In addition, a closed geometry was designed attached to the living room, to validate the solar distribution through internal openings, which played a significant role in this thesis due to the *Closed Balcony* zone. The different settings were input in a stepwise manner, while monitoring the annual heating demand (kWh/m²) output from the two software. Figure 9 shows the different geometries (G1-G4) and simulation steps (1-9). The input data can be found in *APPENDIX D*.

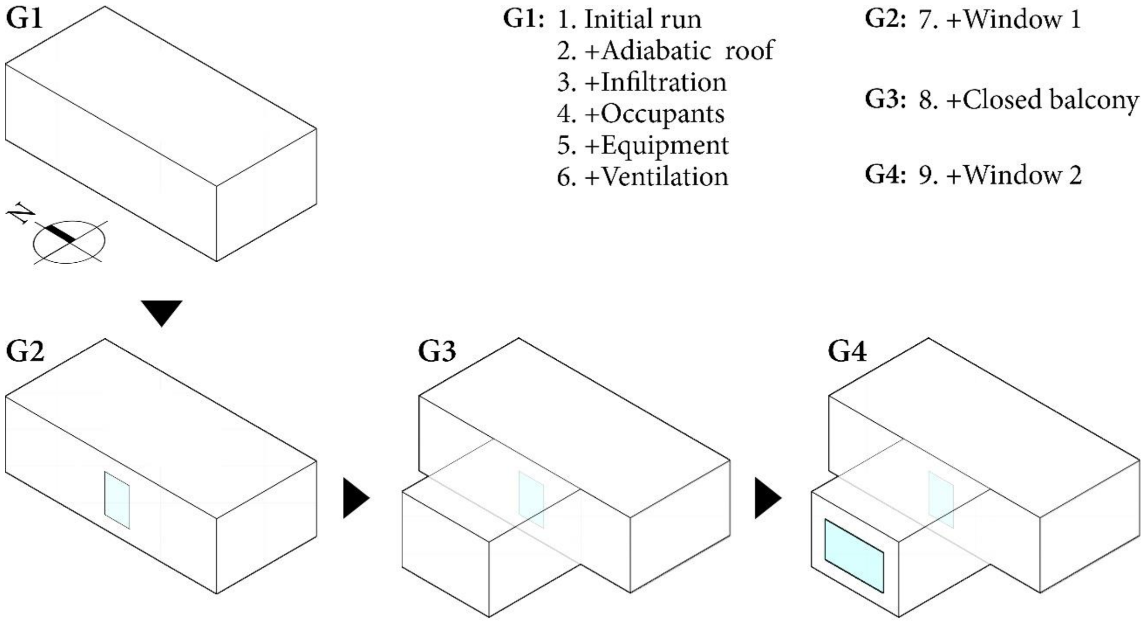

Figure 9: The different simulation steps and corresponding geometries for the validation of the energy model.

2.8 Fenestration definition

This section describes the internal workings of the algorithm that was developed to create fenestration solutions. There were two distinct parts in the script definition developed in the Grasshopper environment:

- A design filter that dictates the rules and boundaries that govern every fenestration geometry. The rules relate to the window size and placement on the façade. Only solutions that satisfied these criteria described below could be considered for the optimization.
- A genetic algorithm that automatically iterates between fenestration designs and assesses them based on a specific process (optimization process).

2.8.1 Rules and boundaries regarding fenestration geometry

Instead of simply assessing different window-to-wall ratios, a design method was utilized that also evaluated the importance of the position and shape of the widows. For every fenestration zone (F1-F5) shown in Figure 5 of section 2.3, a single window was generated, based on a "design filter". In brief, the wall geometry assigned both in the daylight and energy models alters, according to the window size and position that is generated by the algorithm. There are specific geometric constraints that define the window generation. Each fenestration zone is subdivided in a $0,5 \cdot 0,5$ m^2 grid, as shown in Figure 10. The window width, height and sill height have therefore dimensions in integers of 0,5 m. To reduce simulation time and comply with realistic terms, the algorithm is ordered to bypass cases where the window:

1. Has an area smaller than $0{,}5 \cdot 0{,}5$ m² or $0{,}5 \cdot 1{,}0$ m².
2. Is a concave polygon. The majority of windows used in practice today are convex shapes.
3. Has been calculated previously in the process.

To account for the occupant view towards the exterior environment, a "View zone" was set as shown in dashed lines in Figure 10. Any generated window that does not intersect with this zone and lies altogether below or above it, is bypassed by the algorithm. This filter is in line with the occupants' appreciation of windows because they offer a view outside, according to relevant research (Christoffersen, et al., 1999). Moreover, there is a possibility that duplicates can be ordered for simulation (designs already calculated once), due the genetic algorithms internal workings. In case a window design is a duplicate, the algorithm identifies it and automatically uses the previously stored result, without running a simulation. This was crucial in terms of total simulation time.

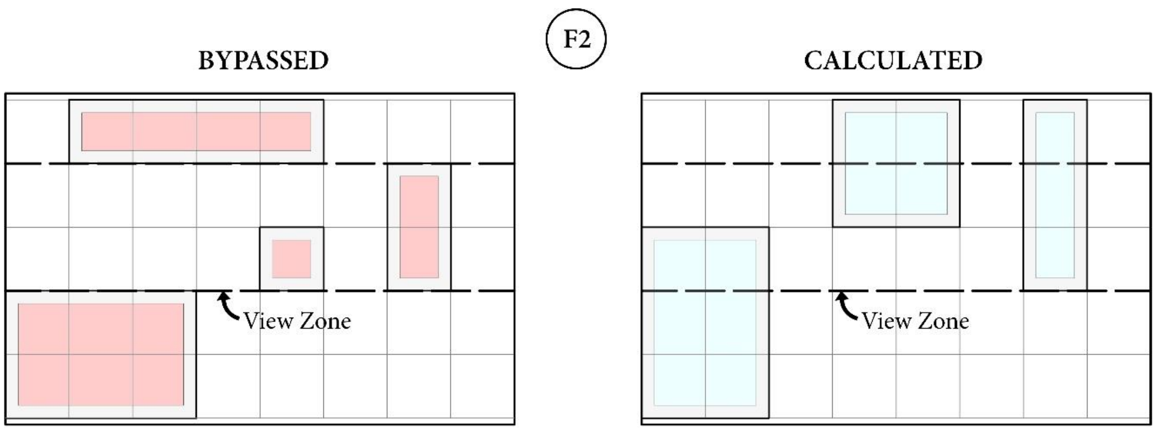

Figure 10: The window generation scheme (shown here for the fenestration zone F2).

The window designs that were input in Radiance and EnergyPlus were also designed in a simplified manner, in order to reduce the amount of surfaces for calculation, without compromising the validity of the results. Figure 11 shows an example of how a window that has passed the previous filter, proceeds as input for the two different simulation engines.

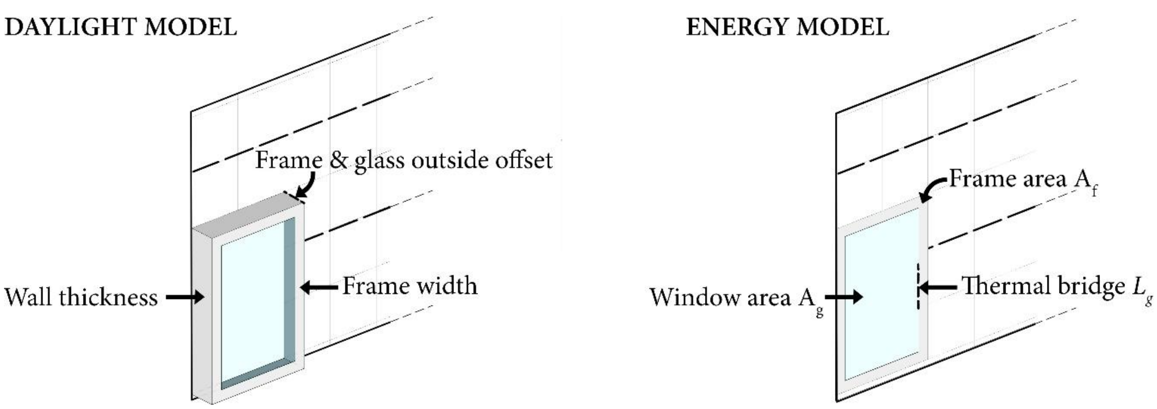

Figure 11: The window geometry input for the daylight and the energy model.

In the case of the daylight model, there is an offset of the window outside the wall surface, in order to model the wall thickness that could potentially block daylight from penetrating inside. The window is assumed placed on the outer part of the wall, as it is the actual case. In the energy model, the window is co-planar with the wall, as shown in Figure 11.

Looking at Figure 11, one can realize that a specific window design constitutes of a glazed part and a frame part. There is also a linear thermal bridge that is different for each window shape. In brief, two windows of the same WWR could have different shapes, thus different overall *U*-Values depending on these parameters. According to ISO10077-1 (2006), the window *U*-value, U_{win}, is calculated using Equation 2, and is dependent on the areas of glazing (A_g) and frame (A_f). Other factors include the *U*-value of the frame (U_f) and glazing (U_g) as well as the length of the linear thermal bridge Ψ of the glazing perimeter (L_g). A constant frame width of 113 mm was adjusted parametrically by the algorithm for all window sizes. The glazing and frame properties are shown in Table 12.

$$U_{win} = \frac{A_g \cdot U_g + A_f \cdot U_f + L_g \cdot \Psi}{A_g + A_f} \qquad [2]$$

Table 12: Window components properties.

Window pane	Triple
Glass U-value U_g	0,60 W/m²
Frame U-Value U_f	1,10 W/m²
Glass thermal bridge Ψ	1,01 W/m·K
Window light transmittance	59r%
Window g value	53f%

2.8.2 Genetic algorithm

Given the number of possible fenestration solutions, a study that would simulate all possible cases would be time-consuming, if not impossible. Radiance has long been pointed out as a burden when attempting multiple simulations, due to its long run-times (Ward Larson & Shakespeare, 1998). Such a study would also be unnecessary, because many fenestration designs could be logically excluded from the study, as they would not meet neither the daylight nor the thermal criteria. For this thesis, the genetic algorithm used to evaluate designs and to proceed faster with the optimization was based on the Strength Pareto Evolutionary Algorithm, SPEA2 (Zitzler, et al., 2001), embedded in the Octopus-explicit components running on the Grasshopper platform.

In brief, the genetic algorithm is generating one window at a time. Once generated, the studied space with that window is simulated by Radiance, Daysim and EnergyPlus. These simulation engines send back to the genetic algorithm the case-specific results, which are used for evaluation. If the evaluation proves that window efficient, the algorithm "remembers" its geometric properties, and tries to test similar ones.

The way the genetic algorithm conceives a window geometry is shown in Figure 12. The window properties (Width, Position, Head height and Sill height) constitute the so-called "Genes". Each Gene can have a different value, which will be translated into a different geometrical attribute on the façade. The grid size is 0,5 m · 0,5 m, so a Gene value of 5 for the Width means a 2,5 m wide window or 5 grids width, and so on. The Position Gene measures the distance of the window from the left side of the wall (looking from the exterior). A complete set of Genes constitutes a Chromosome, a complete window design, which from now on will be referred to as a solution. In the language of genetic algorithms, a phenotype is the way this solution looks in space.

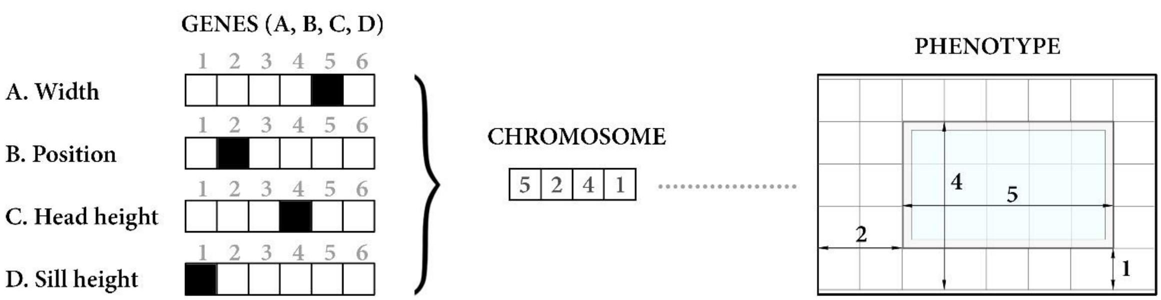

Figure 12: Exemplified scheme of genetic algorithm logics – Genes, Chromosome and Phenotype.

The stepwise optimization process followed by utilizing the Octopus-explicit components is shown in Figure 13. The diagram represents a solution space, where the two axes correspond to the conflicting objectives. The solutions plotted closer to the axes are therefore better performing solutions. The user sets different parameters that can guide the optimization process more effectively, as described below. The process illustrated is the one suggested by Zitler et al. (2001).

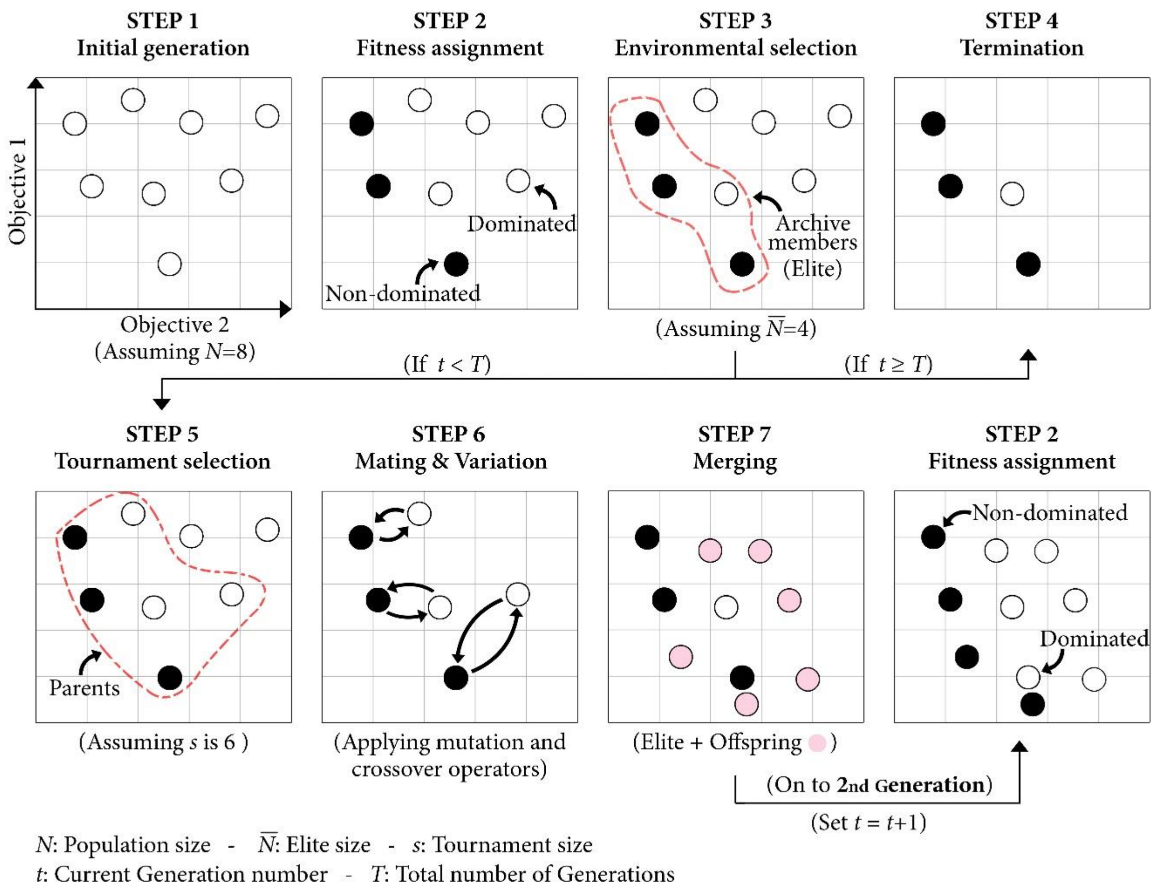

Figure 13: Exemplified genetic algorithm optimization loop, for two conflicting objectives.

The following is a brief description of the process illustrated in Figure 13, which follows the SPEA2 process (Zitzler, et al., 2001). Initially a time T is given by the user:

STEP 1 - *Initial generation*: The genetic algorithm combines Genes in random ways to generate a number of solutions. The algorithm orders the simulation engines to calculate each solution and return its resulting values for Objectives 1 and 2, in this case, the heating demand and the light dependency. The number of random solutions is called population size (*N*), and is set by the user in the beginning.

STEP 2 – *Fitness assignment*: This step is based on the so-called “fitness function”. The fitness function dictates how the different solutions are evaluated, what are the criteria that a solution should fulfil to be considered good. In this case, the best performance is the one that is minimizing both objectives as much as possible, meaning a window design that induces the least possible annual heating demand and light dependency. A solution is called non-dominated (or Pareto optimal), if none of the objectives can be improved, without degrading the other objective. The algorithm is assigning a score to each solution, based on its performance over the fitness function.

STEP 3 – *Environmental selection*: The algorithm selects a user-defined number of solutions, the "archive members". These will from now on be referred to as the Elite, and their number Elite size ($\tilde{N}$). The selection is based on the ranking that took place in the previous step.

STEP 4 – *Termination*: If t=T then the process is terminated and the Elite from STEP 3 are the optimum solutions provided by the algorithm. Every time the loop is restarted, t increases by one, so by setting T, the user defines how thorough the process will be.

STEP 5 – *Tournament selection*: During this step, the algorithm selects a specific number of solutions out of the total population size (STEP 1). This number is called "tournament size" (s). Tournament size is defined by the user before the initialization of the algorithm. The selected cases are the ones that will be used for "mating" in the next step (STEP 6), and are called Parents. A low tournament size can lead to results faster, but it could exclude potentially good Parent solutions. In Figure 13, the tournament size *s* is equal to 6.

STEP 6 – *Mating* & *Variation*: Mating is the process out of which new solutions are generated by the algorithm. The algorithm chooses pairs of Parents, and applies crossover and mutation operators to generate new solutions, the so-called Offspring. Crossover is a process where two Parents exchange Genes. For example, 1234 and 5678 can exchange the third Gene and give two Offspring like 1274 and 5638. Mutation is the process where a number of Genes of a solution is transformed into another value. For example, the Gene value of Width can transform from 5 to 4, meaning that the window width will reduce from 2,5 m to 2 m. Parents are induced to crossover first, and mutation immediately afterwards. This is a way for the algorithm to iterate between designs. The user sets the probability of crossover and mutation and the extent to which they will take place.

STEP 7 – *Merging*: The resulting solutions, the Elite plus the Offspring, are the ones that will be used as a STEP 1 initial generation, instead of a random generation. The algorithm will set the generation number *t* to *t*+1 and will automatically proceed with STEP 2, assigning fitness to this new population of solutions.

2.8.3 Genetic algorithm input considerations

During each step of the optimization, amounts of solutions are kept in the process while others are excluded. The ones that are kept are the ones that will define where the optimization algorithm will converge. Crossover is an operator that helps convergence. However, a high crossover rate can lead the genetic algorithm to so-called "local optima", which is not desired. Mutation can help avoid this problem, but a high rate of mutation is also unacceptable, since it will not allow the genetic algorithm to converge to the desired set of solutions. Figure 14 exemplifies the definition of a locally optimum point. In this example, the lower the position, the highest the fitness.

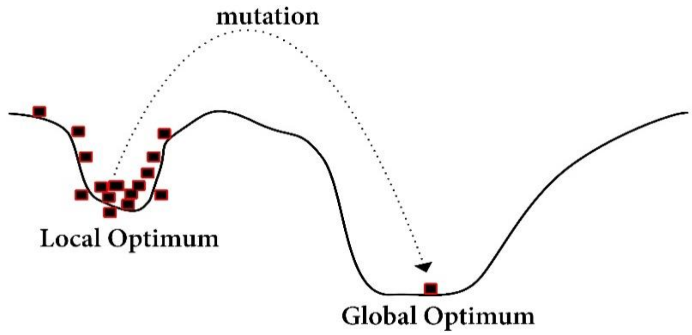

Figure 14: The risk of convergence to a local optimum and the potential solution using mutation.

There are no constant best values for the mutation or the crossover rate. These values depend on the nature of the optimization problem, and the implementation of the algorithm. Reeves and Rowe (2003) have made an extensive study on the principles of genetic algorithms. In their book, they include a specific chapter on how to anneal the mutation rate during the course of a simulation run. The overall good practice they suggest is to initiate the algorithm on a high mutation rate, so that many possible solutions can be generated, and reduce it during the course of different generations.

This annealing process is dependent on various factors, such as the population size, the amount of genes and the number of desired generations. A study on the proper mathematical function that describes the step-wise reduction of the mutation rate was considered too extensive to be included in this thesis. It was however concluded that the mutation rate should be reduced in the course of the optimization. Relevant research also shows that it is related to the amount of elitism (Laumanns, et al., 2001). According to the researchers, the overall best performance occurs for the combination of strong elitism (elitism > 0,7) and high mutation rate (mutation rate ≈ 0,5). The worst performance occurs for a combination of high elitism with low mutation rate.

Prior to the mutation effect, crossover takes place between two Parent solutions. Contrary to mutation, crossover is ensuring that the genetic algorithm is “focused” on the already discovered solutions that perform well in terms of the fitness function. In other words, crossover is leading the algorithm towards convergence, in this case, towards pointing out the optimum solutions for a good trade-off between heating and daylight. It can therefore be concluded that crossover along with elitism are the parameters that ensure that optimum solutions are discovered. Elitism selects them from a list of solutions, and crossover is mixing their genes to provide stronger Offspring.

Table 13 shows the initial settings used for the genetic algorithm used in this thesis. The population size is what defines the number of solutions in the initial generation (STEP 1 in Figure 13). The algorithm starts generating random solutions until this number is reached. Then the optimization steps take place. This indicates the importance of a high population size, to ensure diversity in the solution space. The mutation probability is defining the percentage of genes that will be affected by mutation. This number should be related to the population size.

Table 13: Octopus initial settings

Elitism	Mutation rate	Crossover rate	Population size	Mutation probability
0,60	0,60	0,70	140,00	0,01

2.8.4 Final selection of fenestration design according to multiple objectives

Once the daylighting and heating optimization of the living room zone was finished, a set of 51 Pareto optimal solutions were stored in an Excel database, with all their corresponding dependent and independent variables. Using Pollination (Roudsari, 2015), a web-based application for exploring multi-dimensional data, a refined selection upon these 51 solutions could be made, depending on the objectives of: Specific energy use, Overheating time, DA150lx, DF and UR. Pollination started at the AEC Technology Hackathon (CORE studio , 2014). Figure 15 shows an example where a selection filter for two-window designs and colouring based on the DF performance was applied. Each line represents one fenestration design. It crosses each of the parallel axes based on the performance of the solution on the corresponding variable (axes titles).

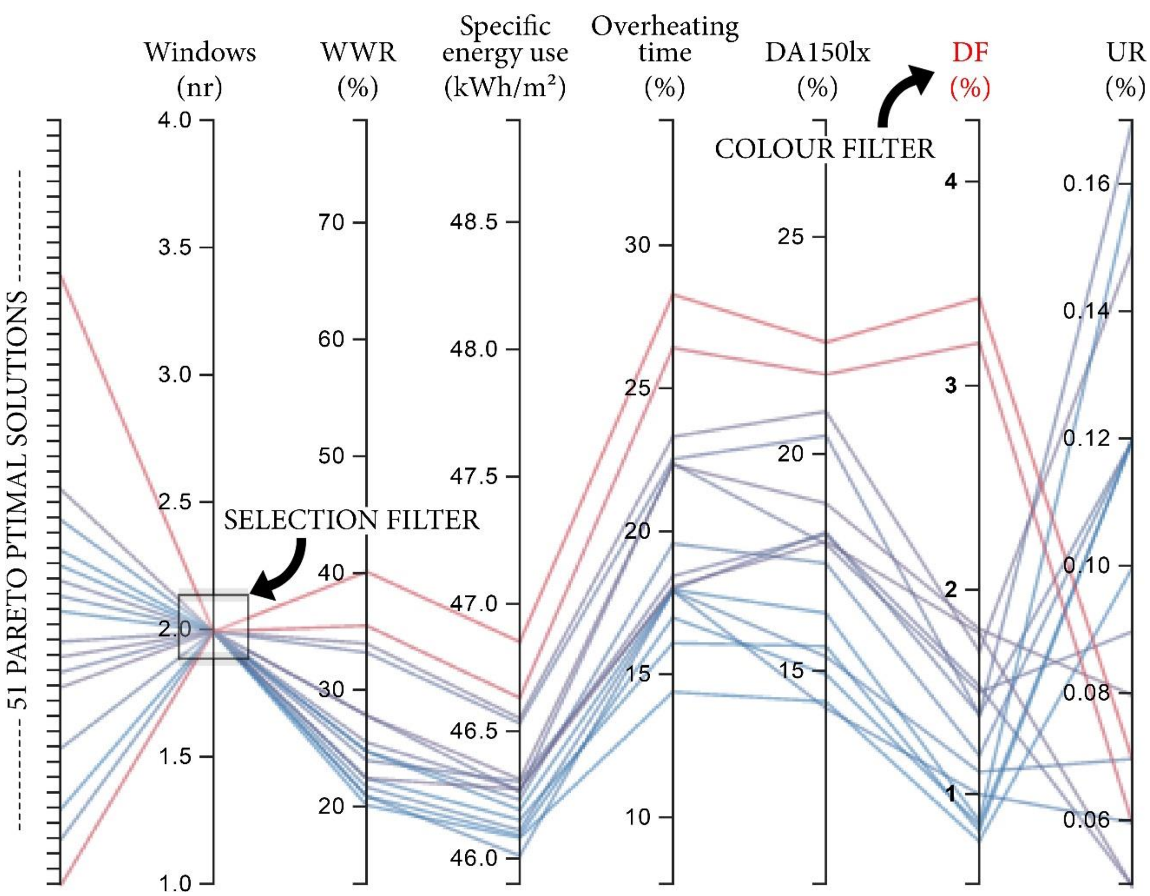

Figure 15: Pollination example for selecting the two-window designs out of the 51 Pareto optimal solutions.

A final choice was made between 51 Pareto optimal designs for heating and daylighting, and 48 Pareto optimal designs for Daylighting and overheating based on the following criteria:

For designs with **two windows**:

- The solutions with the highest possible uniformity ratio UR.
- The solutions that achieve the BREEAM criterion for an average DF of 2,1 %.
- The solutions with the highest DA150lx and the lowest overheating time
- The solutions with the lowest heating demand and the lowest overheating time.

For designs with **three windows**:

- The solutions that achieve the BREEAM criterion for an average DF of 2,1 % and have the highest possible uniformity ratio UR.
- The solutions that achieve the BREEAM criterion for an average DF of 2,1 % and have the lowest possible overheating time.
- The solutions that induce the lowest possible specific energy use and have the highest possible DA150lx.
- The solutions that achieve the BREEAM criterion for an average DF of 2,1 %, have a high UR and the lowest possible overheating time.

3 Results

The results are presented in two parts. The first part includes the preliminary results that were derived in order to set up and validate the simulation model (Preliminary results). The second part regards the analysis for the Bedroom and the Living Room zones. This part presents all fenestration design aspects considering the dependent and independent variables under study.

3.1 Preliminary results

A few preliminary tests had to be performed in order to set up specific conditions for the whole study. These tests concerned mainly:

1. The optimum measurement grid for the daylight analysis.
2. The optimum model geometry and input settings for accurate thermal calculations.

3.1.1 Measurement grid study results

The purpose of this study was to obtain an adequate combination of grid density and number of ambient bounces, in order to achieve low simulation run times without compromising the accuracy of the results. Figure 16 shows the DA150lx values for all simulated cases and their variability outside the upper and lower quartiles. The cases are compared with the Reference case DA150lx. This case corresponds to a 0,25 m grid density and 6 ab, which took 22 minutes of simulation run time on the authors computer (see *APPENDIX E* for computer specifications).

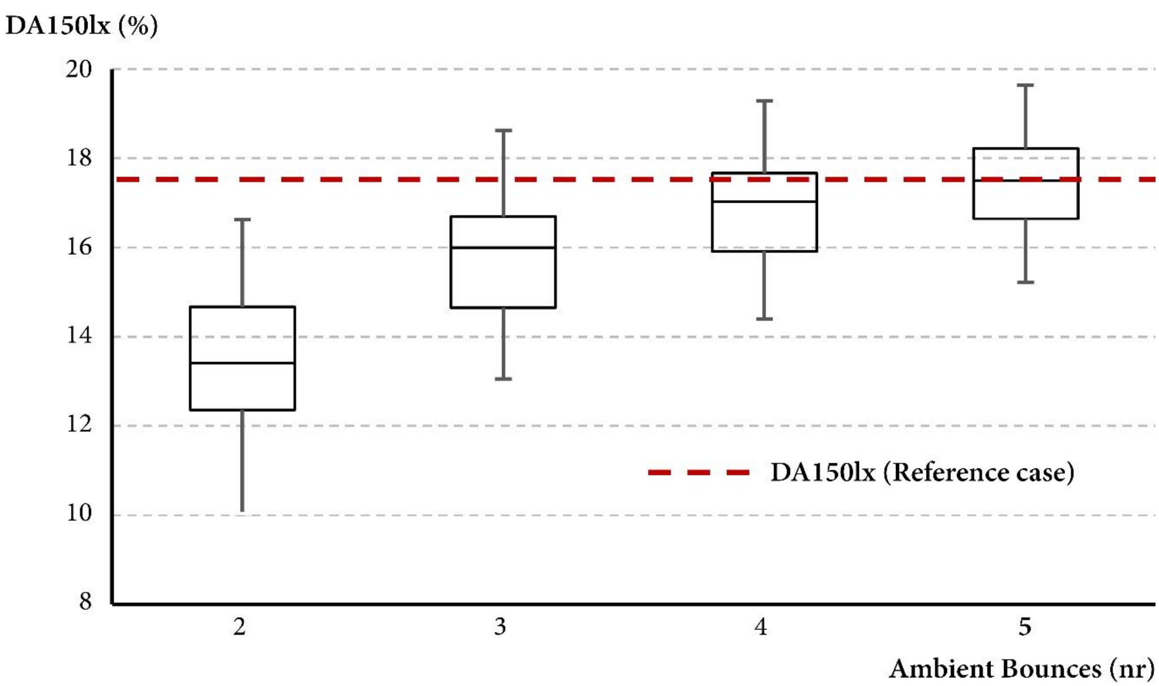

Figure 16: Box plot of DA150lx for different ambient bounces values (27 cases for each value).

The number of ambient bounces has a high impact on the accuracy of the results, due to the geometrical complexity of the studied space. As the number ambient bounces increases, DA150lx increases as more light reaches the back of the room. Sufficient daylight penetration through the exterior balconies cannot be modelled with less than 4 ambient bounces. The variability in the results of DA150lx is reduced when using 4 or 5 ambient bounces, with the latter showing an almost even distribution centered around the Reference DA150lx. Still the choice of 4 ab seems sufficient if only monitoring the DA150lx.

The DA150lx does not provide sufficient information to determine the settings to be used. A low deviation (ΔDA150lx) could be the result of high positive and negative discrepancies that sum up to a low overall value. A better monitoring approach consists of calculating the volumetric difference ΔVol simultaneously, which ensures that the sum of absolute discrepancies is also low. Table 14 illustrates this, showing the ΔVol and the ΔDA150lx. Cases that provide both ΔDA150lx and ΔVol at minimum levels were the ones considered. The final decision was made based on the relative simulation time, which is the percentage of the Reference case simulation time (Tref).

Table 14: ΔVol, ΔDA150lx and relative simulation time for each combination of grid size, ambient bounces and window position.

Tref =22 min		Volumetric difference ΔVol and simulation time as a percentage of Tref															
Amb. bounces		2				3				4				5			
Win. Position		Lo*	Me*	Hi*	Time	Lo*	Me*	Hi*	Time	Lo*	Me*	Hi*	Time	Lo*	Me*	Hi*	Time
Grid size (m)	0,50	6	9	14	21%	4	3	6	51%	3	3	3	59%	3	2	2	60%
	0,75	7	7	13	10%	4	5	6	38%	4	5	4	49%	4	5	4	51%
	1,00	6	9	12	8%	9	10	7	33%	11	12	5	44%	9	10	5	46%
	1,25	8	11	10	7%	11	13	9	29%	10	14	8	40%	11	16	7	42%
	1,50	10	20	16	5%	9	15	15	24%	9	13	14	34%	11	13	15	36%
	1,75	10	20	16	5%	9	15	15	24%	9	13	14	34%	11	13	15	36%
	2,00	11	24	13	4%	10	17	12	24%	9	16	10	34%	9	16	10	35%
	2,25	21	18	13	3%	21	18	13	17%	21	18	13	27%	21	18	13	29%
	2,50	21	18	13	3%	21	18	13	17%	21	18	13	27%	21	18	13	29%
		Difference ΔDA150lx															
Grid size (m)	0,50	25%	26%	34%		11%	12%	16%		5%	5%	7%		2%	2%	2%	
	0,75	26%	24%	36%		12%	9%	17%		6%	4%	9%		4%	1%	3%	
	1,00	23%	21%	36%		6%	4%	15%		3%	0%	8%		0%	-4%	3%	
	1,25	20%	17%	30%		7%	3%	16%		3%	-2%	8%		0%	-5%	2%	
	1,50	18%	14%	28%		9%	2%	12%		5%	-1%	2%		1%	-2%	-4%	
	1,75	18%	14%	28%		9%	2%	12%		5%	-1%	2%		1%	-2%	-4%	
	2,00	13%	11%	25%		5%	-1%	12%		2%	-2%	3%		-1%	-3%	-4%	
	2,25	16%	5%	15%		5%	-7%	-2%		-1%	-11%	-10%		-5%	-13%	-16%	
	2,50	16%	5%	15%		5%	-7%	-2%		-1%	-11%	-10%		-5%	-13%	-16%	
Ref.DA150lx/%		17,5	17,5	15,7		17,5	17,5	15,7		17,5	17,5	15,7		17,5	17,5	15,7	

*Window position - Lo: Low, Me: Medium, Hi: High

ΔVol is mostly dependent on the grid size and ΔDA150lx is influenced mainly by the amount of ambient bounces. ΔVol is less for high grid densities, though the highest inaccuracy occurs for grids larger than 1 m. Cases using 2 or 3 ab show high discrepancies in both the criteria of ΔDA150lx and ΔVol. Cases using 4 ab show a satisfactory performance in both criteria only when very dense grids are selected. These grid sizes induce simulation times that are almost similar to using 5 ab. The latter yield more accurate DA150lx results, as shown in Figure 16.

In order to ensure the validity of the results, 5 ab was the only secure choice. According to Table 14, using 5 ab and a 0,5 m grid ensures the highest accuracy, but induces the longest simulation time. For this thesis workflow, which included approximately 4000 simulations, 5 ab with a grid density of 1 m was the optimum choice. Figure 17 shows the deviation of this case from the Reference case, for the different window positions.

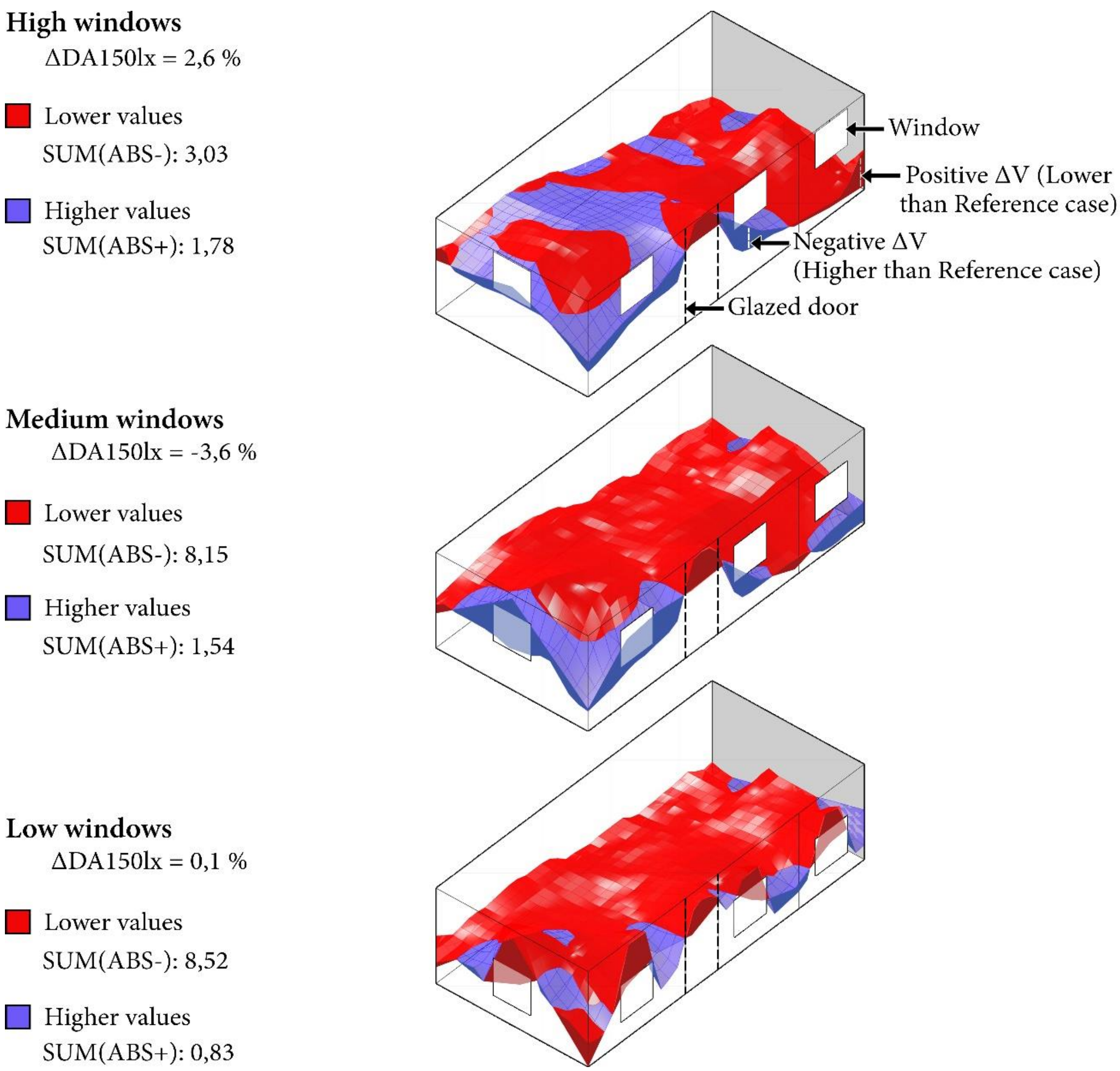

Figure 17: Discrepancies when using 5 ab and 1 m grid density, for the different window positions.

The discrepancies differ slightly between window positions. In the cases of low and medium positions, the DA150lx is mainly lower than the Reference case, uniformly across space. Higher deviations occur close to the external walls, and between window openings. In the case of high window placement, the DA150lx is lower in the back of the living room (close to the kitchen). This is due to the obstructions in front of that area (external balconies). Nevertheless, the discrepancies are low and were therefore considered within the acceptable range of error. Overall, the validity of the model was not compromised, and the simulation time was reduced to less than half.

3.1.2 Energy model validation results

Figure 18 shows the annual heating energy calculation in Designbuilder and Honeybee for the different geometries and simulation settings used. The purpose was that the construction, the admittance of solar gains, the generation of sensible heat gains and infiltration of the outdoor air are modelled in the same way. Figure 18 shows that the Honeybee results were consistently lower by a small amount. The largest discrepancy of 3 % occurred for construction settings, due to slightly different U-Value calculation methods between the two software. This was overcome when the adjacencies corresponding to the final model were set, as the adiabatic condition behaves the same in both software. For the rest of the settings, the discrepancy was constantly below 1,5 %, which was considered sufficiently accurate to accept Honeybee as a valuable simulation tool for this study.

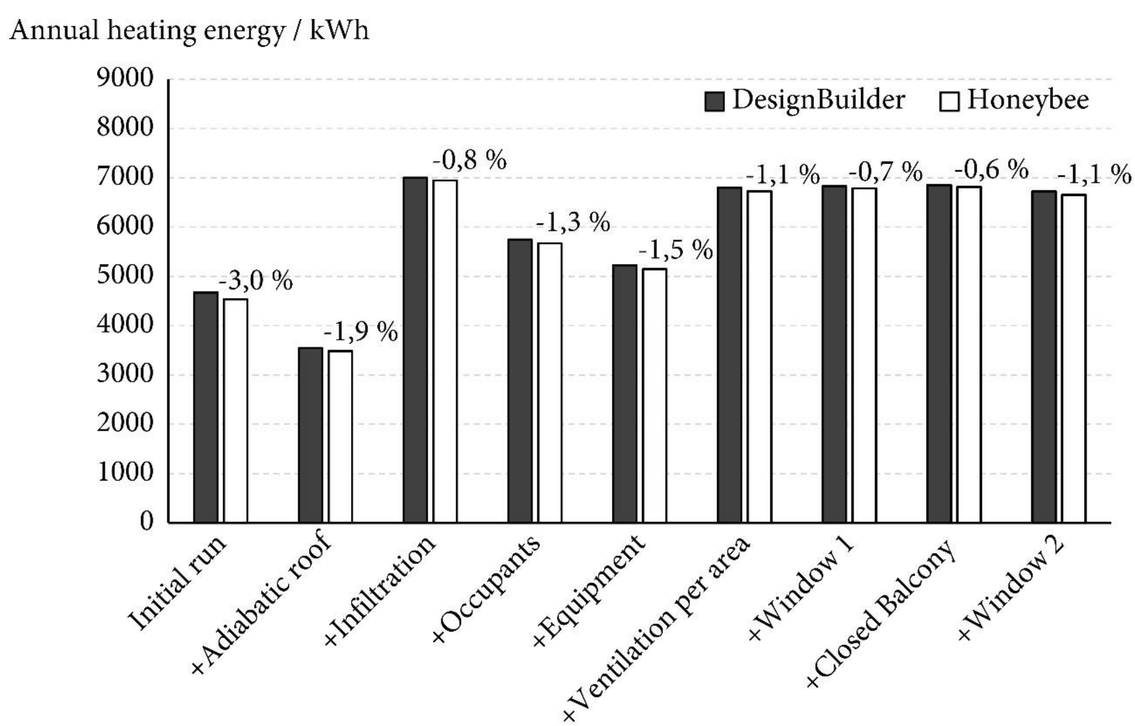

Figure 18: Difference in annual heating energy between Designbuilder and Honeybee simulations, for the different geometries and simulation settings.

3.2 Results

The results for the bedroom and living room zones are presented in different sections, depending on the variable under consideration. The bedroom results focus more on the effect of the orientation and the window geometry (WWR, head height and height-to-width ratio). The Living room study focuses more on the effect of the number of windows used, and their position on different fenestration zones.

3.2.1 Daylighting and heating demand optimization

BEDROOM

Figures 19 shows the performance of different WWR choices and Figure 20 shows the corresponding 20 optimal solutions in terms of light dependency and heating demand, for a north oriented bedroom. A solution is called Pareto optimal if none of the objectives can be improved, without degrading the other objective. It is shown that the light dependency is not a linear function of the percentage of glazing on the façade (Figure 19). Specific cases with a WWR ranging from 10 % to 20 % can actually admit more daylight than some cases ranging from 30 %-40 %. This is a result of the window position and the window height-to-width ratio, described further down. On the other hand, the annual heating demand displays a more straightforward correlation with the WWR. Larger window areas yield a higher energy use for heating, as the overall façade U-value increases with the addition of more glazing. Note that increasing the WWR beyond 30 % - 40 % results in a significant increase in heating demand for a negligible reduction in LD, as demonstrated by previous studies.

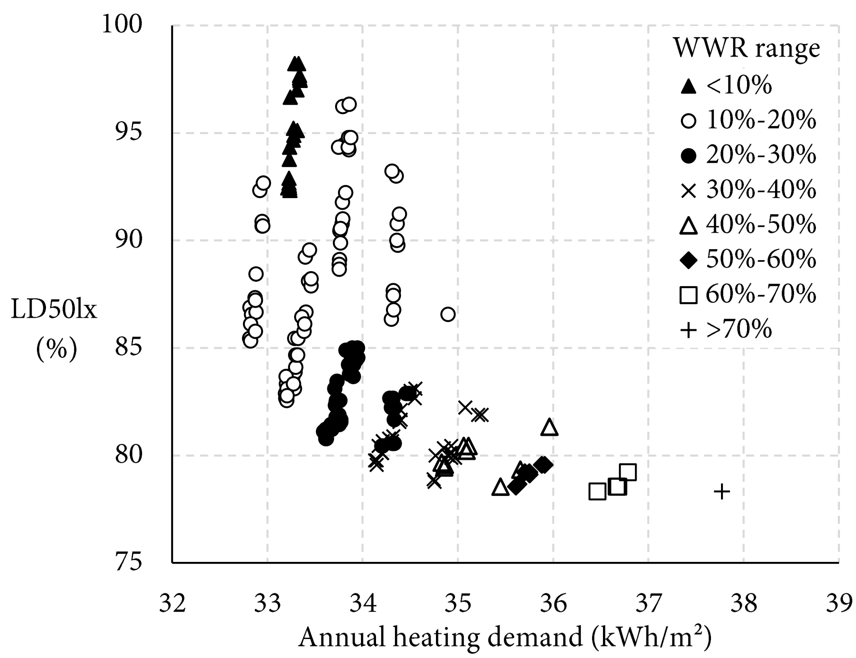

Figure 19: Relation of LD and annual heating demand for different WWR for North orientation.

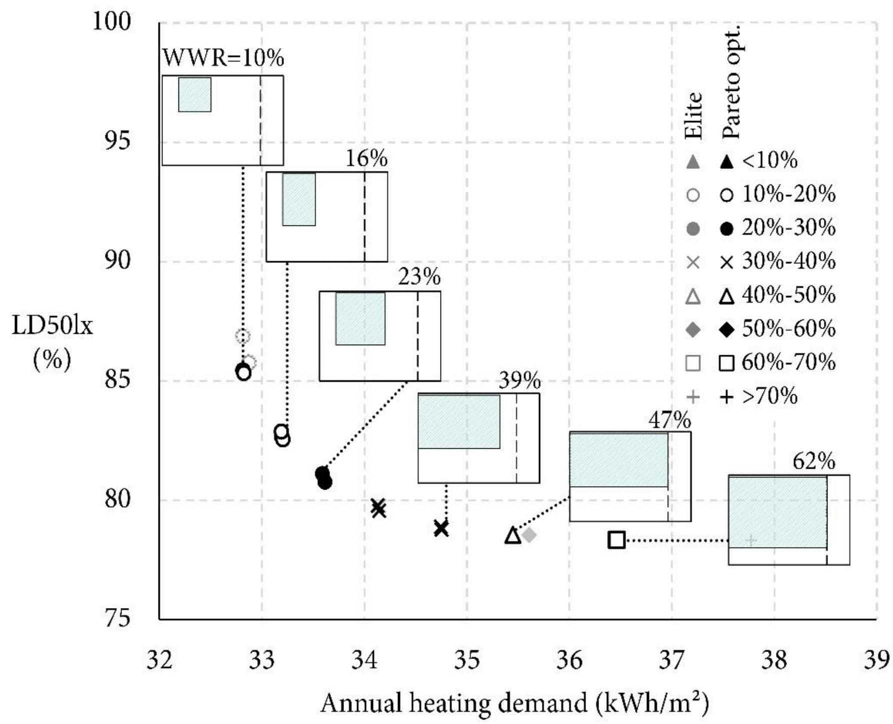

Figure 20: Pareto optimal and elite cases (20 in total) for the optimization of LD and annual heating demand on the North orientation.

The long Pareto front on the north orientation indicates the high conflict between the objectives. The optimum WWRs range from 10 % to 62 %. All windows are placed high on the façade, and are mostly occupying the left side of it (seen from outside), as the room is 8,0 º inclined to the west. Left placed windows are also utilizing the interior surfaces reflectance for light distribution inside the bedroom more, since the walls have a higher reflectance than the wardrobe.

For a south oriented room (Figures 21 & 22), the best choice is to use the highest possible WWR, equal to 78 % in this case. This can be explained by the fact that a higher WWR for south can be used to exploit passive solar gains, as shown further down. As for the consequences on the indoor operative temperature, this is studied further down. Contrary to the north, the minimum number of Pareto optimal solutions indicates that the objectives of daylighting and heating are not in conflict in south. Increasing the WWR results in minimizing both objectives. Moreover, the heating performance of all cases on the south is better that any case on the rest of the orientations. The difference in heating demand as a function of WWR is higher, indicating that the energy used for heating is more sensitive to the WWR choice for this orientation.

A WWR of 78 % is a choice based only on minimizing the heating energy use and maximizing the daylight levels. Considering the overheating time, one could argue that shading is necessary, with a corresponding impact of the light dependency and the utilized solar gains. Note that when the overheating occurs, the occupant will normally also want lower daylight levels (as in warm countries people in e.g. Greece do not want to have full daylight when it is hot outside).

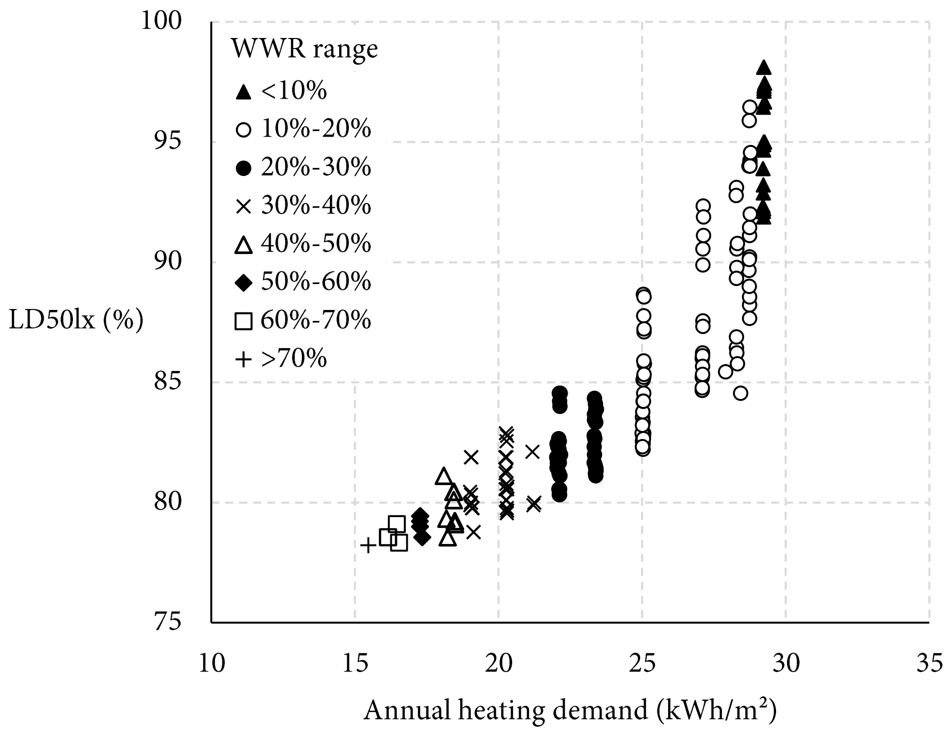

Figure 21: Relation of LD and annual heating demand for different WWR for South orientation.

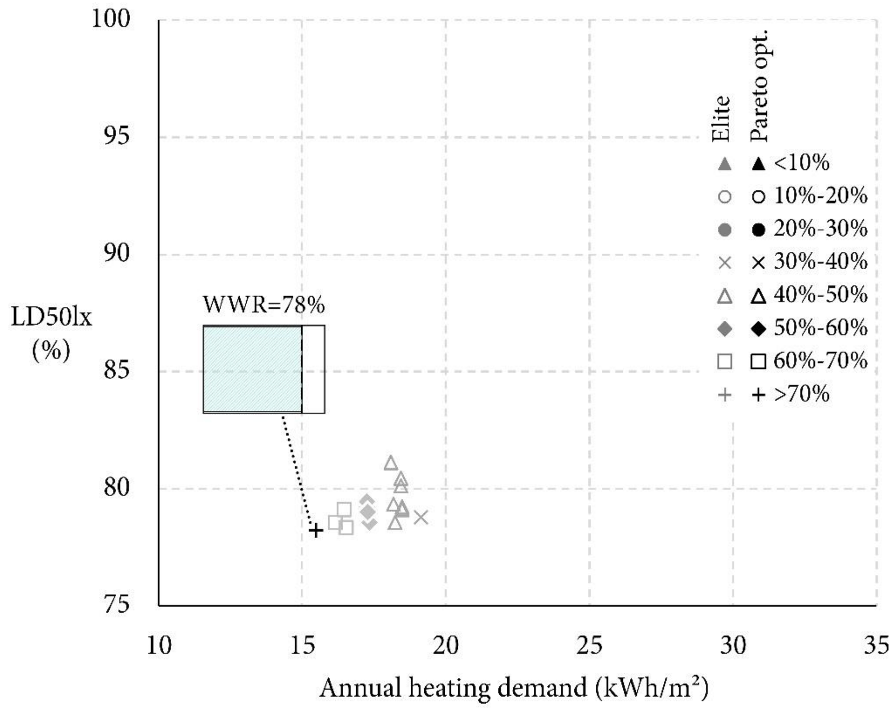

Figure 22: Pareto optimal and elite cases (20 in total) for the optimization of LD and annual heating demand in the South orientation.

For the east orientation, the optimum trade-off between the objectives is achieved for WWRs between 42 % and 62 % (Figures 23 & 24). The least efficient designs are those of a WWR equal to 16 % or less. As the WWR increases, the heating demand is reduced, but only until a WWR in the range of 40 % to 50 %. From that point on, adding more glazing increases the heating demand.

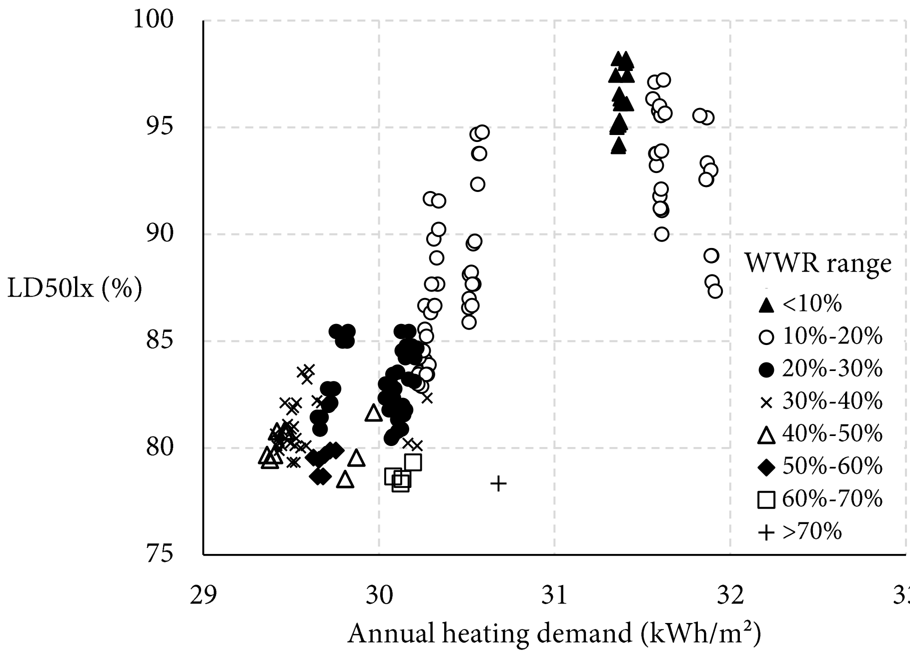

Figure 23: Relation of LD and annual heating demand for different WWR for East orientation.

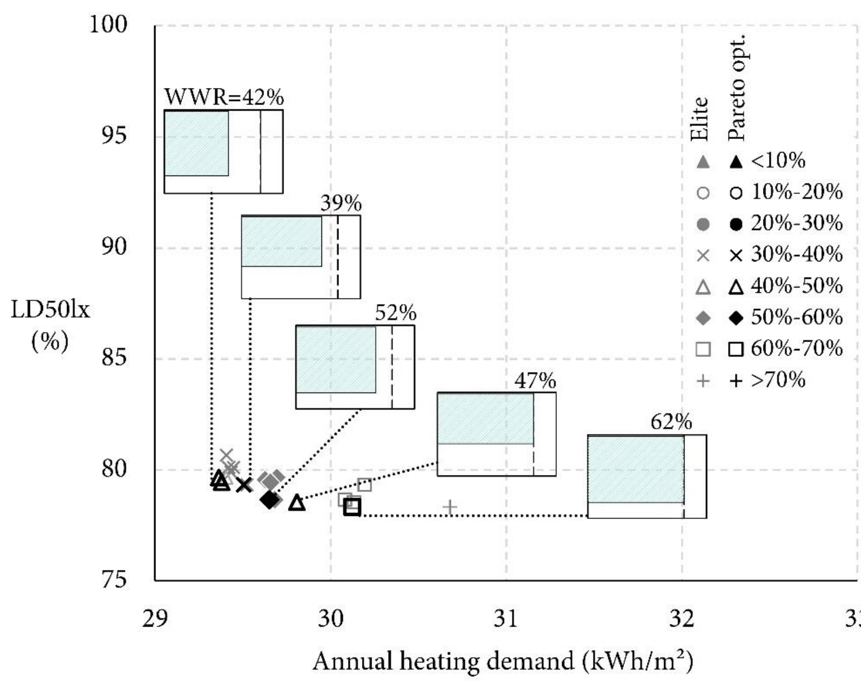

Figure 24: Pareto optimal and elite cases (20 in total) for the optimization of LD and annual heating demand in the East orientation.

The pattern is similar for a west oriented room (Figures 25 & 26), but all designs have a lower light dependency compared to the east because occupancy occurs in the evening. The difference in the light dependency is more evident for lower WWRs, when Figures 23 and 25 are compared.

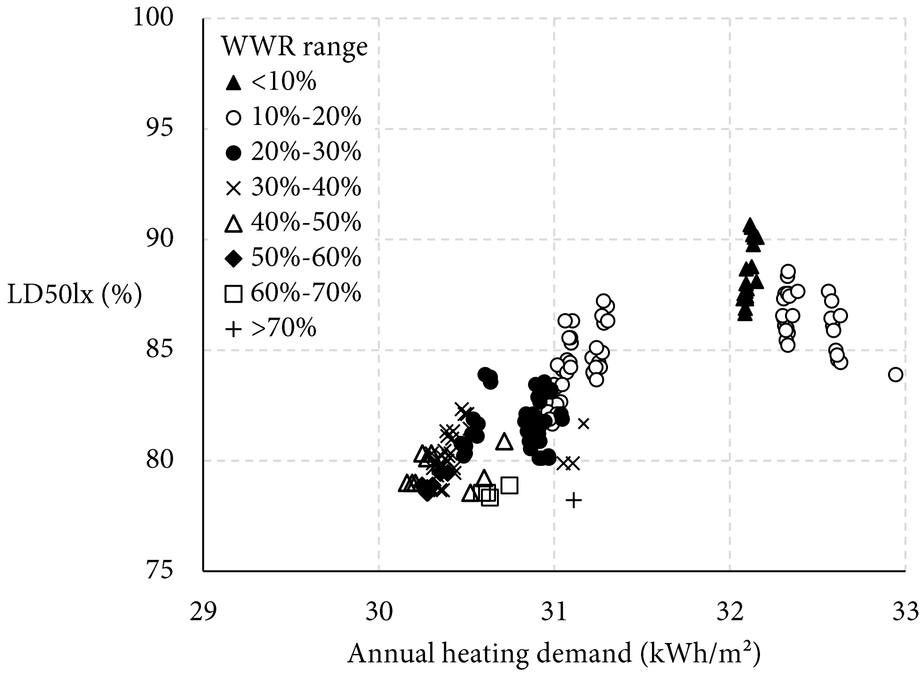

Figure 25: Relation of LD and annual heating demand for different WWR for West orientation.

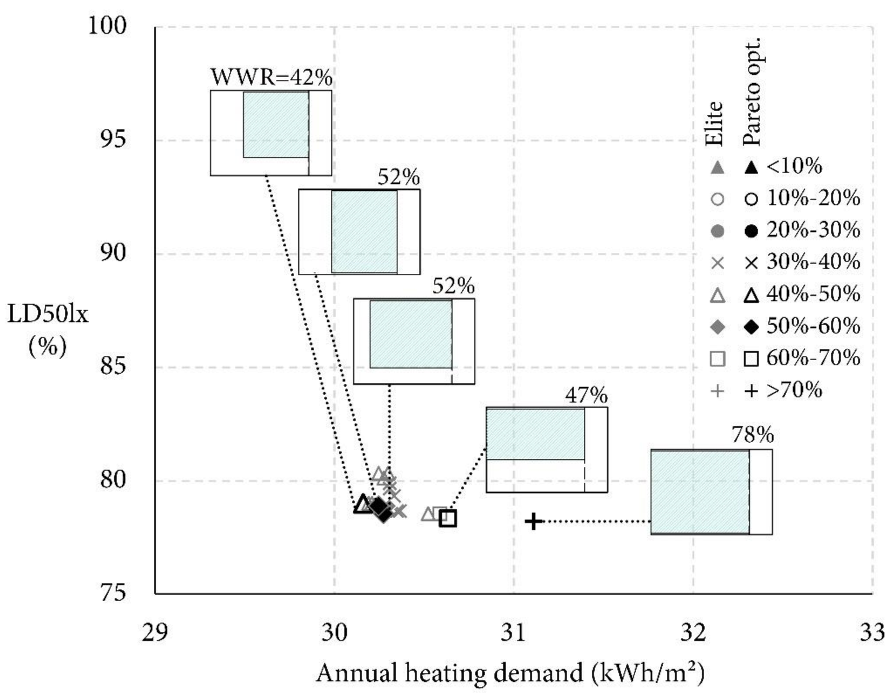

Figure 26: Pareto optimal and elite cases (20 in total) for the optimization of LD and annual heating demand in the West orientation.

Placing the bedroom on the east results in a slightly lower heating demand compared to the west. On the other hand, the light dependency is lower on the west, as the bedroom was assumed occupied from 22:00 to 00:00 hours, when the sun is mostly on the west side throughout the year. For both east and west, WWRs below 16 % are not performing well for none of the objectives. For WWRs larger than 50 %, the light dependency is slightly reduced, whereas the thermal performance deteriorates, as the solar gains cannot compensate for the heating losses due to the increased window size. Finally, it was shown that east-facing windows are better off placed on the left side of the façade (seen from the outside), while the optimum position on the west is on the right side.

Figure 27 shows the 20 best performing cases for each orientation. It is shown that the light dependency reaches the same minimum of approximately 78 % on all orientations. For north and south, the heating demand is more sensitive to the window choice compared to the east and west. The daylight levels are more affected by the window size and position for a north oriented bedroom.

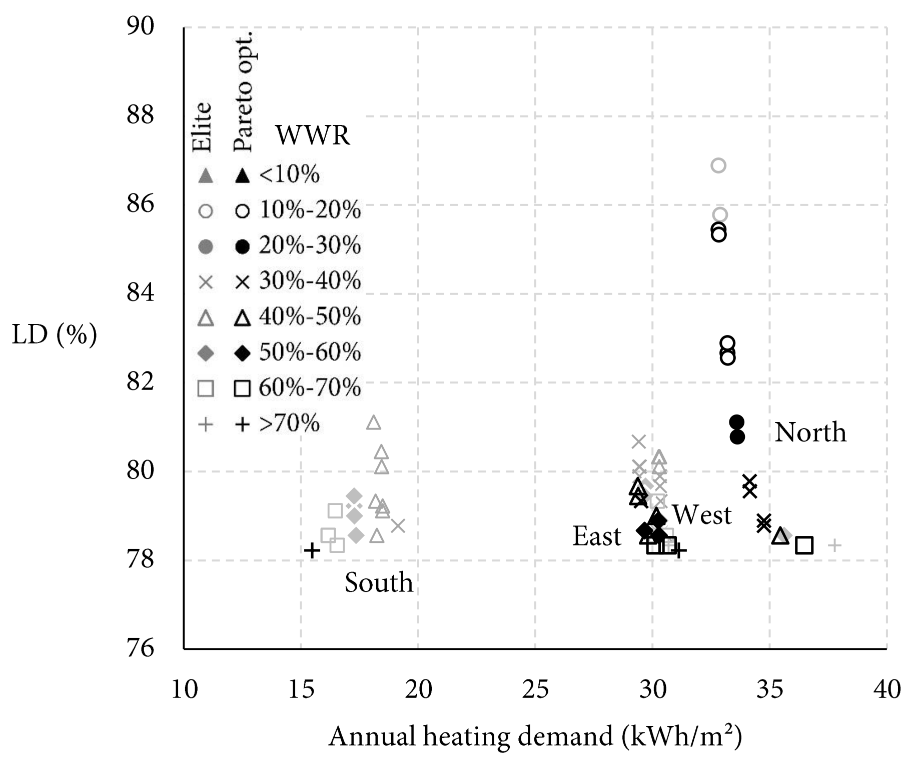

Figure 27: Pareto optimal and elite cases (20 in total) for the optimization of LD and annual heating demand for each orientation.

An overview of the Pareto optimal cases for each orientation is illustrated in Table 15 below. It is shown that there is a higher number of possible design solutions for north facing windows, with a maximum WWR of 62 %. For the east and west orientations the optimum WWR approximately ranges from 40 % - 50 %. On the south, the highest WWR of 78 % is the optimum choice.

Table 15: Pareto optimal fenestration designs in order to maximize DA50lx and minimize annual heating demand of the bedroom for each orientation.

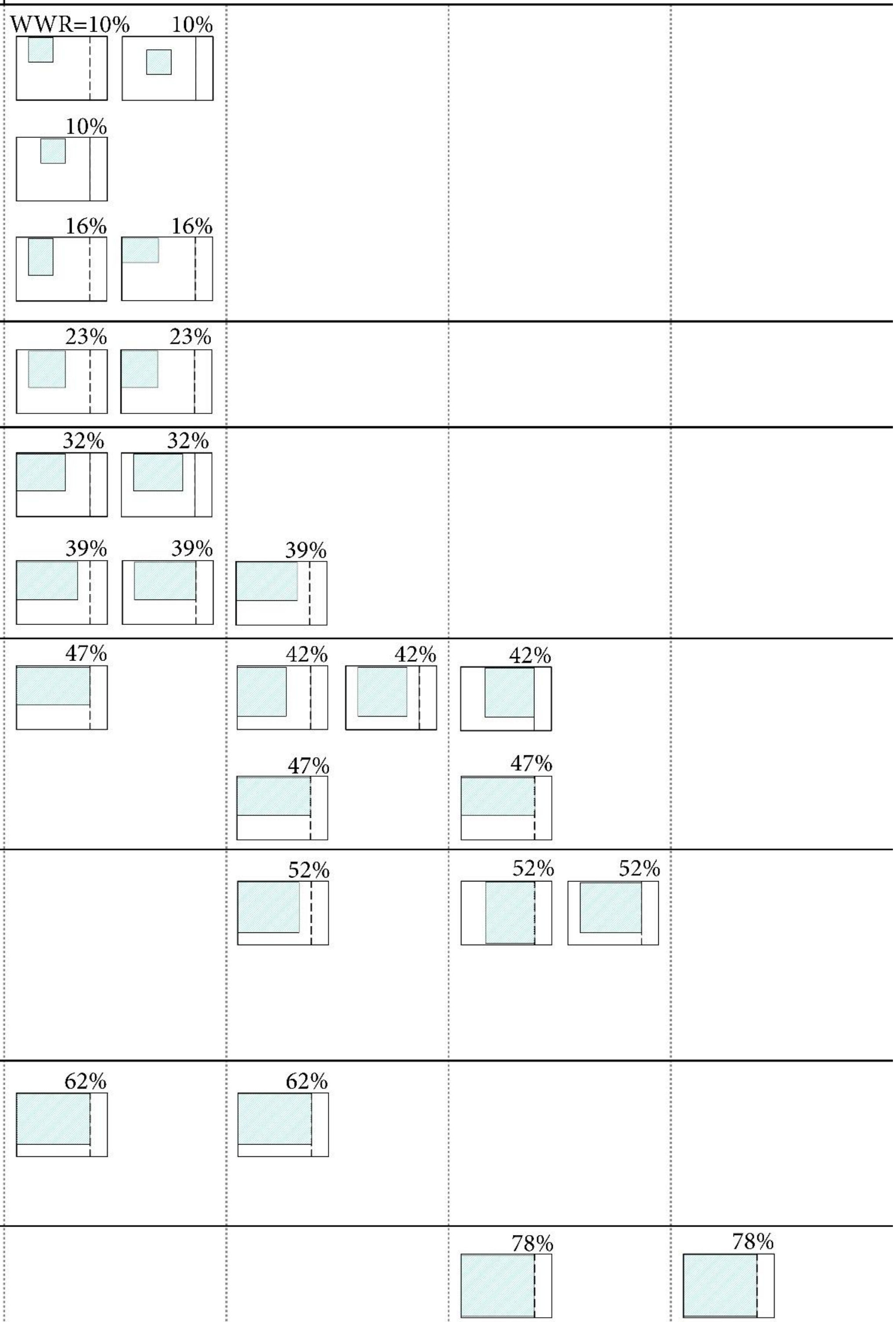

WWR	Orientation: NORTH	EAST	WEST	SOUTH
10% - 20%	WWR=10%, 10%, 10%, 16%, 16%			
20% - 30%	23%, 23%			
30% - 40%	32%, 32%, 39%, 39%	39%		
40% - 50%	47%	42%, 42%, 47%	42%, 47%	
50% - 60%		52%	52%, 52%	
60% - 70%	62%	62%		
>70%			78%	78%

Examining Table 15 one can see that all designs involve windows with the highest possible head height, at 2,55 m. This independent variable affects the daylight penetration inside the room, as it is described further down. Moreover, the optimum windows have a shape that tends to be squared, in other words, the height-to-width ratio of these windows is close to 1,0. For a north orientation, the majority of the Pareto optimal solutions have a WWR that is lower than 40 %. For east and west, a WWR of approximately 40 % to 50 % achieves the optimum trade-off between the objectives, while on the south, the window opening has to be the maximum possible (WWR = 78 %).

Figure 28 shows the DA50lx as a function of the annual heating demand for all simulated cases. Daylighting and heating are conflicting on the north, whereas on south increasing the daylight levels yields a decrease of the heating demand. The most interesting trends appear on the east and west orientations, where decreasing the heating demand leads to a decrease on the DA50lx until a certain point. For specific window designs, it is possible to maximize DA50lx and achieve a low heating demand at the same time. The west orientation shows the highest performance on the DA50lx for most window alternatives, whereas the south orientation is better for a low annual heating demand.

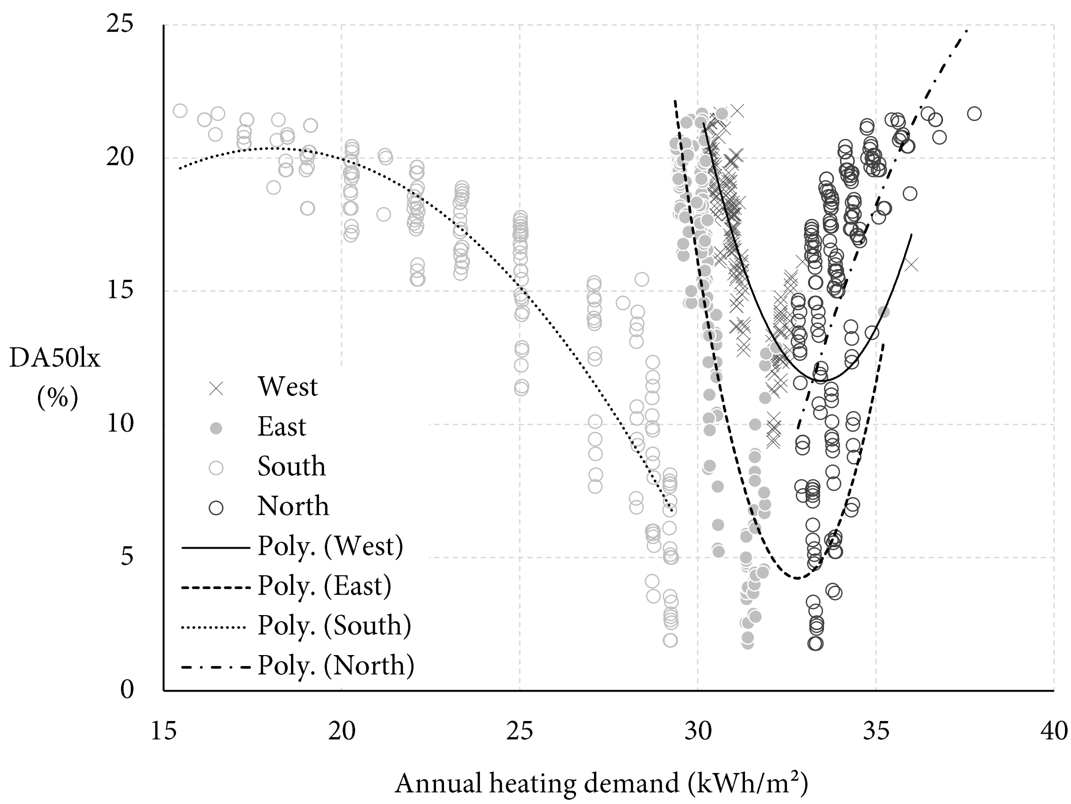

Figure 28: DA50lx as a function of the annual heating demand for all window alternatives on each orientation.

Figure 29 shows the correlation of the annual heating demand with the DF for each orientation. It is shown that an east oriented bedroom can achieve a lower energy use for equal DF levels, compared to the west. This result can be somewhat misleading, in choosing east over west, as the DF remains the same regardless of the orientation. In the case of the light dependency LD, which is climate-based, the west orientation was shown to perform better on daylighting compared to the east.

Achieving a DF of 2,1 %, as per the BREEAM (2014) minimum requirement results in a different energy use for heating, depending on the orientation. It is shown that the DF requirement is reached for a WWR over 30 %. For the same window choice of e.g. 32 % WWR (circled case in Figure 29), the heating demand is 30,2 kWh/m² on east, 31,1 kWh/m² on west, 20,9 kWh/m² on south and 34,9 kWh/m² on north.

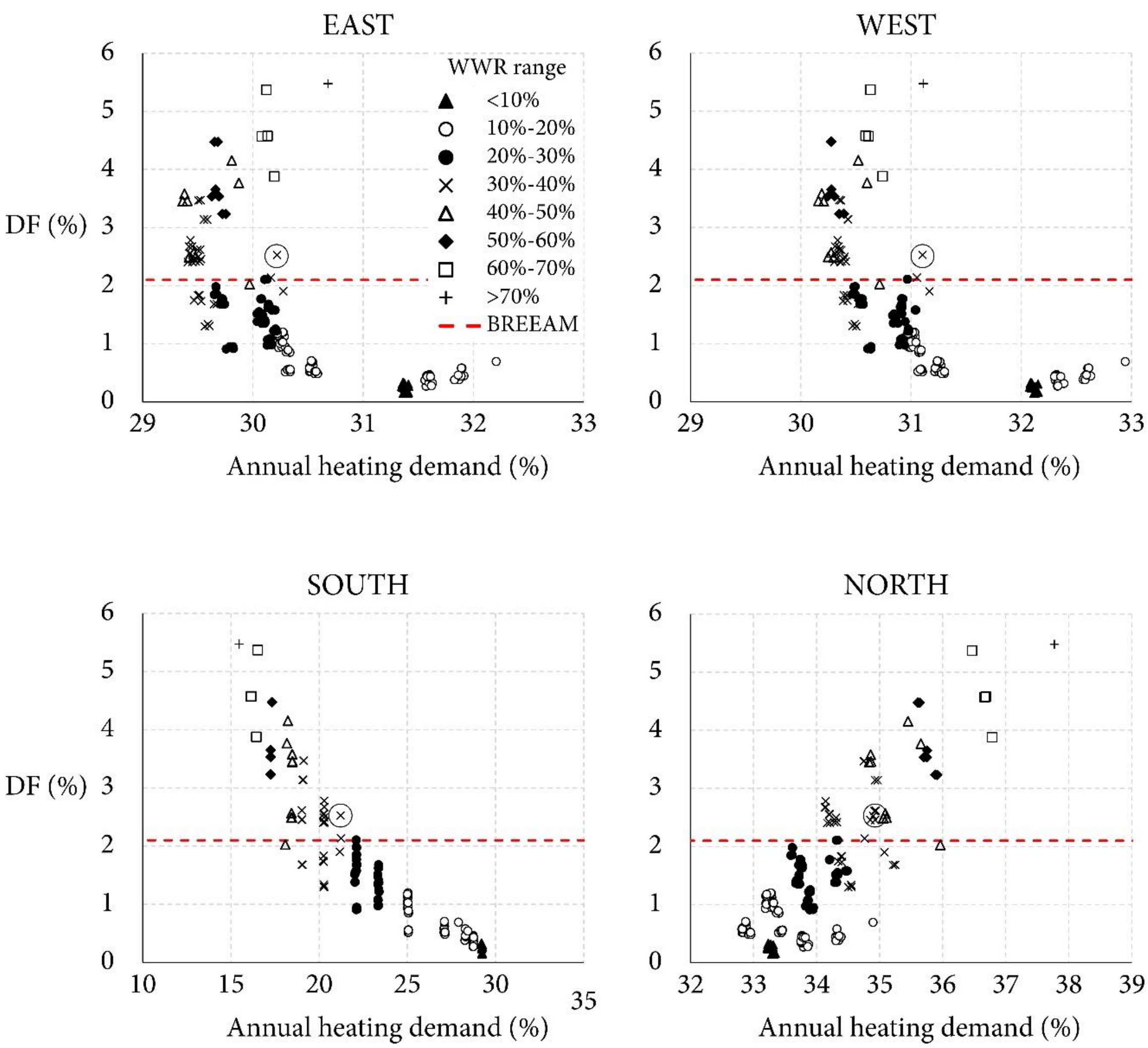

Figure 29: DF and annual heating demand of the bedroom for each orientation, as a function of the window-to-wall ratio.

Figure 30 shows the point DF as defined by the Green Building Council (Miljöbyggnad, 2016) and the corresponding annual heating demand for all window alternatives. For each orientation, only a 10 % of the window alternatives exceeds the set requirement of a point DF equal to 1,2 %. On average, a northern bedroom must have a heating demand of at least 34 kWh/m² in order to satisfy the daylight criterion. For south, east and west the corresponding values are 18 kWh/m², 29 kWh/m² and 30 kWh/m² respectively.

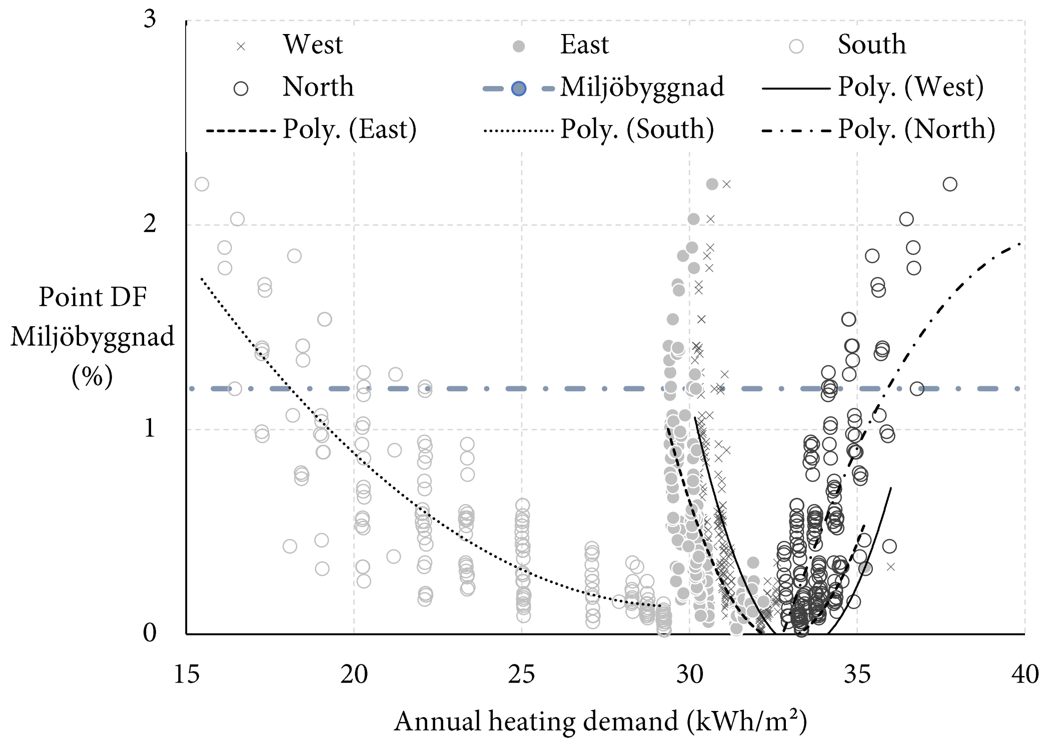

Figure 30: Correlation of the annual heating demand and the point DF defined by the Green building Council, for all window alternatives.

LIVING ROOM

The living room study presented here includes mainly the west-facing apartment (*apartment 1*). The results of the study on the east apartment are only presented whenever a comparison between the two orientations is considered necessary, hence, whenever there are considerable differences.

Figure 31 shows the evolution of the optimization algorithm in finding the optimum solutions in terms of daylighting and specific energy use. Daylighting includes only the living room zone, while the specific energy use considers the total apartment. The process is illustrated here for every fifth generation, until the 20th generation is reached, when the solutions formed the final Pareto front (black crosses).

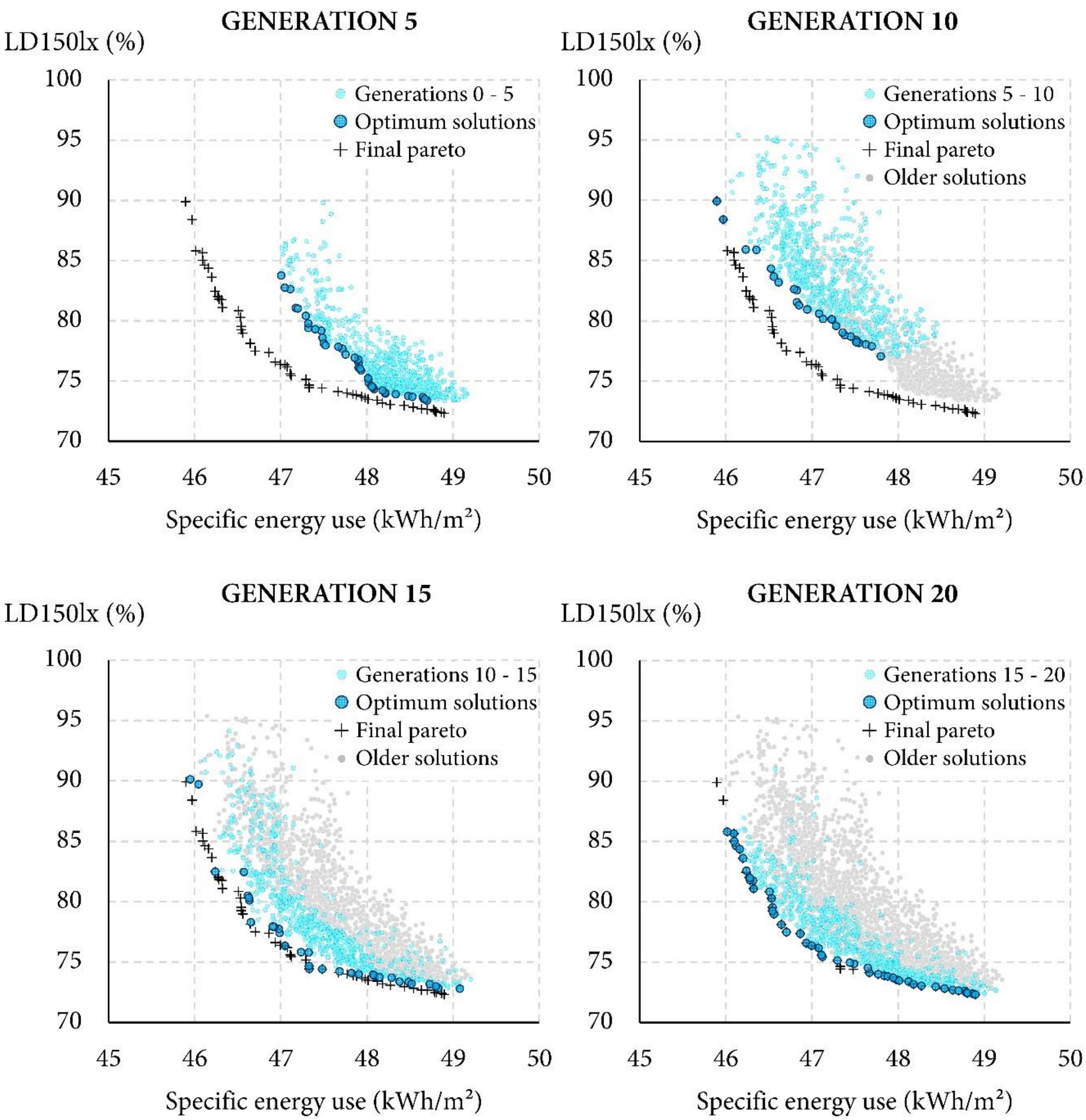

Figure 31: The solution space after generations 5, 10, 15 and 20, during the optimization of LD150lx and the specific energy use for the west apartment.

The upper left chart shows that during the initial five generations, the optimization algorithm was bounded in local optima (bottom right of the Pareto front). In other words, it was generating highly glazed designs, due to their good performance (only) in terms of LD150lx. In the next five generations, the WWR boundary rule was applied, in order for the algorithm to explore parts of the solution space for which the specific energy use is lower. Designs with a WWR higher than 50 % were not allowed until the end of the 10th generation. After that, the algorithm proceeded from the 11th to the 20th generation considering all possible fenestration sizes. It is shown that the evolution of the optimum solutions is higher in the beginning, whereas it is not significant between the 15th and the 20th generation. For this reason, the process was terminated after the 20th generation.

Figure 32 shows the 51 Pareto optimal solutions and their corresponding WWR. A thumbnail (phenotype) is superimposed for each range of WWR. Examining the phenotypes leads to interesting findings: When a low WWR is to be used (10 % - 20 %), fenestration zone F3 is utilized by the algorithm. This zone is not as shaded by the balcony as F4 or F5. Increasing the WWR leads the algorithm to generate solutions where F3 and F5 are combined, thus a wide spread window allocation and west-oriented windows are preferred for daylighting and heating respectively. When larger glazing areas (WWW > 35 %) are required, the algorithm populates the north façade (F2) for the first time in the Pareto front. The F2 window is placed high and not in contact with the F3 window, for more daylight distribution with the least possible glazing area. Although utilizing the northern façade improves the daylighting performance, it also yields a higher energy use for heating. Examining the highly glazed designs, it is evident that only for very high WWRs does the algorithm populate fenestration zone F4. The existence of the glazed balcony door (grey hatch on phenotypes) was already providing daylight close to that area, and the balcony over F4 has a negative effect: Any window placed on that zone will be contributing more to the thermal losses than the daylight gains. Finally, there is a negligible increase in daylighting gain when increasing the WWR beyond 50 %, but the heating demand increases significantly.

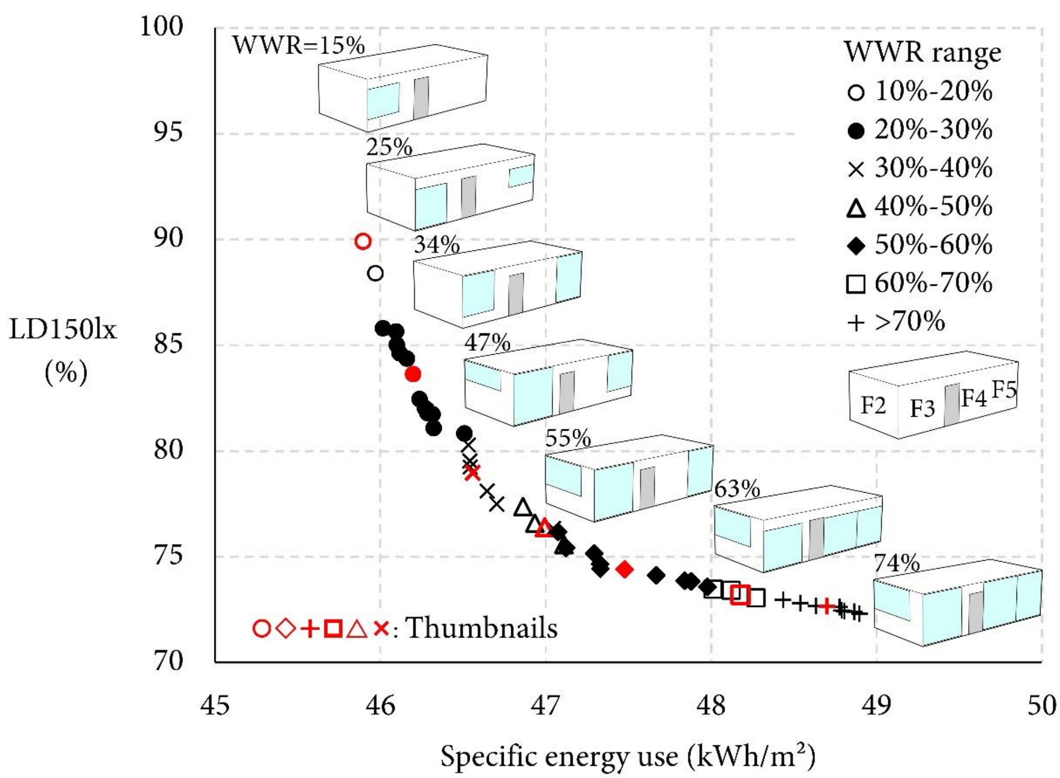

Figure 32: Pareto optimal solutions in terms of LD150lx and the specific energy use of the west apartment.

The following table shows the phenotypes of all the Pareto optimal solutions, per WWR range.

Table 16: Pareto optimal solutions for each WWR for the west apartment.

WWR	West
10% - 20%	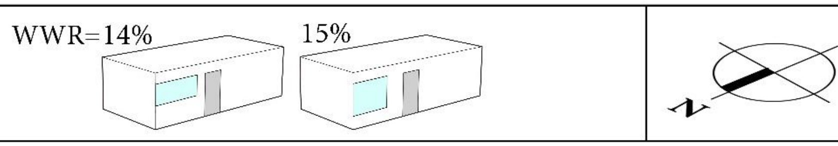
20% - 30%	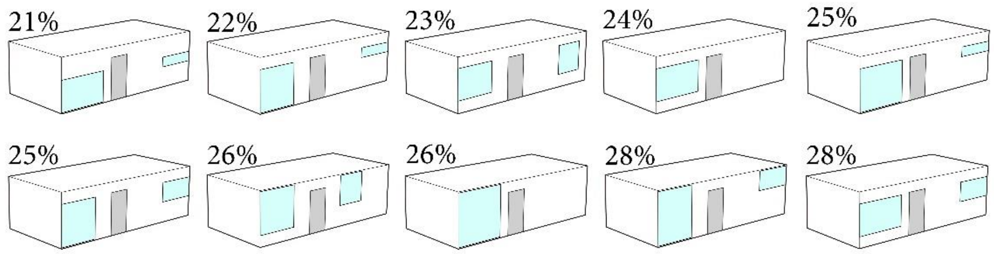
30% - 40%	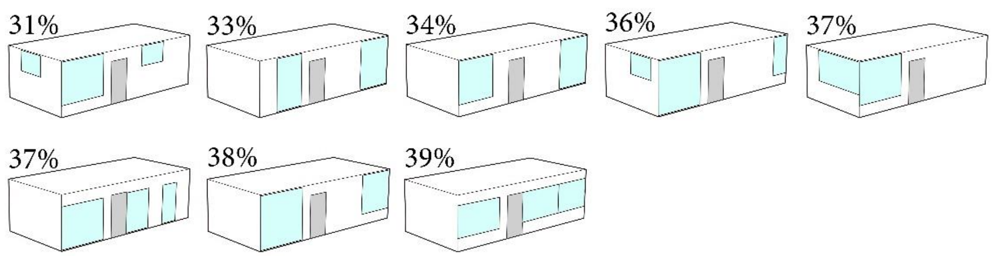
40% - 50%	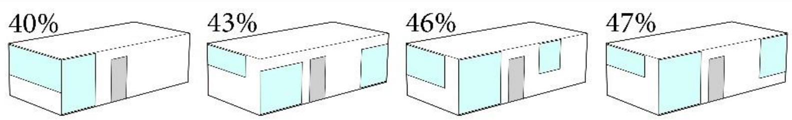
50% - 60%	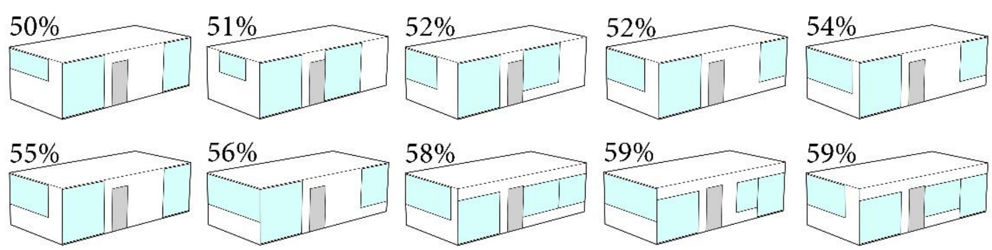
60% - 70%	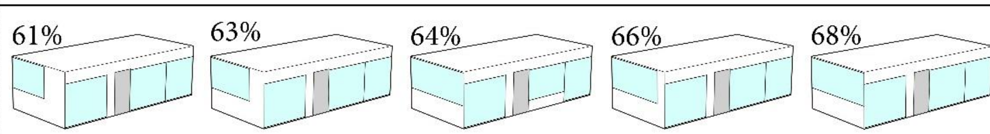
>70%	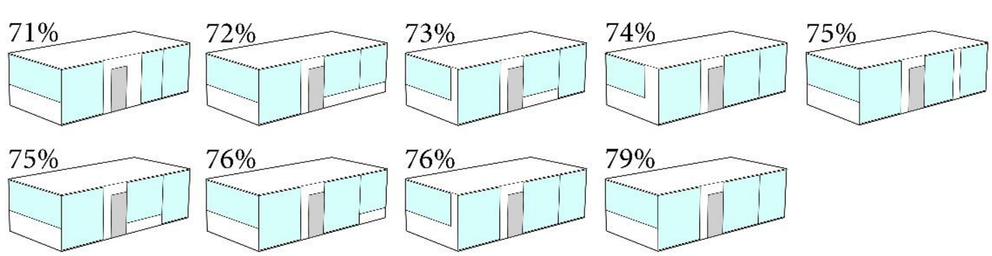

Table 16 illustrates the same narrative: West oriented openings are the optimum choice for small WWR, with the preference on fenestration zone F3. For WWR between 20 % and 30 %, the combination of F3 and F5 is the optimum design choice. A northern window is mostly generated for WWRs above 40 %, and fenestration zone F4 is populated for WWRs above 50 %. The majority of the windows is placed high on the façade and they are more square-shaped (height-to-width ratio ≈ 1).

3.2.2 Effect of independent variables

BEDROOM

The effect of the window head height and height-to-width ratio was examined for the bedroom, as there is no balcony shading to influence the results. Table 17 shows the daylighting performance of all cases for each orientation with respect to the window-head-height. The lighter values indicate higher DAs and thus a better performance.

Table 17: Percentage of simulated designs for which the DA50lx exceeded a given value, for different window head heights (all orientations included).

Head height		2,55 m				2,05 m				1,55 m			
Orientation		E*	N*	W*	S*	E	N	W	S	E	N	W	S
	1	100	100	100	100	100	100	100	100	100	100	100	100
	2	100	100	100	100	100	100	100	100	89	96	100	96
	3	100	100	100	100	94	100	100	100	87	87	100	87
	4	99	100	100	100	88	94	100	96	87	87	100	87
	5	94	100	100	100	76	91	100	94	85	87	100	87
	6	94	97	100	100	76	82	100	84	74	85	100	87
	7	88	96	100	96	76	81	100	82	70	85	100	83
	8	83	93	100	94	76	76	100	78	65	74	100	76
	9	83	90	100	90	73	76	100	76	57	74	100	72
DA50lx	10	83	86	100	86	73	76	100	76	54	63	89	67
(%)	11	83	83	100	83	69	75	100	76	52	57	87	63
	12	81	83	100	83	69	70	93	73	46	52	87	57
	13	81	83	94	83	63	67	76	69	39	46	80	50
	14	78	79	85	82	58	63	76	66	35	37	63	46
	15	76	76	83	79	51	58	70	60	30	35	50	35
	16	74	76	81	76	43	46	60	51	20	24	39	28
	17	65	68	76	74	39	39	49	43	9	17	20	20
	18	51	53	65	57	31	34	39	37	2	7	11	7
	19	43	43	50	43	21	22	27	22	0	0	2	0
	20	22	26	35	29	7	10	10	10	0	0	0	0

*E: East - N: North - W: West - S: South

Table 17 shows that windows with a high head height (2,55 m above floor level) are consistently performing better. This is the result of daylight penetrating deeper in space when the head height is high. A rise of the illuminance on the back-end sensors is the reason for a higher DA50lx. For the west orientation, none of the designs has a DA50lx lower than 10 %, and there is a lower variability between the different window head heights. This is the result of the received direct solar irradiation, which is higher for a west bedroom due to the assumed occupancy schedule of 22:00 to 00:00 hours.

The following table shows the effect of the height-to-width ratio of the window on the DA50lx, for each orientation. It is shown that square-shaped windows consistently perform better. Vertical windows perform better than horizontal for lower DA150lx levels, meaning, for lower WWRs. For higher WWRs, horizontal windows perform better. It should be noted that square-shaped windows have also a better thermal performance, as their frame to glazing ratio is lower. This explains why the optimization algorithm converged to highly placed squared windows, as it was shown in Table 15 of section 3.2.1.

Table 18: Percentage of simulated designs for which the DA50lx exceeded a given value, for different window height-to-width ratios (all orientations included).

Height-to-Width		<0,75 (horizontal)				0,75-1,25 (squared)				>1,25 (vertical)			
Orientation		E*	N*	W*	S*	E	N	W	S	E	N	W	S
DA50lx (%)	1	100	100	100	100	100	100	100	100	100	100	100	100
	2	95	97	100	97	100	100	100	100	98	100	100	100
	3	92	95	100	95	100	100	100	100	93	100	100	97
	4	92	92	100	93	100	100	100	100	85	97	100	93
	5	79	92	100	92	100	100	100	100	80	93	100	93
	6	75	88	100	89	96	100	100	100	80	90	100	85
	7	74	85	100	85	92	100	100	100	73	80	100	80
	8	71	75	100	77	90	96	100	98	70	80	100	80
	9	66	75	100	75	90	96	100	94	67	78	100	75
	10	66	71	96	73	90	90	100	92	65	75	97	72
	11	64	67	95	70	87	90	100	90	63	72	97	70
	12	62	64	92	66	83	88	100	90	62	67	92	67
	13	55	62	78	64	79	85	98	87	62	63	80	62
	14	52	53	73	60	73	77	90	83	58	62	68	62
	15	51	52	64	52	67	71	88	75	52	62	62	60
	16	45	49	55	51	63	63	79	65	42	58	58	52
	17	36	40	47	45	58	62	63	63	35	47	50	42
	18	29	32	37	32	52	54	58	56	18	37	35	28
	19	19	19	27	19	44	46	50	46	13	22	15	13
	20	9,6	14	14	14	27	31	31	31	0	13	10	3,3

*E: East - N: North - W: West - S: South

LIVING ROOM

The independent variables examined for the living room were the number of windows used and the fenestration zones selection for their placement. Figures 33 and 34 show all simulated solutions for the living room of the west apartment, classified by WWR and number of windows respectively.

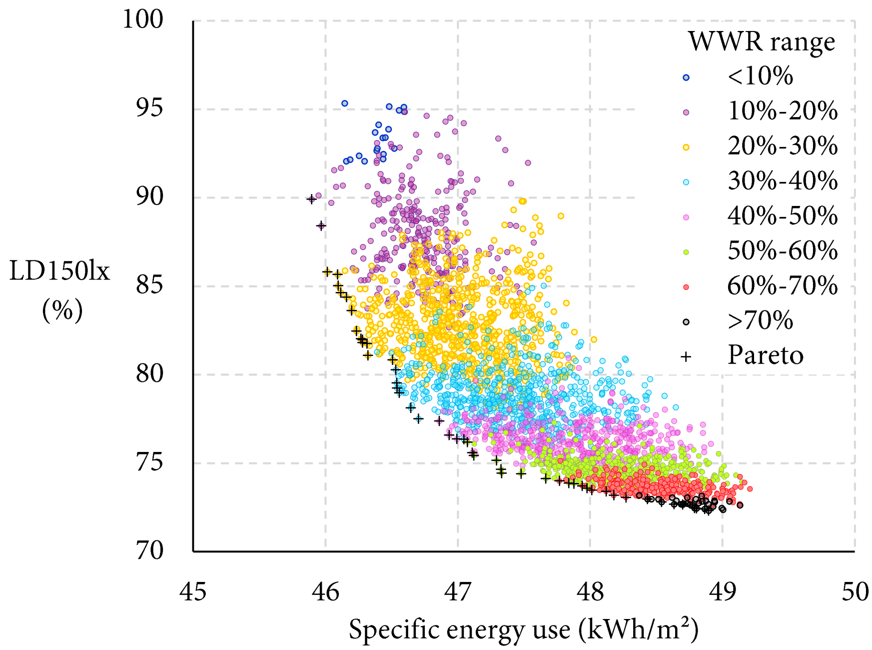

Figure 33: LD150lx and specific energy use for all simulated designs, sorted by WWR range.

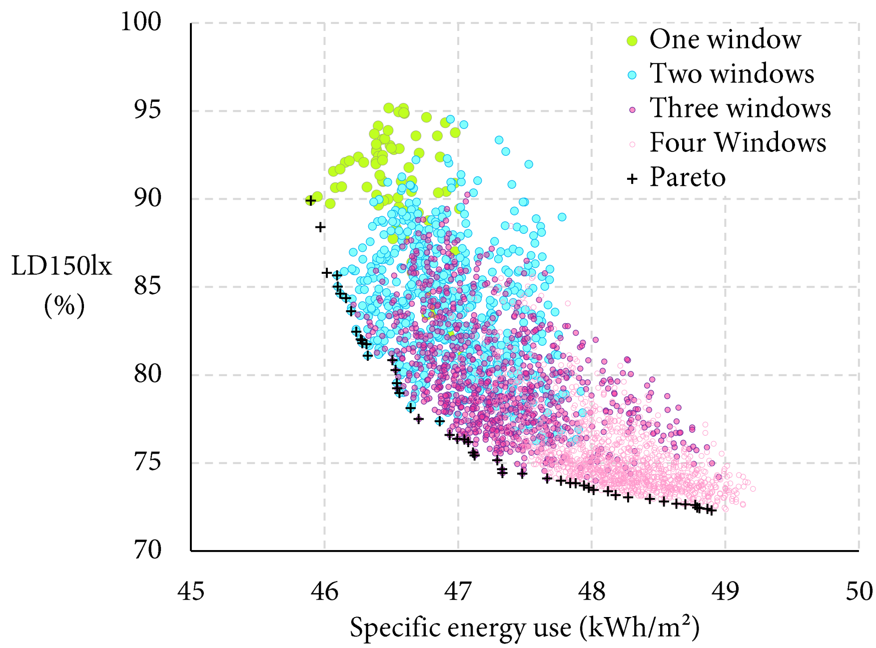

Figure 34: LD150lx and specific energy use for all simulated designs sorted by number of windows.

Figure 33 shows that the LD150lx is mostly reduced when increasing the window area until approximately a WWR of 40 % - 50 % (Figure 33). Increasing the glazing area beyond that percentage leads to negligible daylight gains and considerable increase in heating demand. It is interesting to note that a fenestration design with a WWR of 10 % to 20 % can actually perform worse that one of 40 % to 50 %, both for the daylighting and the heating objective. This is a result of the fenestration zone utilized each time. Figure 34 shows that the Pareto optimal solutions (black crosses) consist mostly of two, three or four windows. Although using one window leads to a low energy use, it results to very poor daylight conditions. On the other hand, using four windows does not yield considerably higher daylight levels, compared to using three. The most effective part of the Pareto front is populated by two- and three-window solutions.

Figure 35 shows the performance of all fenestration designs with two windows, when different fenestration zones are utilized for the window placement.

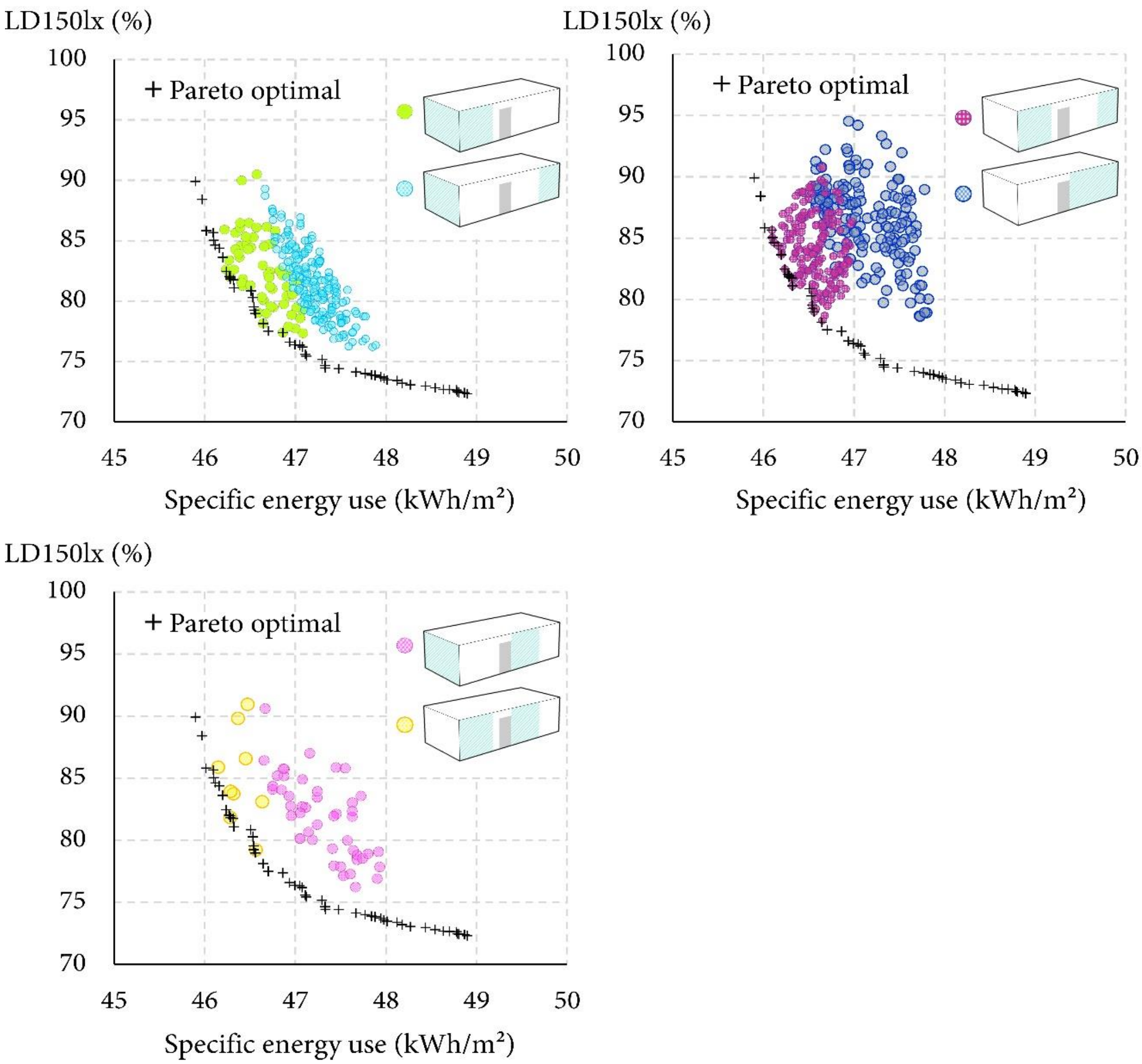

Figure 35: LD150lx and specific energy use for two-window designs, allocated in different fenestration zones.

The solutions that are closer to the Pareto front are the desired ones. The upper left chart shows that if a window is placed on the northern fenestration zone (F2), then the second window should be placed in F3 instead of F5. The upper right chart shows that if both windows are to be placed on the west façade, then it is preferable to position them on F3 and F5. The daylight levels will be approximately the same with utilizing zones F4 and F5, but the energy use will be lower. The bottom left chart shows that if F4 is to be utilized for one window, then the second one should be placed on F3. Overall, the solutions utilizing F3 are consistently better performing and closest to the Pareto front.

Figure 36 shows the specific energy use as a function of the overall U-Value (walls + windows) and the annual solar gains as a function of the WWR, when one window is placed on the northern fenestration zone. The left chart shows that when placing the second window on F3 (green points), a lower heating demand can be achieved with the use of the same insulation level. The right chart explains this by showing that the solar gain potential per glazing area is higher for two windows on F2 and F3.

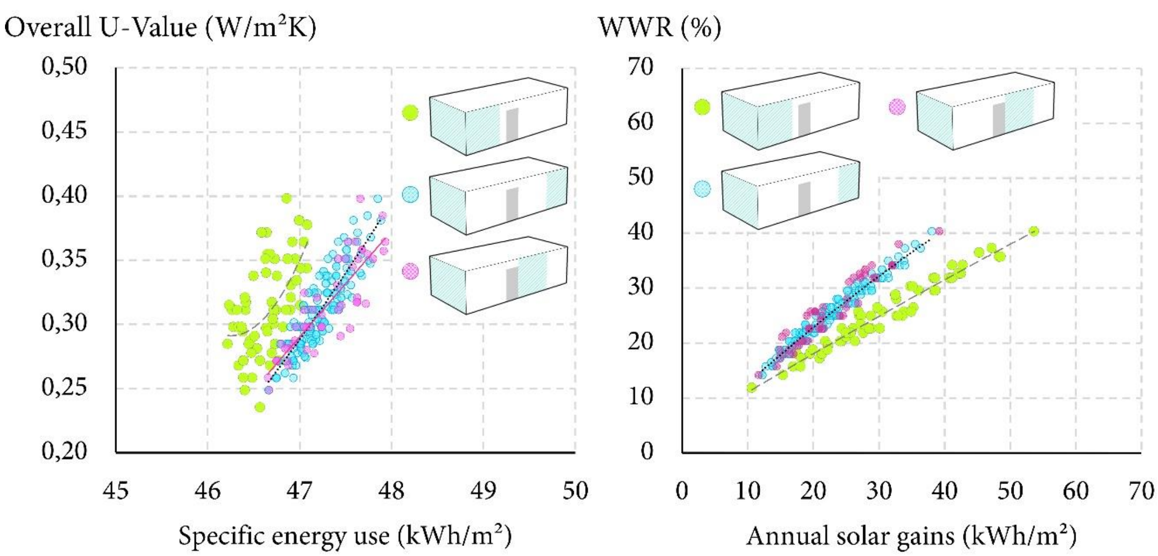

Figure 36: The specific energy use as a function of the overall U-Value and the annual solar gains as a function of the WWR, when one window is placed on the northern fenestration zone.

As shown in Figure 34, using three windows results in higher daylight levels compared to using two. The issue here is the higher energy use caused by the extra opening. Figure 37 shows the performance of four different cases, each one missing a window on one of the fenestration zones. It is shown that avoiding placing a window on F2 or F4 results in the best performing solutions (green and light-blue points). The poorest choice is to place one window on the north (F2), and the other facing the balcony area (F4 and F5). It seems that avoiding using F3 is not a good choice.

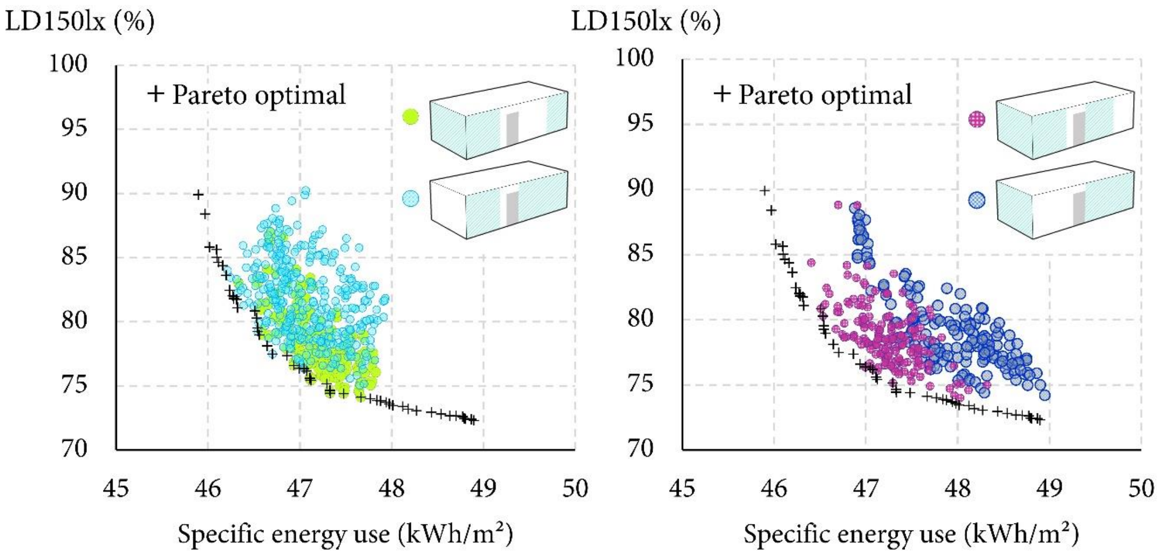

Figure 37: LD150lx and specific energy use when placing three windows.

Figure 38 shows the specific energy use as a function of the overall U-Value (walls + windows) and the annual solar gains as a function of the WWR, when fenestration zone F3 is not utilized (blue points) and for all other combinations of three windows (purple points). It is shown that more insulation is required to achieve a given specific energy use, if a window is not placed on F3 (left chart). As in the two-window cases, the solar gains admitted are less for a given WWR, if fenestration zone F3 is not utilized. In other words, F3 represents an optimal window placement due to the passive solar gains.

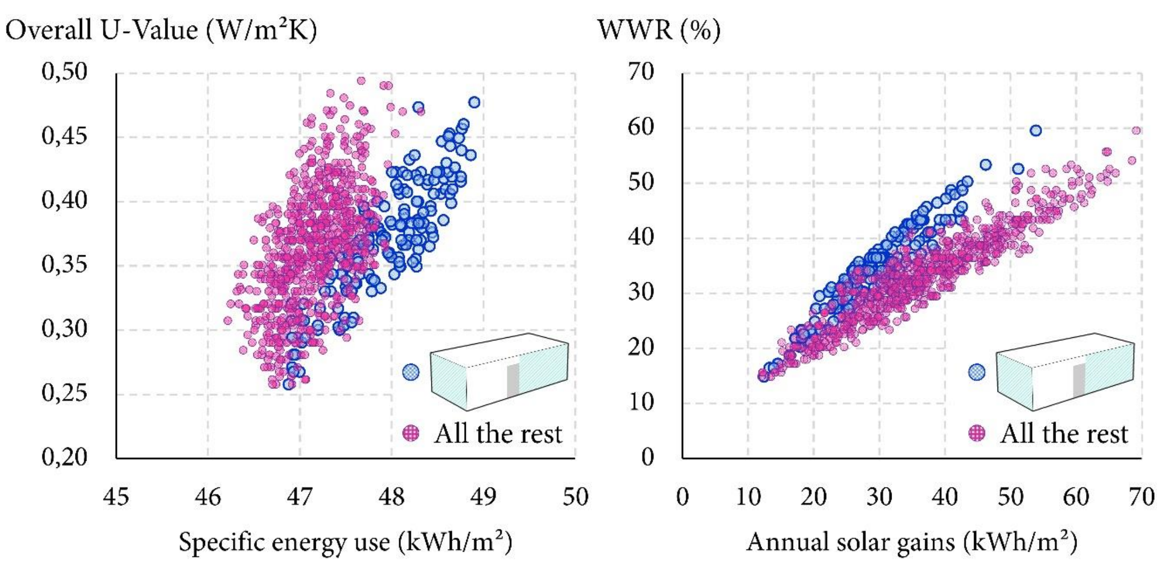

Figure 38: The specific energy use as a function of the overall U-Value and the annual solar gains as a function of the WWR, when placing three windows on the living room.

Figure 39 shows the specific energy use of the west apartment, as a function of the DF and the UR, for the placement of two windows in different fenestration zones. The crosses indicate that a solution is Pareto optimal according to the heating and daylighting optimization described previously in section 3.2.1. The left chart shows that in order to achieve the BREEAM (2014) average DF of 2,1 %, the two windows should be placed either on F2-F3 (green points) or on F2-F4 (pink points) or on F2-F5 (light-blue points). This shows a contradiction between the daylight certification requirement and the thermal performance of the apartment: All three pre-mentioned combinations have always a window on the northern façade (F2) that results in a higher heating demand. There are only two fenestration designs that are Pareto optimal (black crosses) and still pass the BREEAM criterion. These cases are the ones placing the second window on F3, which was shown to induce a higher solar gain. The lowest DF is reached when placing both windows on the fenestration zones facing the balcony area (F4-F5, blue points).

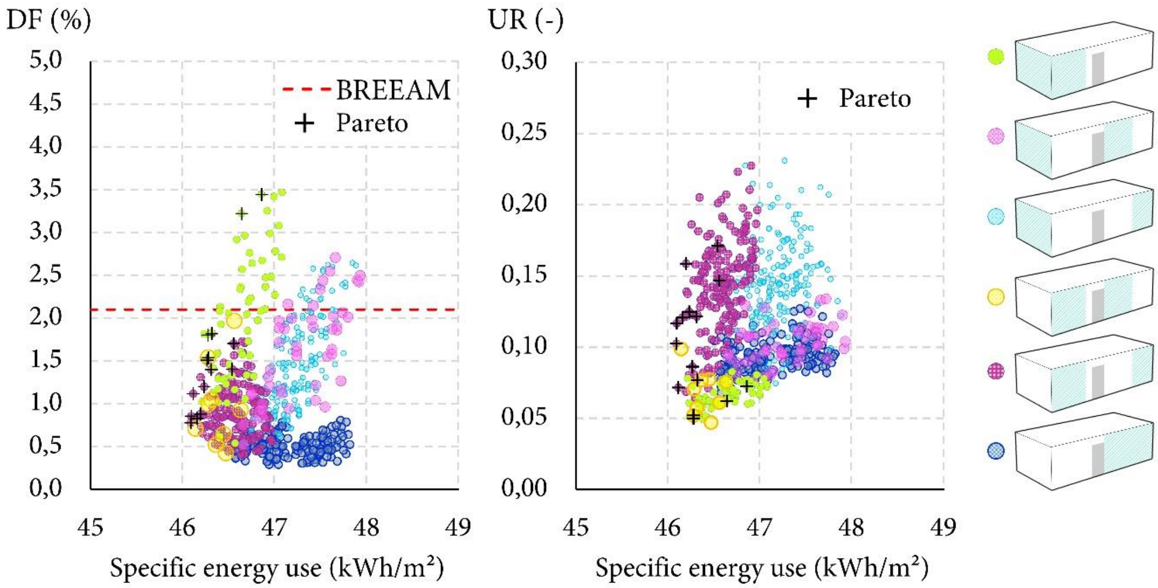

Figure 39: Specific energy use of the west apartment, as a function of the DF and the UR, for the placement of two windows in different fenestration zones.

On the other hand, the uniformity ratio UR shown on the right chart is the lowest possible when placing the windows on F2 and F3 (green points). For a design solution to be Pareto optimal and achieve a higher uniformity ratio simultaneously, the two windows should be placed on F3 and F5 (purple points). The same UR levels can be achieved for F2-F5, where the windows are spread as much as possible on the building envelope, but in that case, the specific energy use is always higher. It is therefore shown that achieving a low energy use, a high DF and a satisfying UR is not possible, when placing two windows on the living room zone.

Figure 40 shows the specific energy use of the west apartment, as a function of the DF and the UR, for the placement of three windows in different fenestration zones.

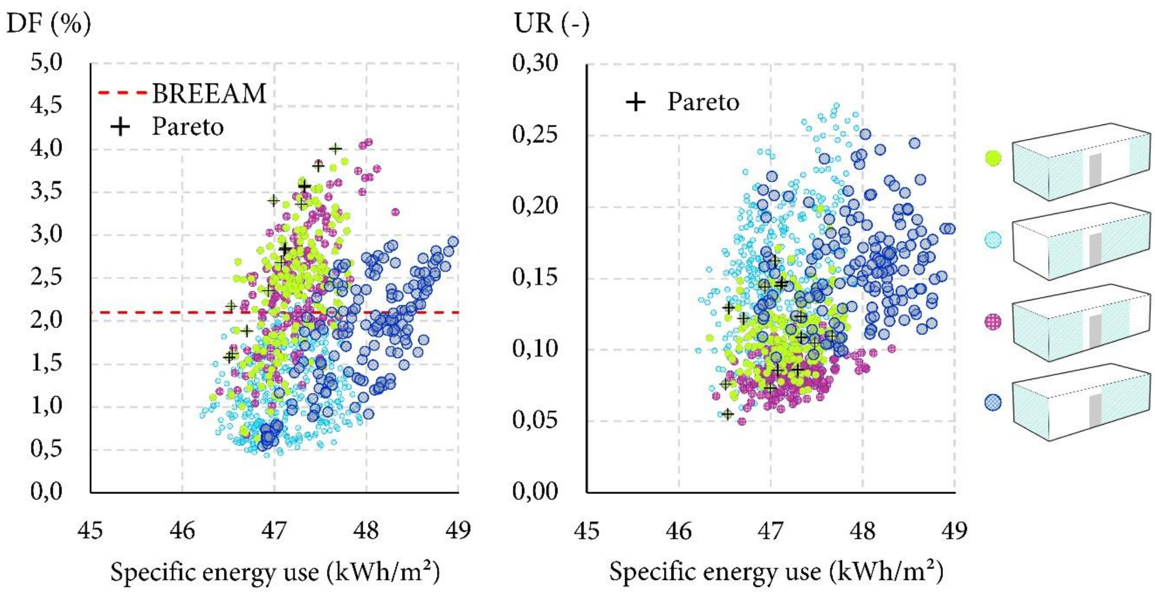

Figure 40: Specific energy use of the west apartment, as a function of the DF and the UR, for the placement of three windows in different fenestration zones.

The left chart shows that placing three windows instead of two yields higher DF levels, but the energy use is higher too. The only choice that does not achieve the BREEAM criterion is the one lacking a window on the north façade F2 (light-blue points), which is the one that can yield the lowest heating demand possible. The fenestration design that achieves the BREEAM DF criterion and includes Pareto optimal solutions at the same time is the one that does not include a window on F4 (green points). Examining both graphs, it is evident that the designs achieving the highest DF levels are the ones that achieve the lowest DF uniformity ratios (green and purple points). If the energy use is not a priority for a designer, then avoiding a window on F3 (blue points) can result in high DF and UR levels simultaneously. This shows that even with three windows, achieving visual comfort and low energy use are contradicting goals.

The electricity used for lighting is a variable that depends on the daylight levels of the living room. Figure 41 shows the electric energy intensity for lighting as a function of the window-to-wall ratio, when two windows are placed in different fenestration zones. It is shown that spreading the windows as much as possible over the building envelope results in the lowest possible electricity use for lighting (F2-F5, light-blue points). The most demanding design in terms of electric lighting is the one where the two windows are placed next to each other and in front of the balcony area (F4-F5, blue points). The overall electricity use as well as the variation between the designs is relatively small, as the illuminance threshold for lighting was set to only 150lx.

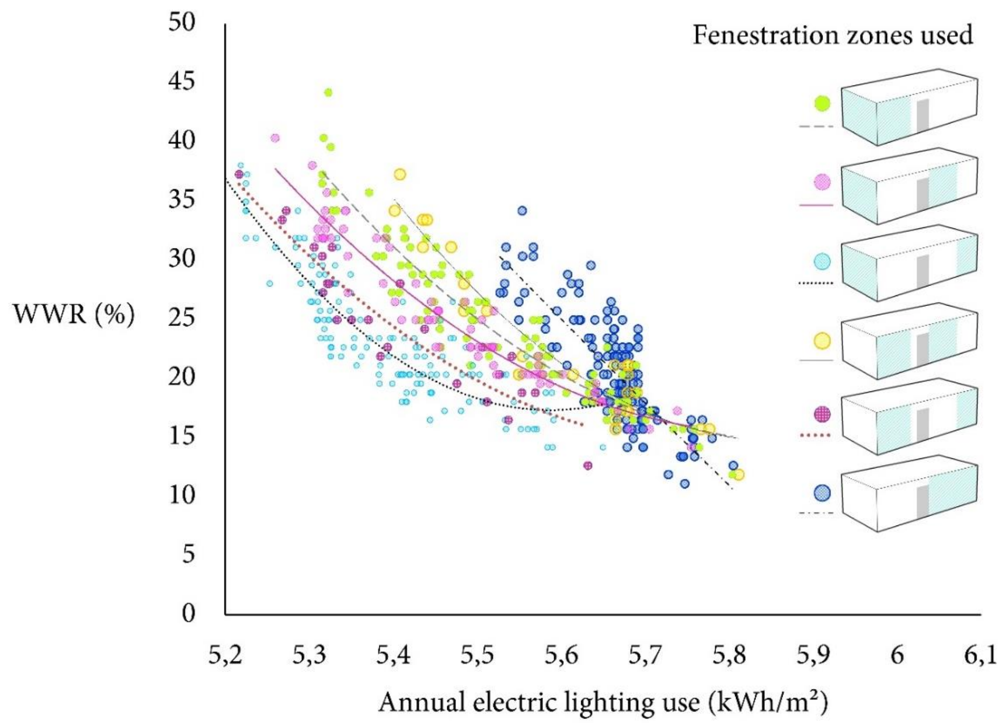

Figure 41: Annual electric lighting use for different placement of two windows.

IMPORTANT NOTE

A limitation of this study was that the heating demand was calculated for each fenestration solution with an unlimited indoor air temperature. This in turn can result in slightly different heating demands, as in reality occupants would ventilate space by the use of the openings when the operative temperature exceeds 27 °C or 28 °C. In other words, the heat gained by solar irradiation is slightly overestimated in the current study. An hourly study showed that (excluding the summer months), the operative temperature exceeds 27 °C partly during April, May and September. During April and May this only occurs for two or three days, whereas in September in occurs for most of the first half of the month.

3.2.3 Impact of solar gains

BEDROOM

The annual heating demand of the bedroom was previously shown to vary, as a function of WWR, but not always in a straightforward way. Especially for the east and west orientations, the overall trend was that it decreased until a specific WWR was reached, after which it started increasing. The reason behind this is exemplified in Figures 42, 43, 44 and 45, where the annual heating demand is shown as a function of the solar gains through the window for each orientation.

Figure 42 shows the effect of the solar gains for an east oriented bedroom. For WWRs smaller than 20 %, the heating demand is the highest possible. It is interesting that a WWR between 10 % and 20 % can yield the same energy use as a WWR larger than 70 %. The WWR of 70 % compensates for its high U-value by exploiting nearly 100 kWh/m² of solar gains annually. The amount of solar gains is proportional to the size of WWR. The heating demand is decreasing until a WWR in the range of 40 % - 50 %. For higher WWRs, the heating demand increases, even though the solar gains are increasing simultaneously. The reason for this is that after a specific overall U-value (wall + window), the transmission losses become so high that the energy gained by solar radiation is not sufficient to compensate for the increase in heating demand. The same trend of the heating demand for different WWRs can be seen in Figure 43 for a west oriented bedroom. The difference is that the solar gains are slightly lower for each window design, leading to an increased heating demand for all cases, compared to the east orientation.

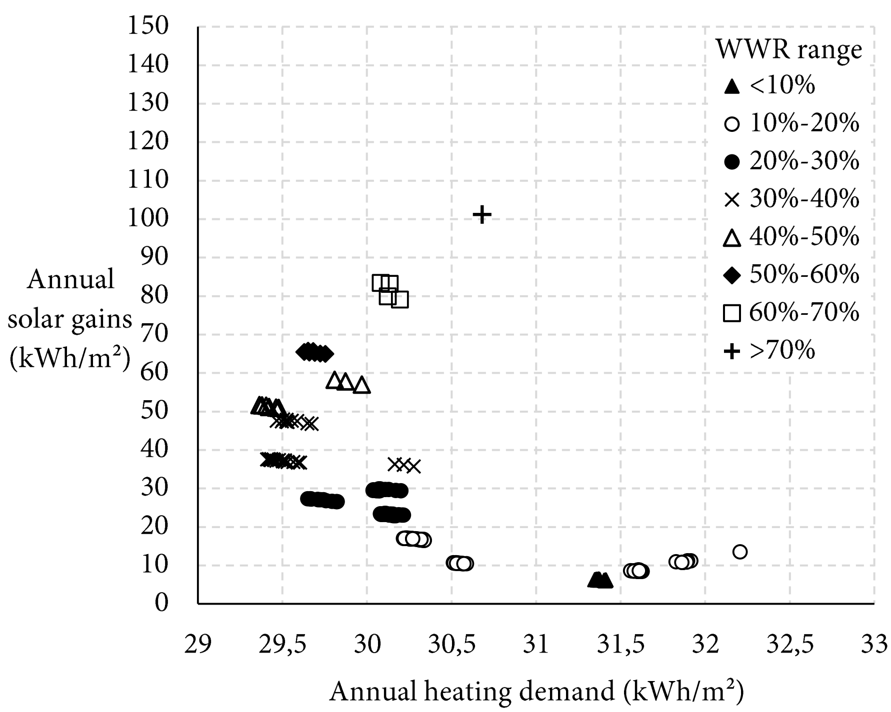

Figure 42: Annual heating demand for East bedroom as a function of solar gains.

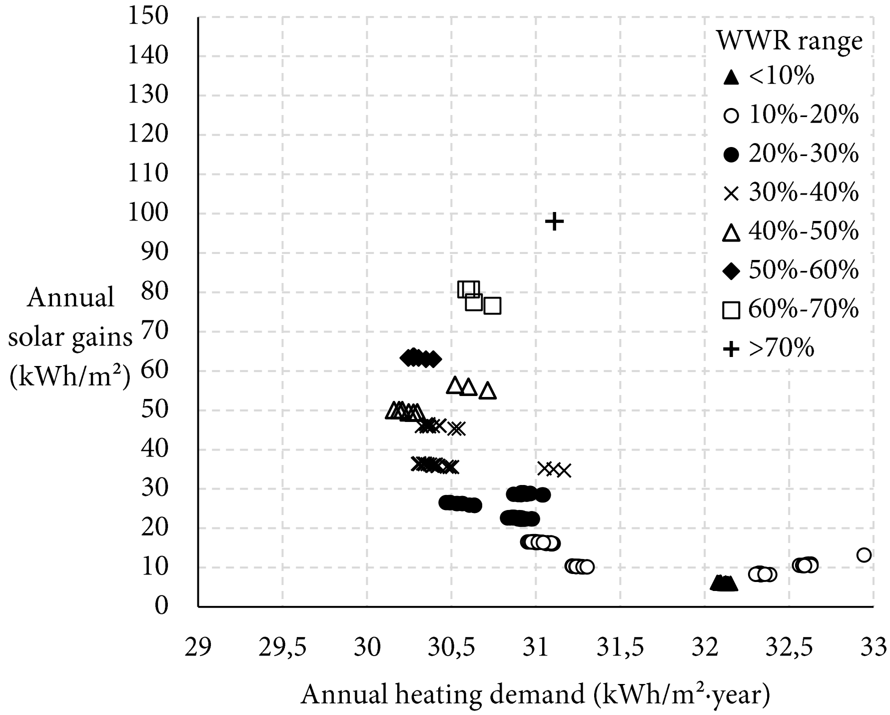

Figure 43: Annual heating demand for West bedroom as a function of solar gains.

The effect of solar gains on the annual heating demand for the north orientation is more straightforward. The low amount of solar radiation on the north façade (Figure 44) results in the heating demand being mostly dependent on the window U-value, in other words, larger WWRs result in a higher heating demand. Nevertheless, one can clearly observe the importance of the window shape as a factor that influences the window U-value. For instance, the heating demand of cases within a WWR range of 40% - 50 % (triangles in Figure 44) can differ. This derives from the fact that a window geometry of really high or low height-to-width ratio has a higher frame area per window area, leading to an increased U-value, since the frame U-value is higher compared to the glazing, and the linear thermal bridge is higher too.

On the south orientation (Figure 45), the high amount of solar gains results in a clear pattern: Larger windows induce a lower annual heating demand. This explains why the Pareto optimum design for this orientation was the one with the highest possible WWR of 78 %. The heating demand decreases faster as the WWR increases from <10 % to 40 %, where it can range from 29 to 18 kWh/m² annually. For larger windows, it can only decrease from 18 to approximately 15 kWh/m², even though the solar gains increase faster. Overall, passive solar gains for heating can be more efficiently exploited by orienting the bedroom towards the south.

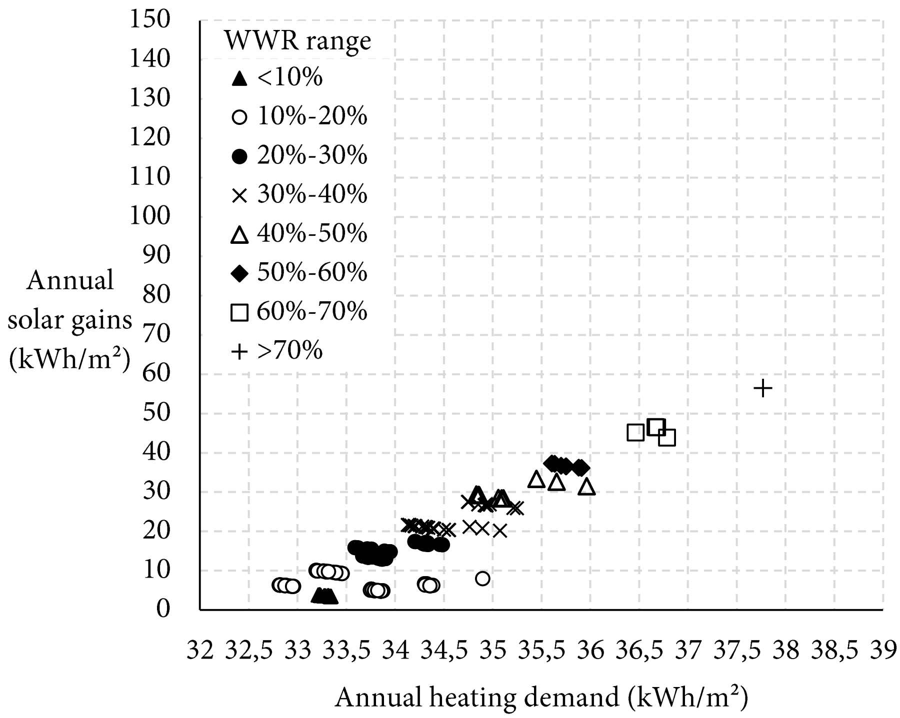

Figure 44: Annual heating demand for North bedroom as a function of solar gains.

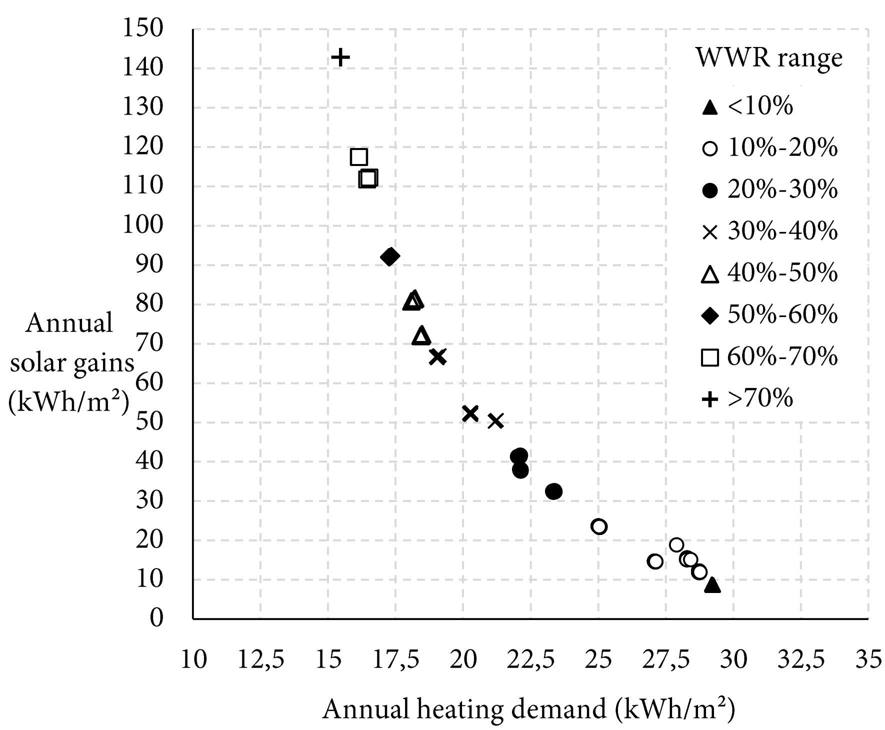

Figure 45: Annual heating demand for South bedroom as a function of solar gains.

The correlation of the achieved DF level and the admitted solar gains for different WWRs is shown in Figure 46. The increase of the daylight levels when increasing the window area is proportional to the incident solar gains. The difference between east and west is negligible for low WWRs, and more visible for larger ones. For a south oriented bedroom, achieving the BREEAM DF requirement results in receiving approximately 50 kWh/m² of solar gains annually, with probable overheating issues during summer. On the other hand, the same criterion on the north is achieved with solar gains of only 20 kWh/m² annually. Overall, the trend is that higher WWRs induce higher daylight levels, and that north is the orientation where higher daylight levels can be achieved for the least possible incident solar irradiation.

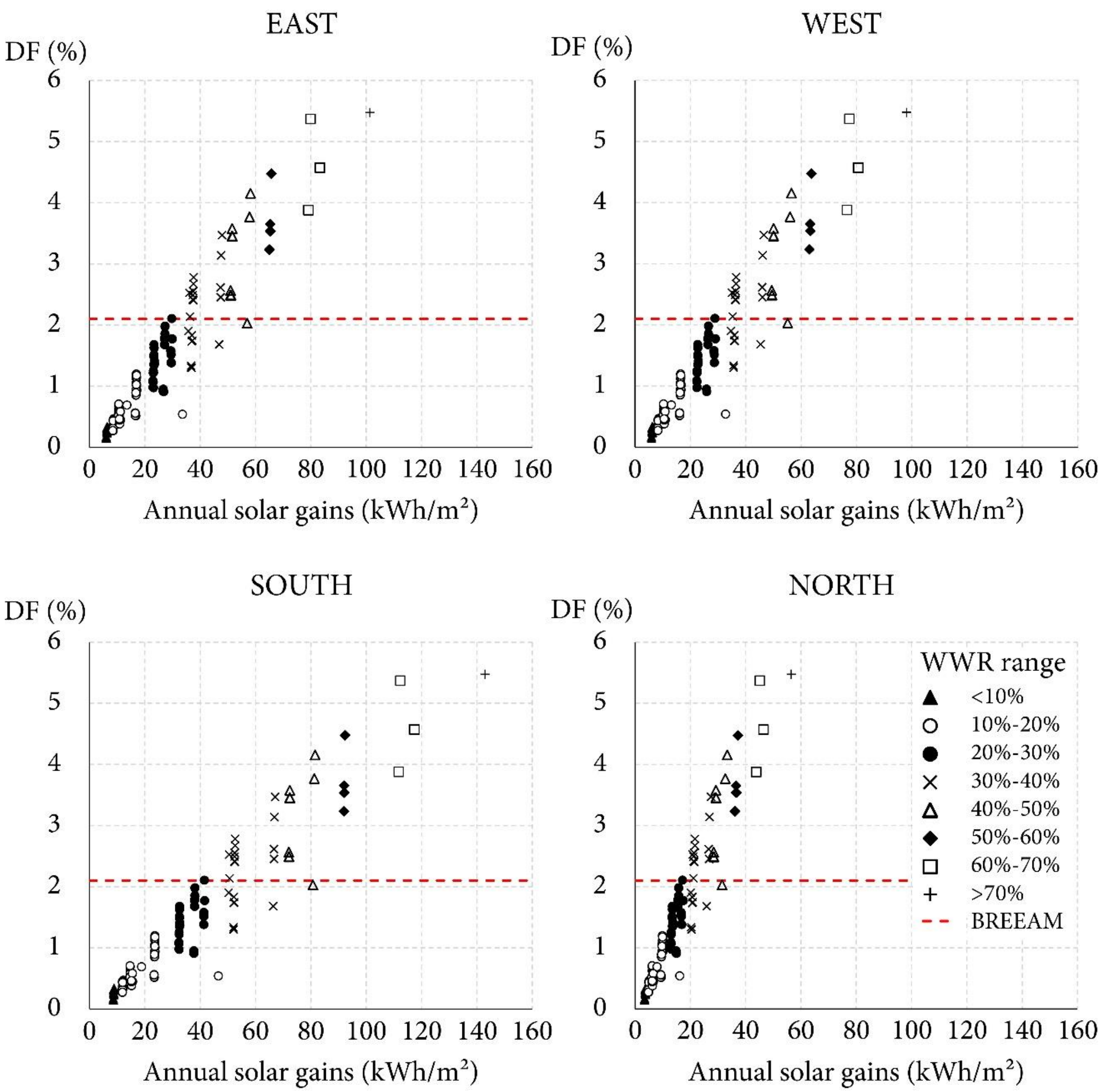

Figure 46: Correlation of the DF and annual solar gains for different WWR and orientations.

Figure 47 indicates that the DA is not linearly proportional to the solar gains. It is shown that beyond a WWR of 40% - 50%, the DA50lx levels do not increase anymore. On the contrary, the solar gains are increasing more dramatically. This benchmark occurs for a DA50lx of approximately 21 %.

In the case of a west oriented bedroom, the DA50lx is higher for smaller WWRs compared to the rest of the orientations. North is the orientation where the maximum DA50lx can be achieved with the least possible solar gains of 57 kWh/m² annually. It is also clear that the same WWRs result in the same solar gain, although not in the same DA50lx, since the light admitted depends on the window shape and position as previously discussed.

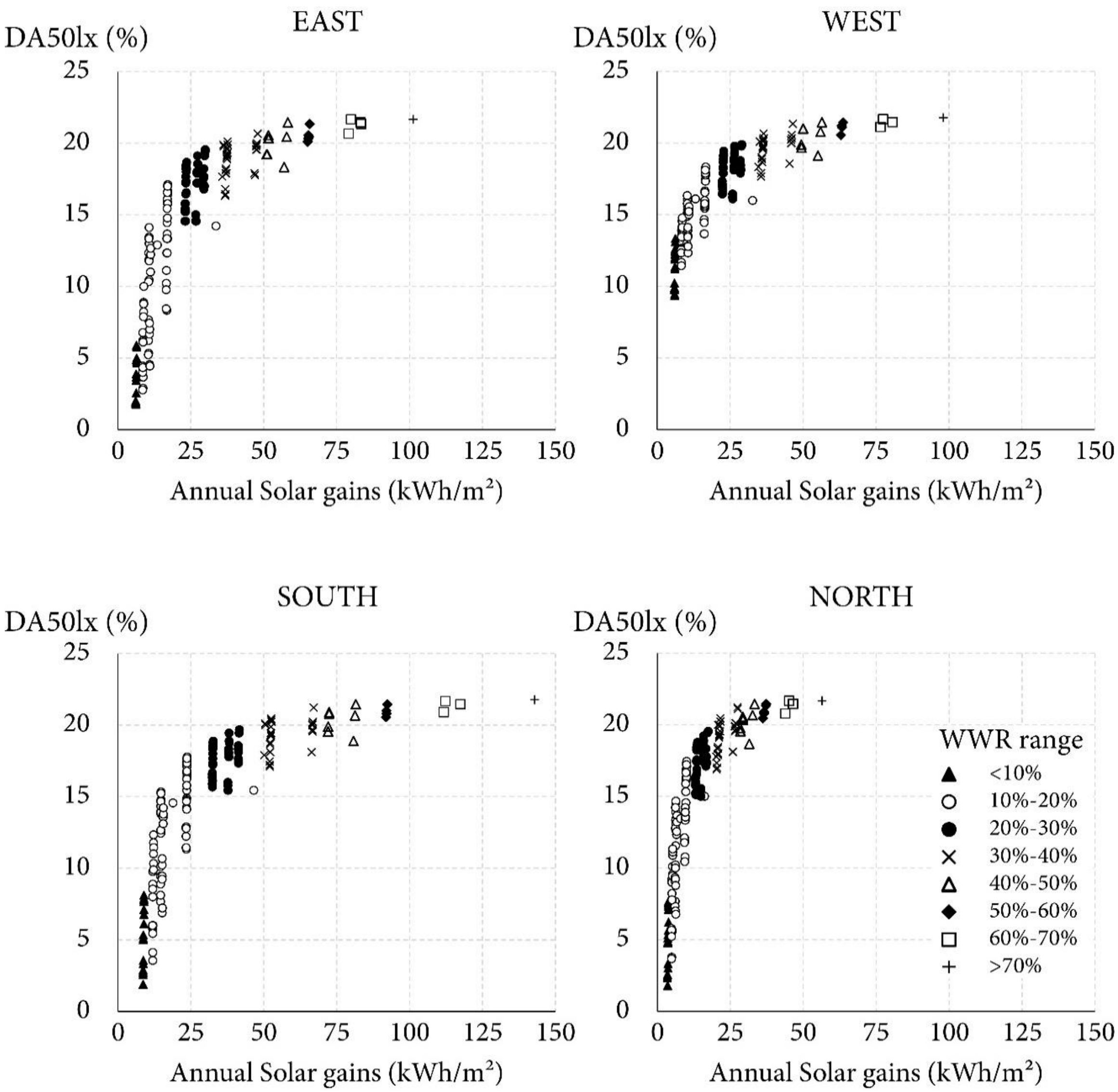

Figure 47: Correlation of the Da50lx and annual solar gains for different WWR and orientations.

Figures 48 and 49 show the DF and the DA50lx as a function of the admitted solar gains, for each orientation.

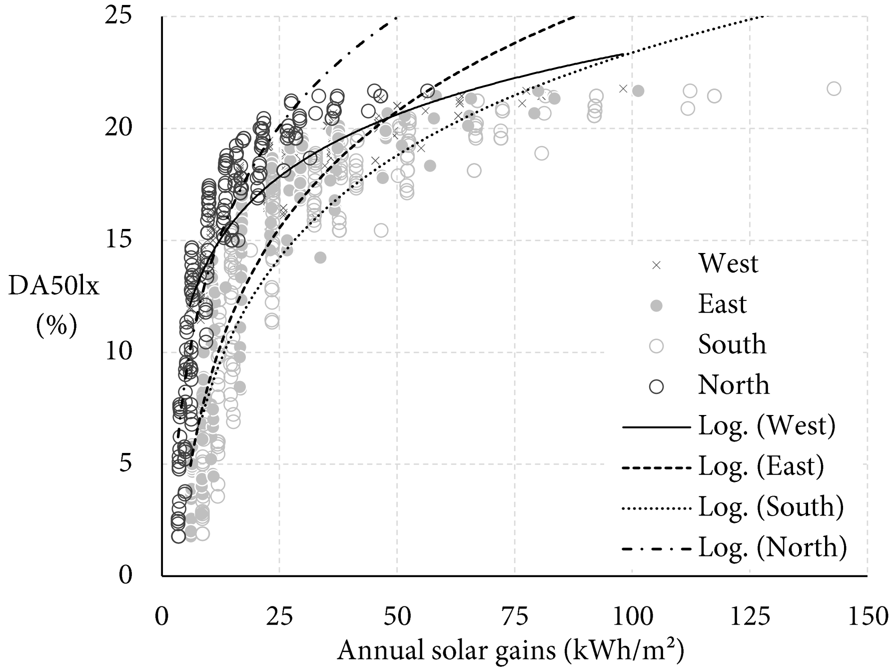

Figure 48: The DA50lx as a function of the solar gains for all possible fenestration designs.

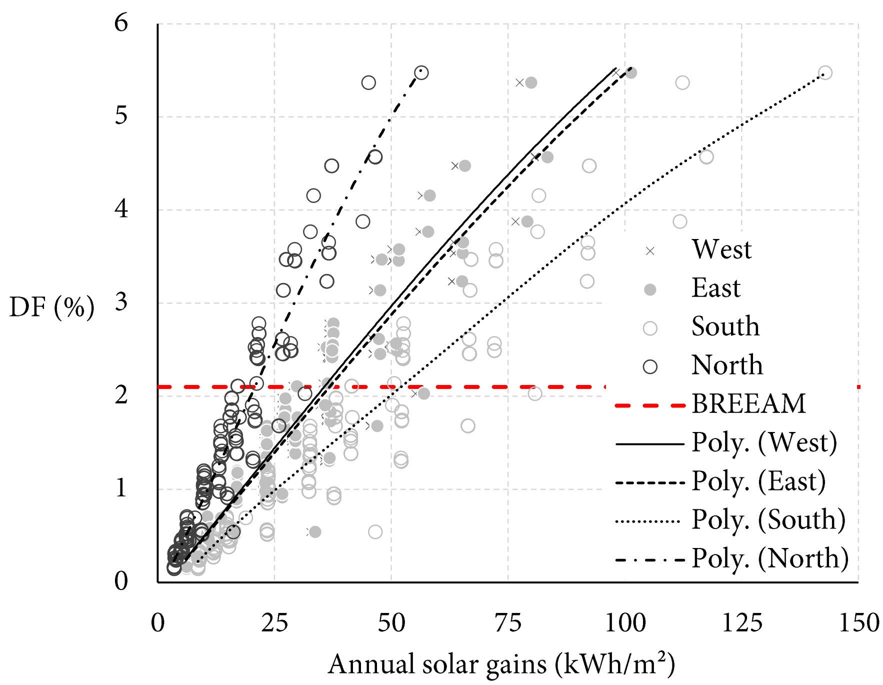

Figure 49: The DF as a function of the solar gains for all possible fenestration designs.

When monitoring the relation between the DA50lx and the incident solar gains, contrary to the DF results, there is a specific point over which the DA50lx during occupancy cannot increase any more, even if the glazing area is increased (Figure 48). This is because the threshold of daylighting is already reached so increasing WWR will only result in more overheating. On the other hand, the DF increases almost linearly with the increase of the incident solar gains (Figure 49). The DA50lx plot shows that north and west are the orientations that receive less solar gains per DA50lx achieved. There is no significant increase of DA50lx after approximately 21% for all orientations.

If the DA50lx is plotted with the DF, as in Figure 50, then an optimum DF benchmark can be defined. According to Figure 50, assuming the DA stabilizes at 21 %, the optimum DF for the bedroom should be 3,5 %. Any value higher than that will most probably result in more solar heating rather than more daylight when it is actually needed.

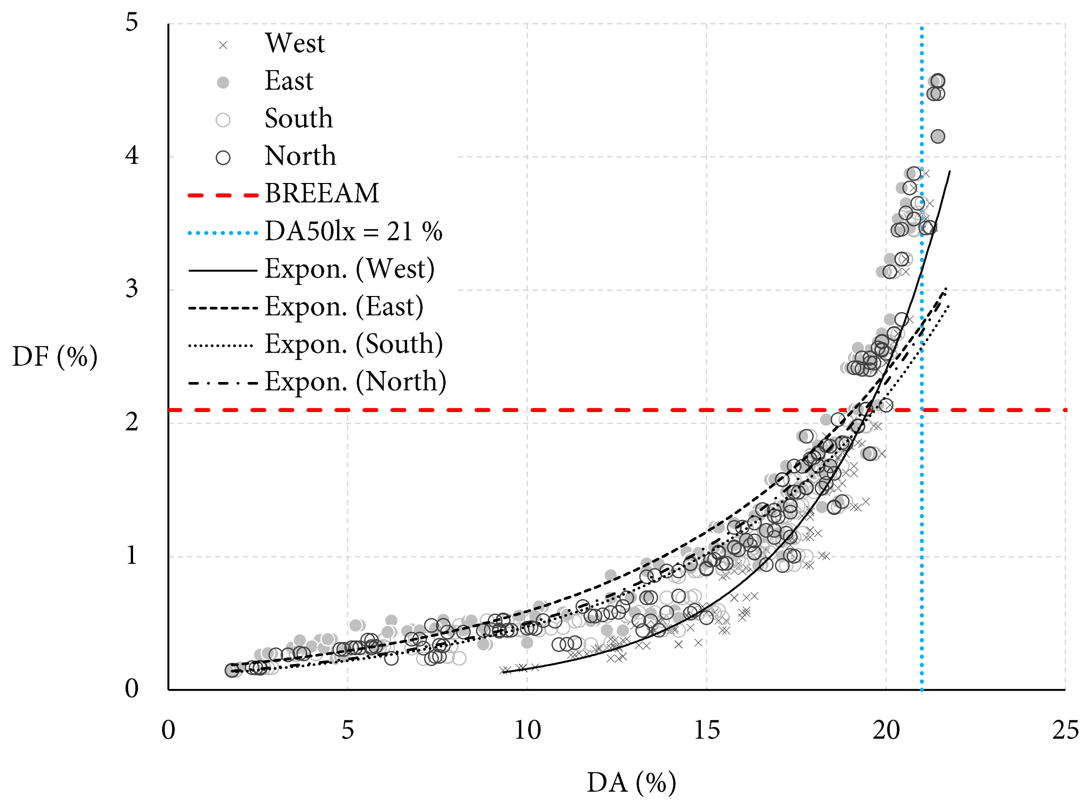

Figure 50: Trend of the correlation between the DF and the DA50lx for all window alternatives.

LIVING ROOM

Figure 51 shows the impact of the admitted solar gains on the specific energy use of the apartment and the DF levels of the living room, for different number of windows. The left chart shows that the solar gains are proportional to the number of windows and specific energy use. The Pareto optimal solutions are shown here to be the ones with the highest possible solar gain, for a given heating demand. The right chart shows that the DF increases when higher solar gains are admitted and that approximately 50 kWh/m² of solar gains are required for a Pareto optimal solution to achieve the BREEAM average DF criterion. The two charts indicate that the optimization objectives of heating and daylight are both proportional to the amount of solar heat gains.

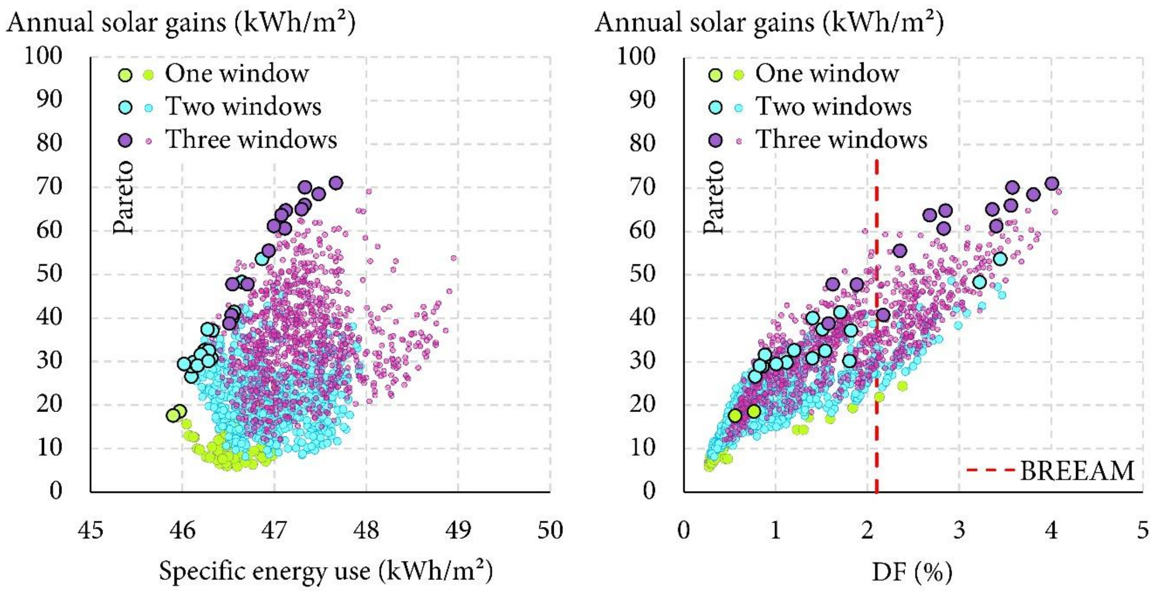

Figure 51: Impact of the admitted solar gains on the specific energy use of the apartment and the DF levels of the living room, for different number of windows.

The following two figures show the effect of the admitted solar gains on the DA150lx of the living room, for the use of two windows (Figure 52) and three windows (Figure 53). Examining Figure 52 shows that placing the two windows on either F2-F4 (pink points) or F2-F5 (light-blue points) leads to high DA150lx levels with the least possible solar gain. These are the fenestration designs that receive mostly diffuse or indirect irradiation, as they have windows on the north façade and behind the balcony. The figure also shows that the Pareto optimal solutions are those that receive at least 28 kWh/m² of solar gains annually (fenestration zones F3-F4 and F3-F5).

Figure 53 shows that when using three windows, high DA150lx levels can be achieved with the least amount of solar gains when avoiding placing a window on F3 (blue points). The rest of the designs though (light-blue, purple and green points) are the ones that include Pareto optimal designs in terms of heating and daylighting. These designs are shown to be the ones with the highest possible solar gain each time.

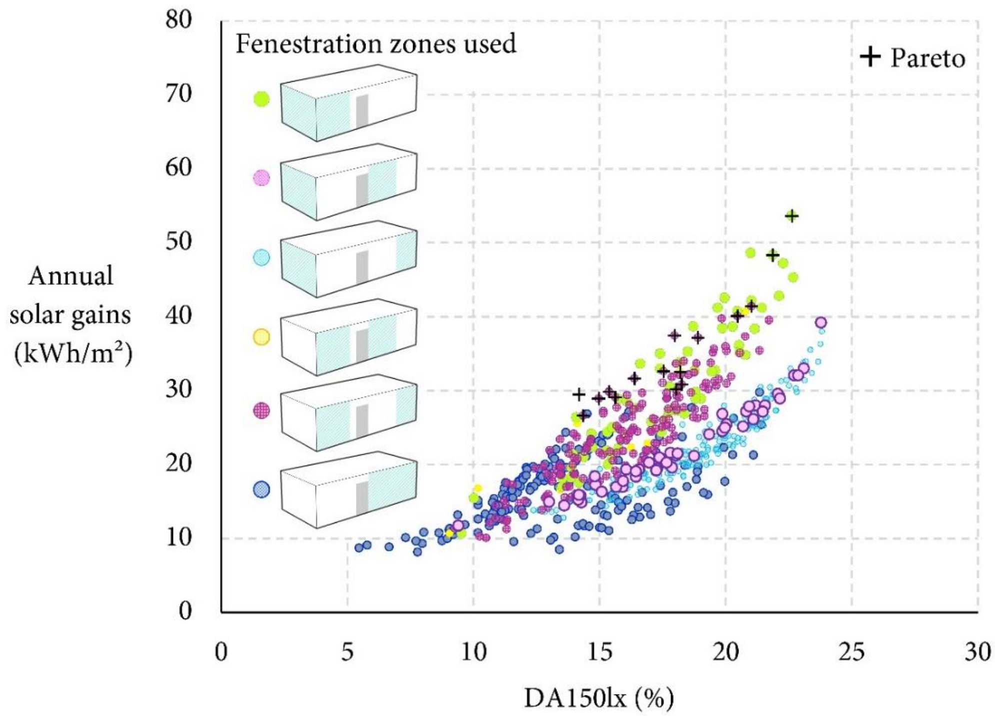

Figure 52: DA150lx as a function of the annual solar gains when two windows are placed in different fenestration zones.

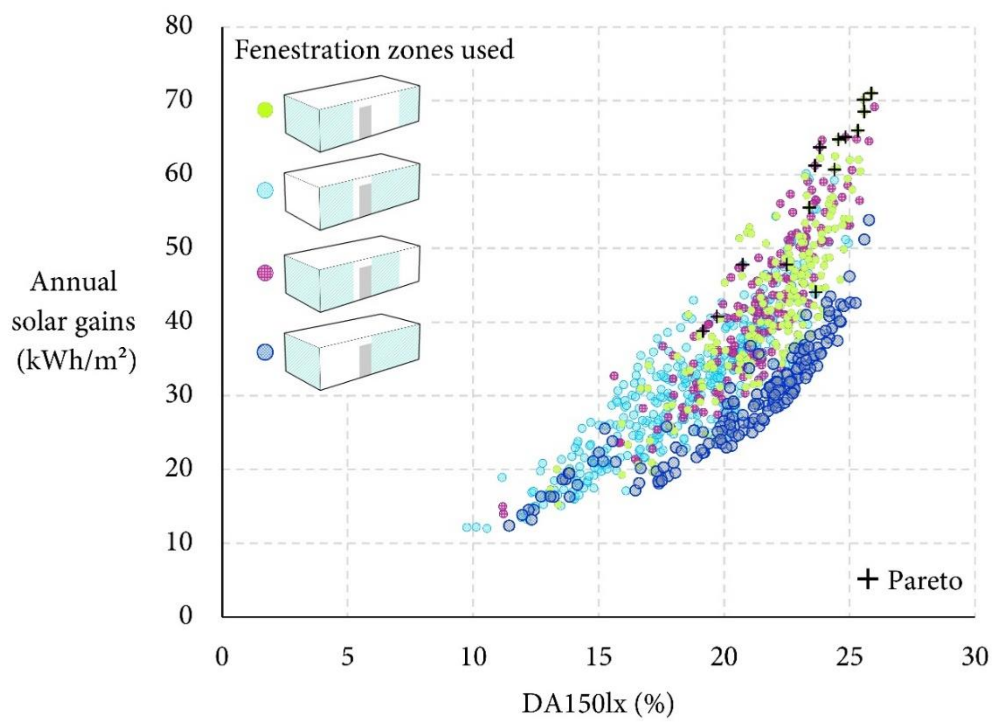

Figure 53: DA150lx as a function of the annual solar gains when three windows are placed in different fenestration zones.

Figure 54 shows the impact of solar gains on DA150lx for the west and east apartments. The solutions shown here are the 600 best solutions in terms of trade-offs between LD150lx and the specific energy use. The two trends are approximately the same, but it is evident that the west orientation achieves a higher DA150lx for a given amount of solar gains. Moreover, the algorithm found more small WWRs on the west orientation, shown here at the bottom left of the scatter plot. The reason behind this is that the living room occupancy schedule of 22:00 to 00:00 hours allows for more optimum solutions with small windows on the west.

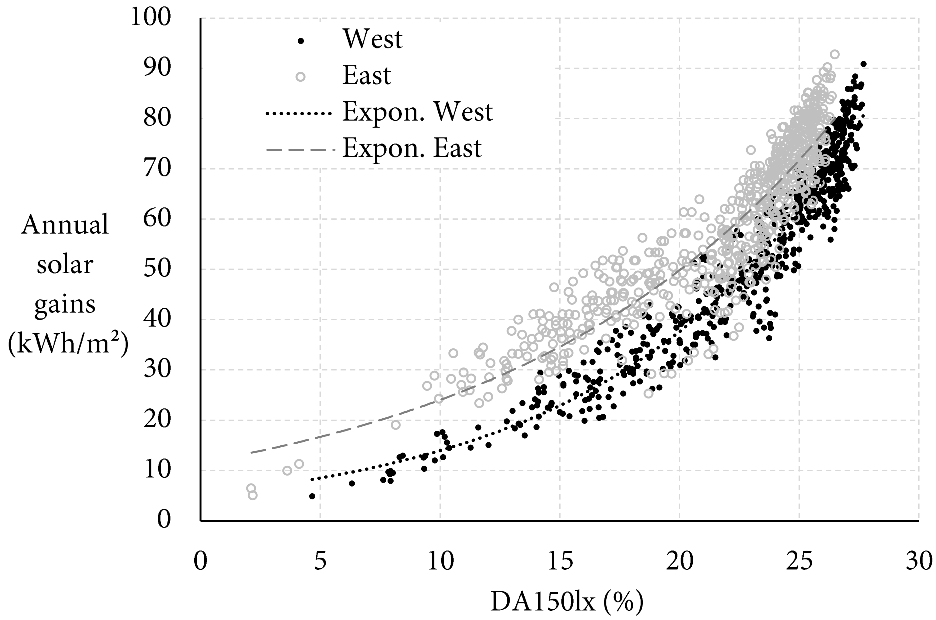

Figure 54: DA150lx as a function of the admitted solar gains on west and east apartments, for the 600 best fenestration designs in terms of heating and daylighting.

3.2.4 Overheating time

BEDROOM

The studied apartment does not have an active cooling system. It is reasonable to assume that increased solar gains can result in overheating in the bedroom during occupancy time. Figure 55 shows the percentage of time for which the operative temperature exceeds 25 °C, as a function of DA50lx, in other words, the overheating "cost" of increasing the bedroom daylight levels. It is shown that the safest location for the bedroom is on the north side of the apartment, as it is the actual case today. Until approximately a DA50lx of 21 %, the west orientation is also a good choice, as it can achieve higher DA levels for less overheating time. If higher daylight levels are required, then for all orientations apart from the north, the overheating time is rapidly increasing as a function of DA50lx. These trends are in direct correlation with the amount of solar gains received, as it was shown in Figure 48.

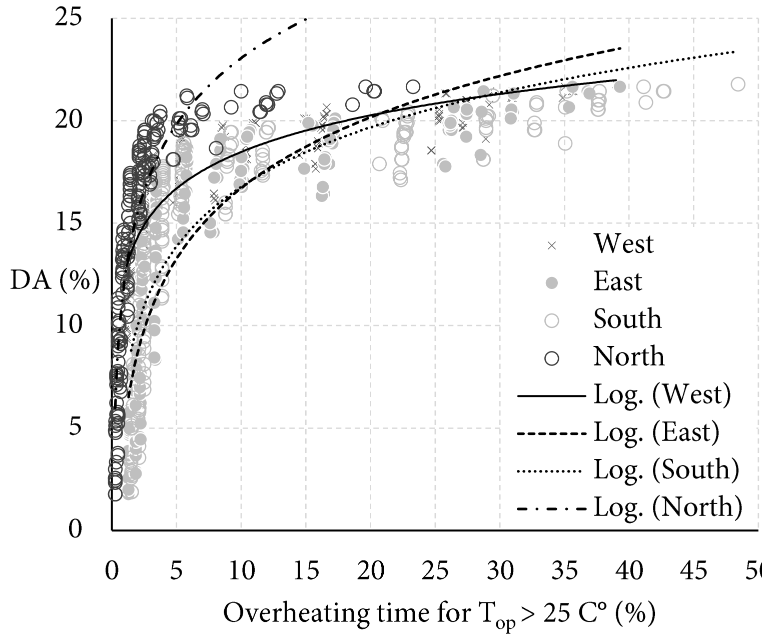

Figure 55: DA150lx as a function of the overheating time (T_{op} > 25 °C) for different orientations.

Figure 56 shows the difference between a north and a south oriented bedroom. The results indicate that it is not wise to increase the WWR on the south orientation, as the optimization of heating and daylighting suggested. The Pareto optimum solution of south has an overheating time of 50 %. On the contrary, using larger glazing areas on the north makes more sense, as approximately the same DA50lx levels can be achieved with significantly lower overheating time. This is the result of the bedroom being highly insulated. Persson et al. (2006) have mentioned this in the context of highly insulated houses in Sweden.

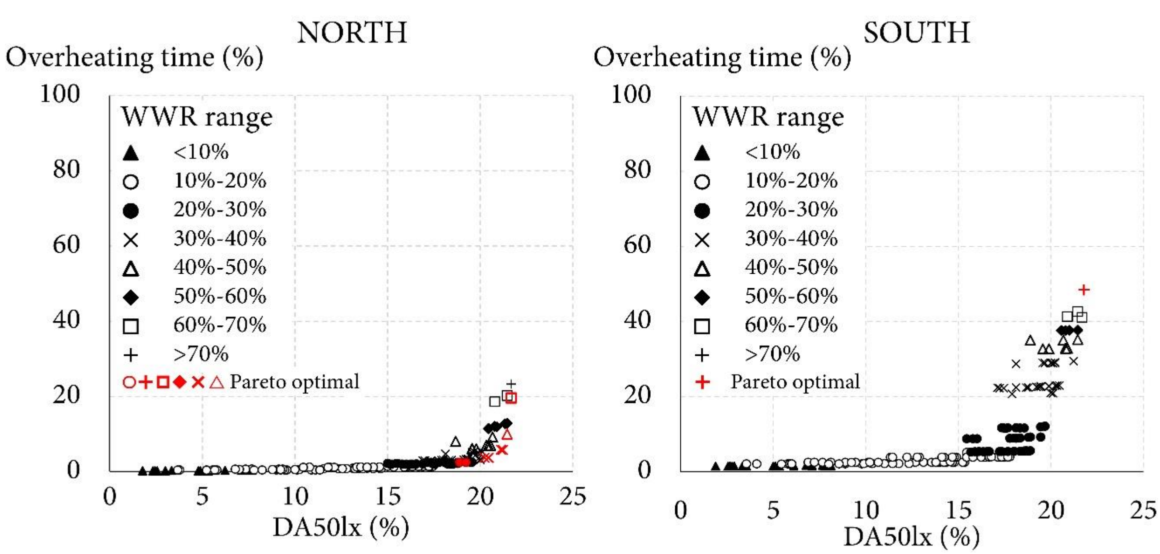

Figure 56: The overheating time for different DA50lx levels reached, as a function of the WWR.

LIVING ROOM

FEBY does not provide benchmark values for the overheating time that a residential space should comply with. One report (Sandberg, 2011) suggests that the operative temperature should not exceed 26 °C for more than 10 % of the occupancy time between April and September, for the "worst" part of the building. On the other hand, the Passive House Institute (2015) states that the operative temperature should not exceed 25 °C for more than 10 % of the year. In practice, occupants in houses have a higher flexibility to open a window or pull down a shading device when their thermal comfort is affected by high operative temperatures. Nevertheless, the following results show the trend of the overheating time as a function of window-to-wall ratio and the window placement, with the intention to define the solutions that result in the least possible overheating.

Figure 57 shows the overheating time of the living room as a function of the window-to-wall ratio, for the west and east apartments. The overheating time is shown for two operative temperature benchmarks: for 25 °C and 28 °C. The overheating time for T_{op} > 25 °C follows the same trend on both orientations: for WWRs between 5 % and 30 % it increases rapidly from 4 % to 20 % of the occupancy time. After a WWR of 30 % overheating increases slower, until a maximum 35 % of the occupancy time. For the benchmark of T_{op} > 28 °C, the case is different: the east orientation is overheating slightly more than the west. Moreover, the overheating time increases slowly until a WWR of approximately 50 %. For larger glazing areas, the time when Top > 28 °C is increasing at a higher rate until a maximum of 20 % of the occupancy time.

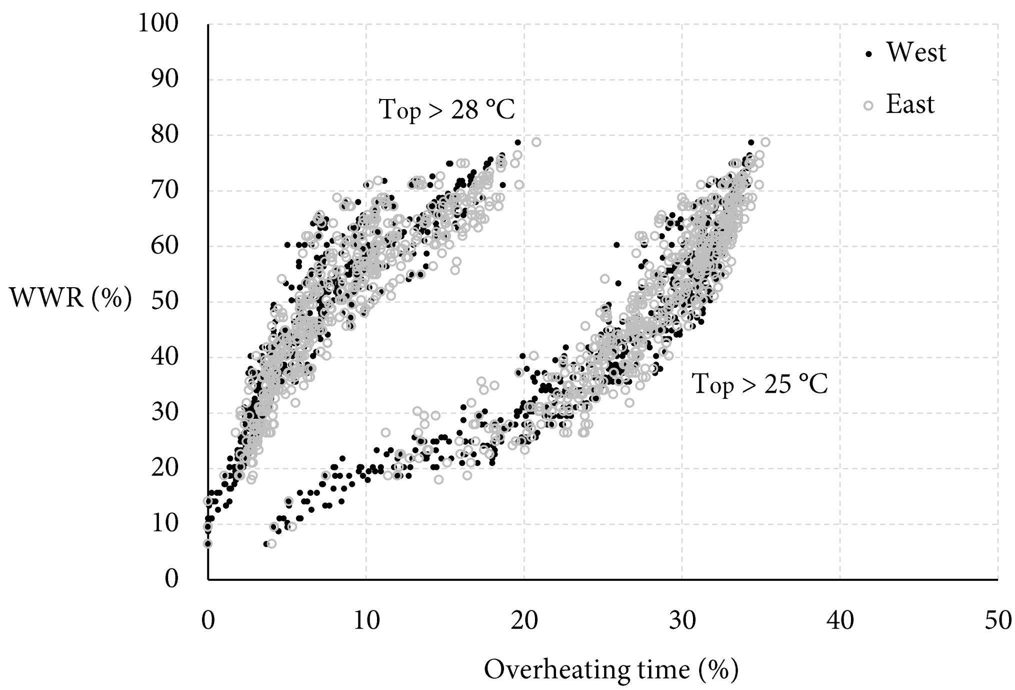

Figure 57: Overheating time of the living room as a function of the window-to-wall ratio, for the west and east apartments (600 cases, two T_{op} benchmarks of 25 °C and 28 °C).

Figure 58 shows the Pareto optimal solutions for two different sets of optimization objectives, in terms of LD150lx and overheating time (Top>25 °C). The black points are the optimum solutions when optimizing for heating and daylighting, and the white points are the one when optimizing for daylighting and low overheating. It is shown that the two cases only converge on the high overheating times (above 30 %), that in reality represent the highest WWRs. For the rest, the results indicate that for a given LD150lx, the heating and daylight optimization (black points) leads to solutions with higher overheating times. This indicates that the daylight/heating optimization is in conflict with the daylight/overheating optimization. In other words, the solutions that yield lower heating demands are the ones that result in higher overheating times.

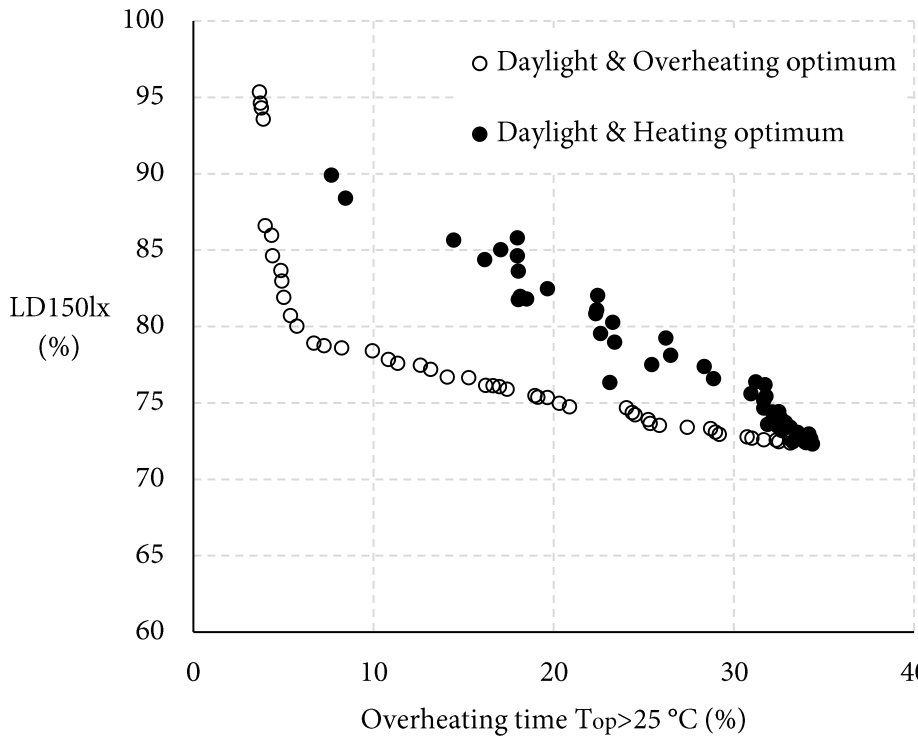

Figure 58: Pareto optimal solutions of the daylighting/heating optimization (black points) and the daylighting/overheating optimization (white points).

Figure 59 shows the distribution of the DA150lx and the overheating time (T_{op} > 25 °C) depending on the number of windows used to fenestrate the living room of the west apartment. The highest increase for both DA150lx and overheating occurs when increasing the number of windows to two. Using either two or three windows results in the same range of overheating time, although for three windows time is distributed more on higher values. What is interesting here is that using four windows instead of three does not yield a considerable increase of DA150lx, but it induces a high increase of the overheating time. In other words, placing windows on all possible fenestration zones is more likely to increase the operative temperature than to increase the daylight levels.

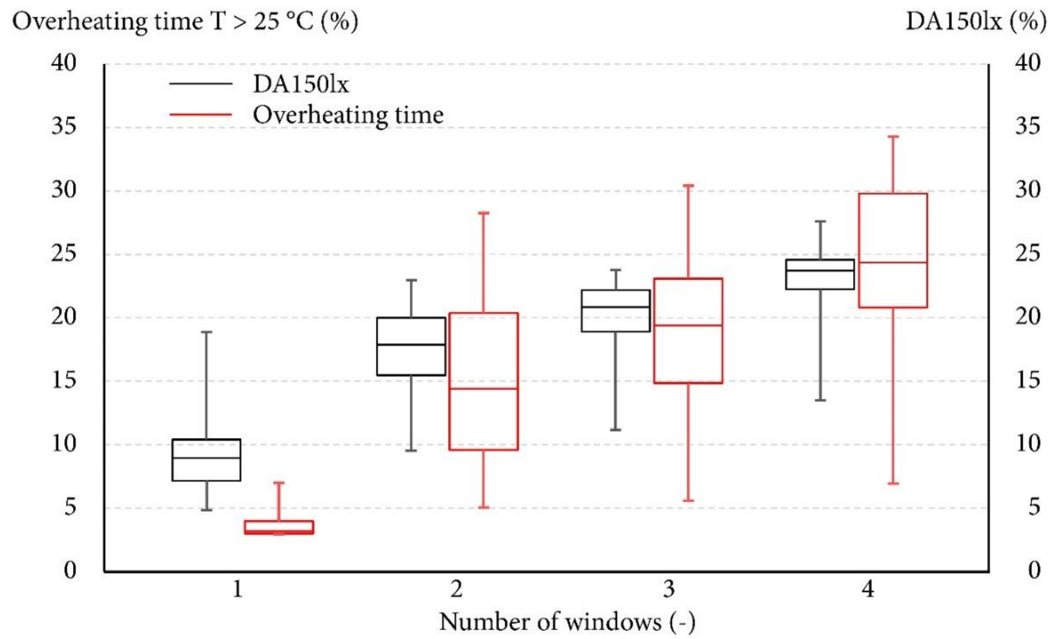

Figure 59: Distribution of DA150lx and overheating time (T_{op} > 25 °C) depending on the number of windows used to fenestrate the living room of the west apartment.

Figure 60 shows the performance of placing three windows in different fenestration zones in terms of LD150lx and overheating time (Top>25 °C). The Pareto front here represents the optimum cases in terms of the trade-offs between daylighting and overheating. The results indicate that the optimum choice is to place windows on the northern façade (F2) and on the fenestration zones that are shaded by the balcony (F4, F5). In other words, the fenestration zone that yields the lower heating demand (F3) has to be avoided if daylight and overheating are to be optimized (blue points).

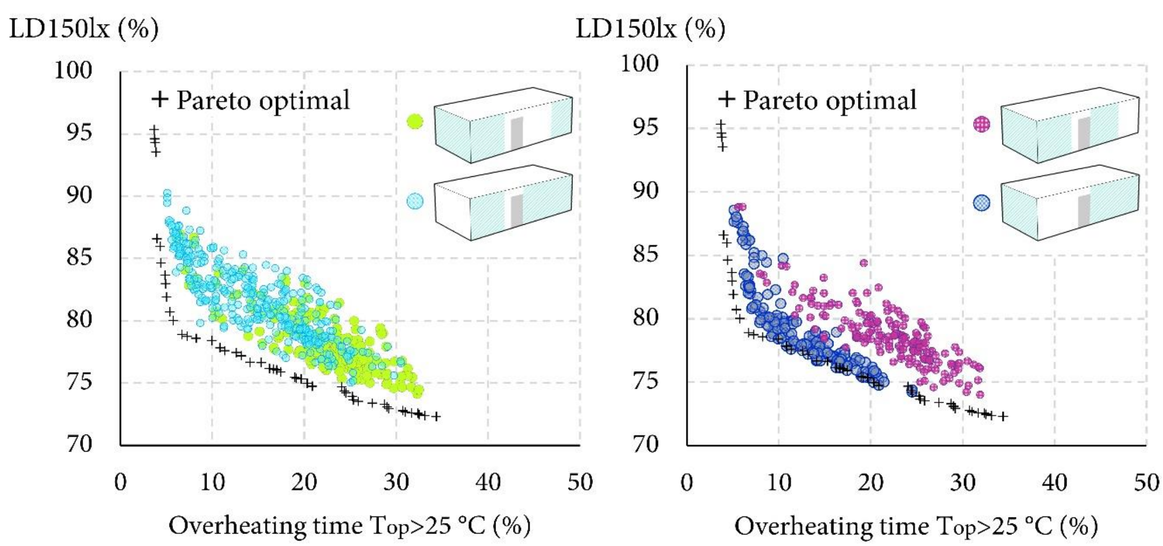

Figure 60: performance of placing three windows in different fenestration zones in terms of LD150lx and overheating time (Top>25 °C)

For the case of two windows (Figure 61), the results are exactly the opposite from the daylighting and heating optimization (Figure 35 in section 3.2.2). Placing the windows on F2-F3 (green points) induces high overheating times, compared to using F2-F5 (light-blue points). Placing both windows on the balcony area (F4-F5, blue points) yields the optimum trade-off between daylighting and overheating time, if overheating is to be minimized. If higher overheating times can be tolerated, then placing windows on F2-F4 (pink points) or on F2-F5 (light-blue points) are the optimum choices. Overall, the optimum choices are combinations of the northern façade (F2) and the fenestration zones within the balcony area, which is approximately the real case.

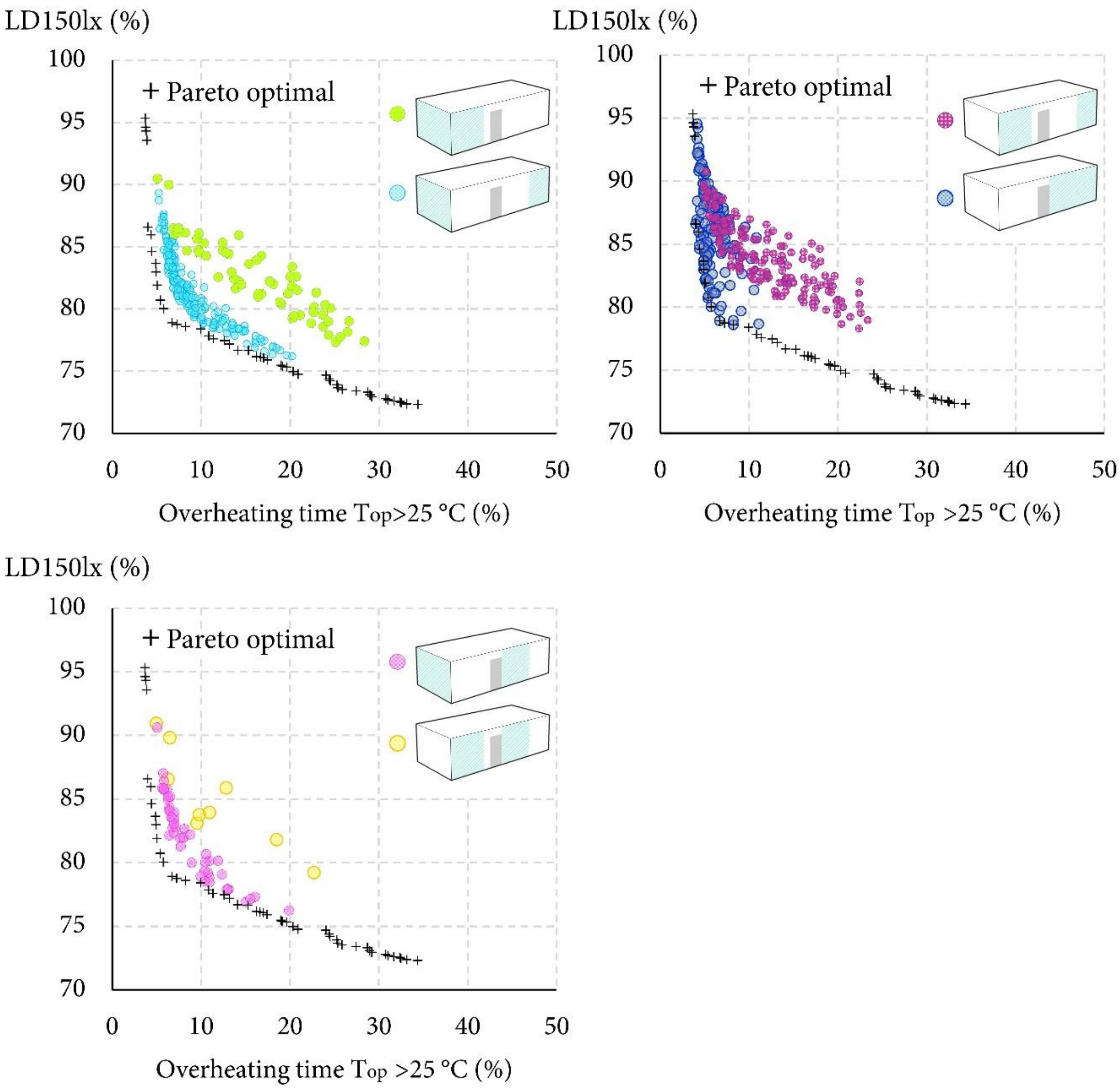

Figure 61: Performance of placing three windows in different fenestration zones in terms of LD150lx and overheating time (T_{op}>25 °C), compared to the Pareto optimum cases for daylighting and overheating time.

The following two figures show the daylight levels achieved and the corresponding overheating time, for cases with two and three windows. Additionally the Pareto optimal solutions of the daylighting-overheating optimization are plotted (black X). Figure 62 shows the overheating time (T_{op} > 25 °C) for the use of two windows in different fenestration zones, and the corresponding DF. In general, the figure shows that the overheating time is proportional to the DF levels achieved. The solutions that have the shortest overheating time for a given DF level are the ones that have at least one of the windows placed on the north (F2-F3, F2-F4 and F2-F5). The only Pareto optimal solutions that meet the BREEAM criteria have almost the highest possible overheating time. None of the Pareto optimal solutions from daylighting and overheating optimization (black X markers) can meet the BREEAM criteria.

When using three windows (Figure 63), avoiding placing a window on F3 results in the lowest overheating times and can also achieve the BREEAM criterion for an average DF above 2,1 %. This configuration is Pareto optimal for the optimization of daylighting and overheating. On the contrary, the daylighting and heating optimization suggests that fenestration zone F4 should be omitted (green points and black crosses). This configuration leads to the highest possible overheating times. Examining both Figures 62 and 63, it is evident that it is impossible to satisfy the BREEAM criterion and keep the overheating time (T_{op}>25 °C) below 10 % as the Passive House Institute suggests.

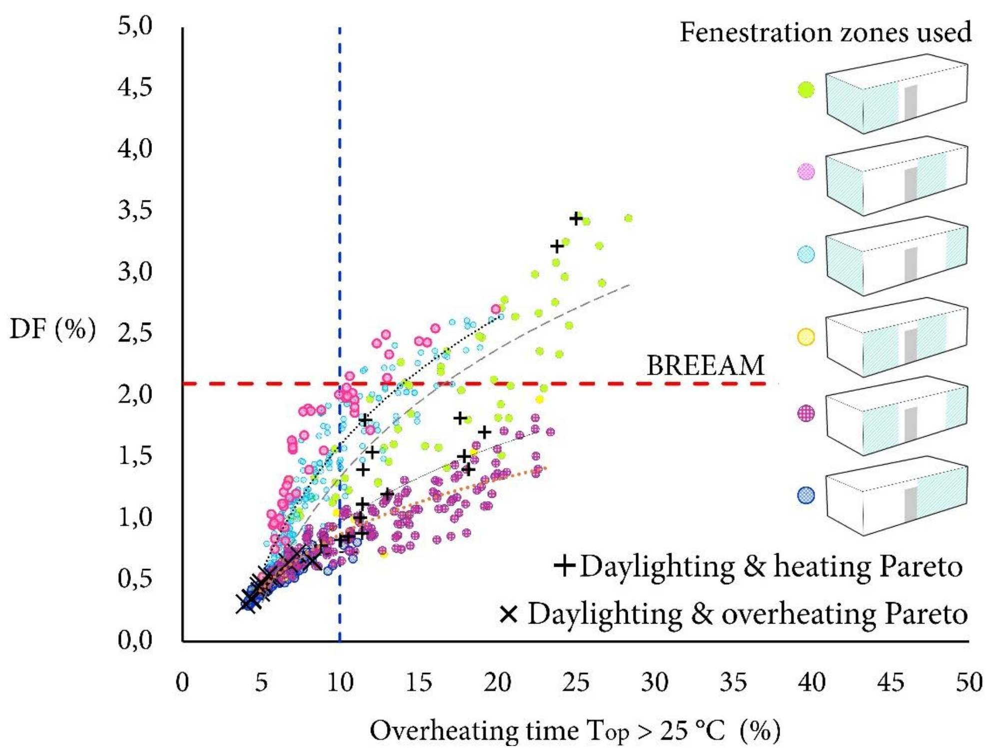

Figure 62: Overheating time (T_{op} > 25 °C) as a function of the DF for the use of two windows in different fenestration zones.

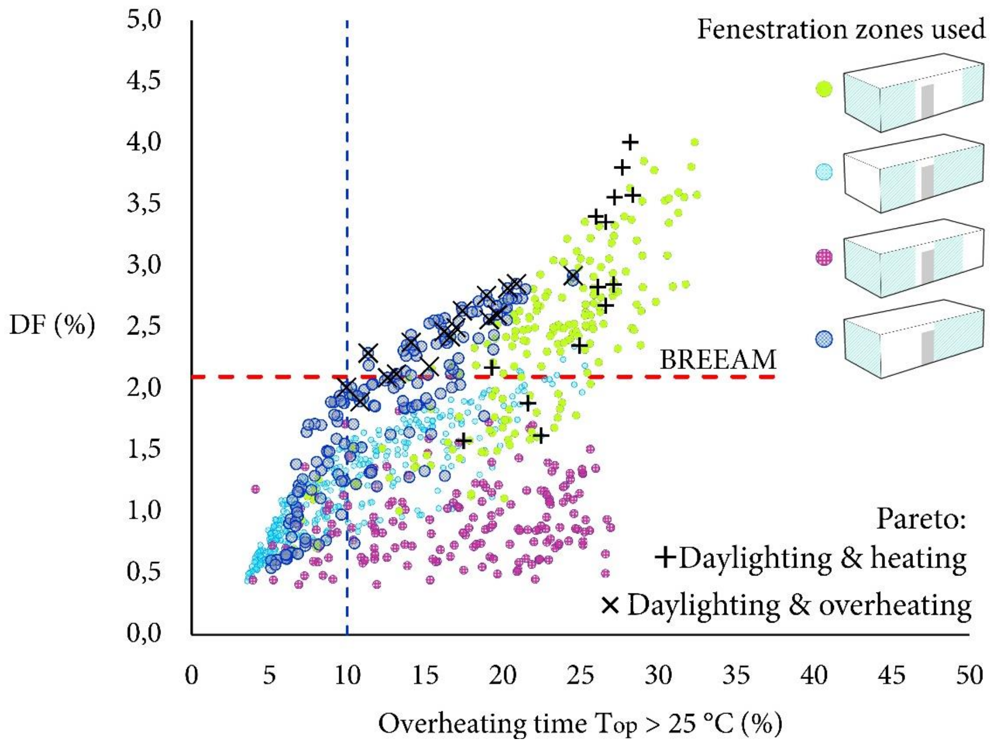

Figure 63: Overheating time (T_{op} > 25 °C) as a function of the DF for the use of three windows in different fenestration zones.

3.2.5 Interdependence of daylight performance indicators

BEDROOM

These results aim at illustrating the interdependence between different daylight performance indicators. Figure 64 shows the correlation between DF and DA50lx for each orientation, considering different WWRs. This figure shows that equal DA50lx levels correspond to the same DF levels for all orientations. The exception is on the west, for WWRs smaller than 20 %. Regarding the Pareto optimal window designs, it is shown that most of them pass the BREEAM criterion. The ones that fail are the WWRs below 30 % for the north orientation.

Overall, Figure 64 shows that the relationship between DF and DA50lx is not linear, but exponential. As the DA50lx increases, DF increases exponentially. The increase in DA50lx is not the same when going from a DF of 1 % to 2 % compared to going from 3 % to 4 %.

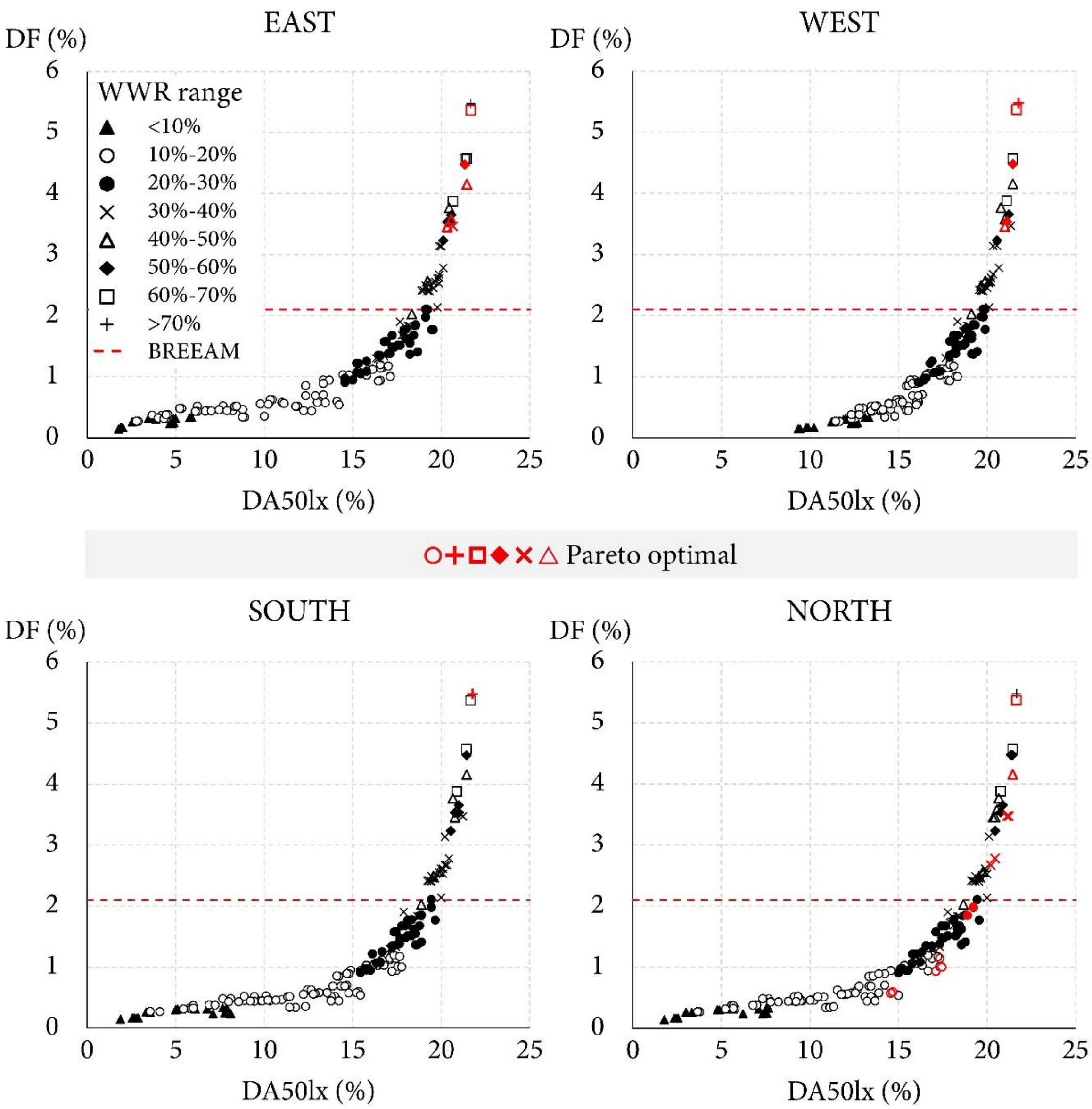

Figure 64: Correlation of DF and DA for different WWRs and orientations of the bedroom.

Figure 65 shows the correlation of the DA50lx with the minimum point DF according to the Green Building Council. Even though the west achieves higher DA levels on average, it seems that in order to satisfy the minimum point DF the DA50lx has to be the same for all orientations, just above 21 %. It is also interesting that only a 10 % of the cases for each orientation can achieve the requirement for a minimum point DF of 1,2 %. The similarity between the orientations can be attributed to the low illuminance threshold of 50lx, used for the DA. For higher thresholds, the direct solar component becomes more important and thus the optimum orientation is determined by the occupancy schedule used. Overall, the minimum WWR to meet the requirement is 20 % to 30 %.

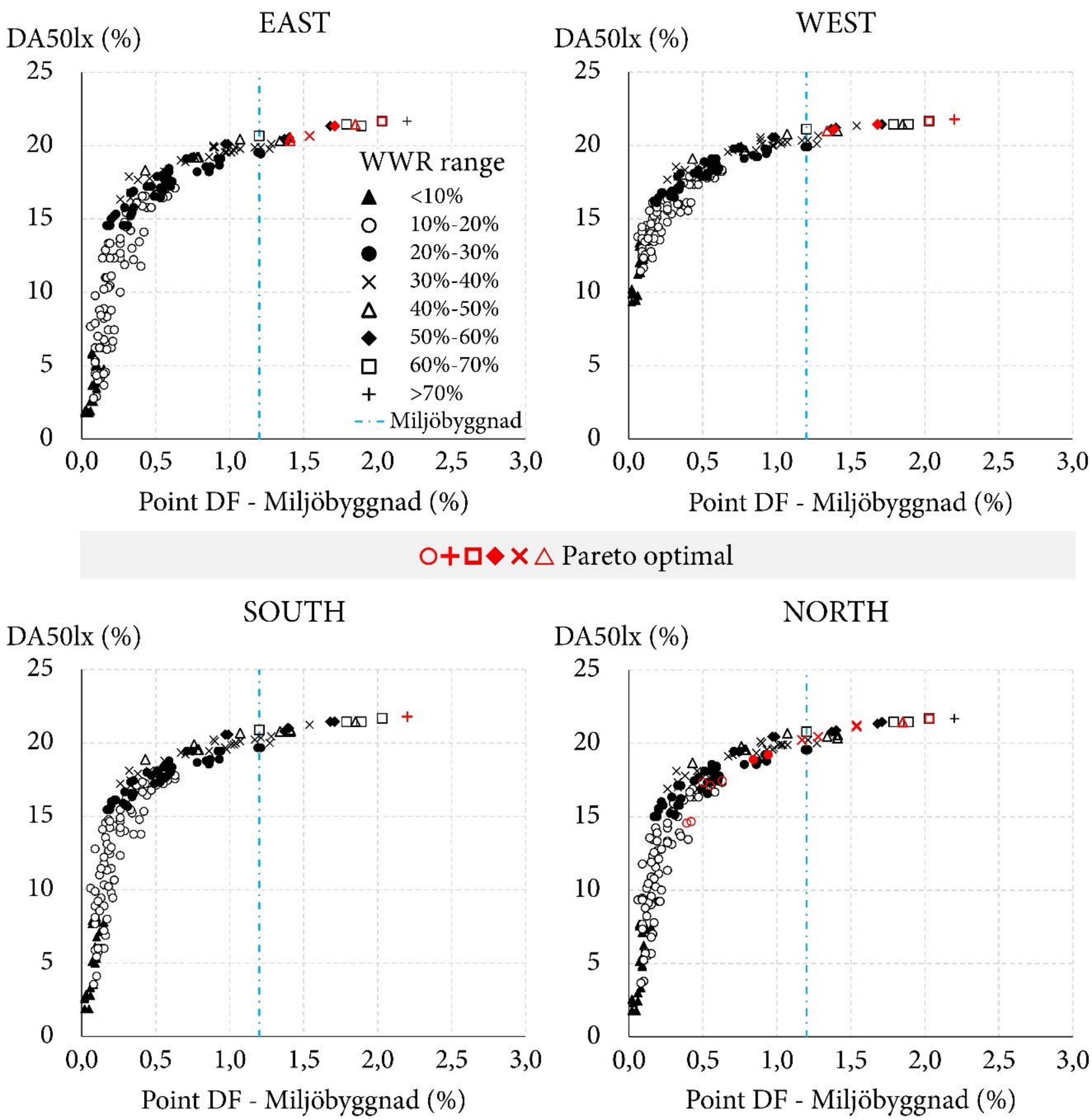

Figure 65: Correlation of DA50lx and the minimum point DF according to the Green Building Council, as a function of the WWR.

The minimum point DF is set by the Green Building Council in order to ensure that even the darkest area in a room is illuminated by a minimum amount of daylight. An average DF of all points of a room can convey more information about the available daylight, with respect to the occupant perception. To find a correlation between the latter two, the median DF and the minimum point DF were plotted in a single figure, for all window designs (Figure 66).

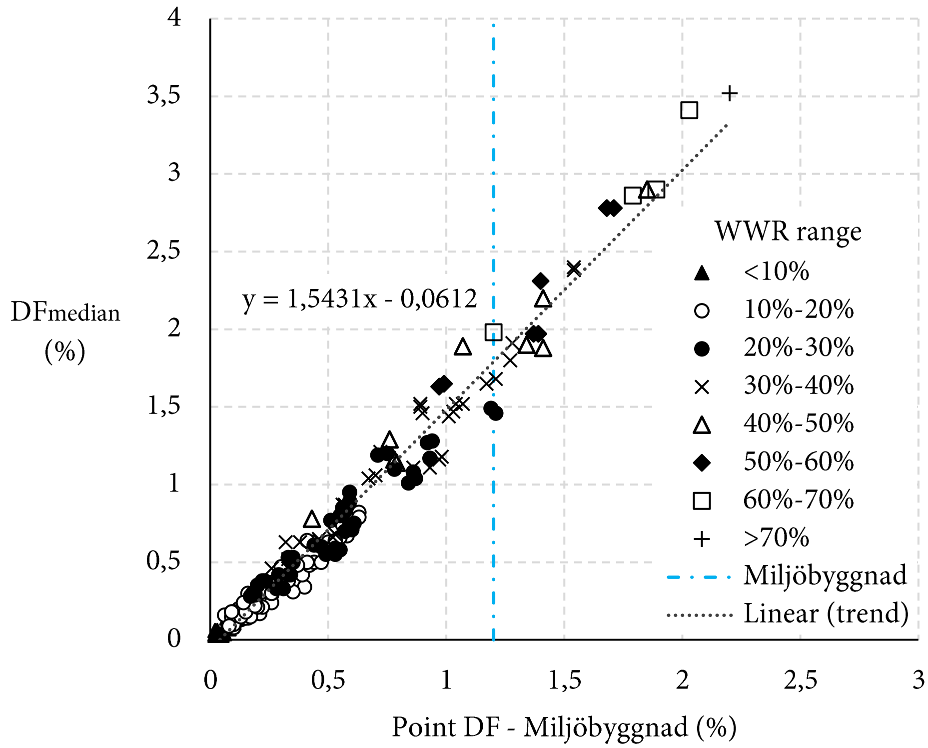

Figure 66: Correlation of DA_{median} and the minimum point DF according to the Green Building Council.

Figure 66 shows that there is an almost linear correlation between the two performance indicators, with a coefficient of determination R^2= 0,98, in a total of 185 simulated cases. The correlation can be approximated to: minimum point DF = 0,67 · DF_{median} · This means that instead of using the geometric rules of the Green building council, a DF simulation across multiple sensor points can be used to define whether or not there are dark areas inside the room.

LIVING ROOM

Although there is a considerable amount of overcast sky conditions in the Swedish context, using the DF metric might not always be the best practice, since it cannot capture the hourly differences that the climate-based metrics can. The problem here concerns the bi-objective optimization of daylighting and heating. The following two figures show the daylight levels for 600 different fenestration designs, and the corresponding specific energy use. In Figure 67 the daylight metric used is the DA150lx, whereas in Figure 68 it is the average DF. It is shown that for a given energy intensity, the west orientation achieves higher daylight levels when using the DA150lx (Figure 67), while the east is performing better when the daylight metric used is the DF (Figure 68). In addition, the proportion of the variance when using DA150lx is lower compared to using DF.

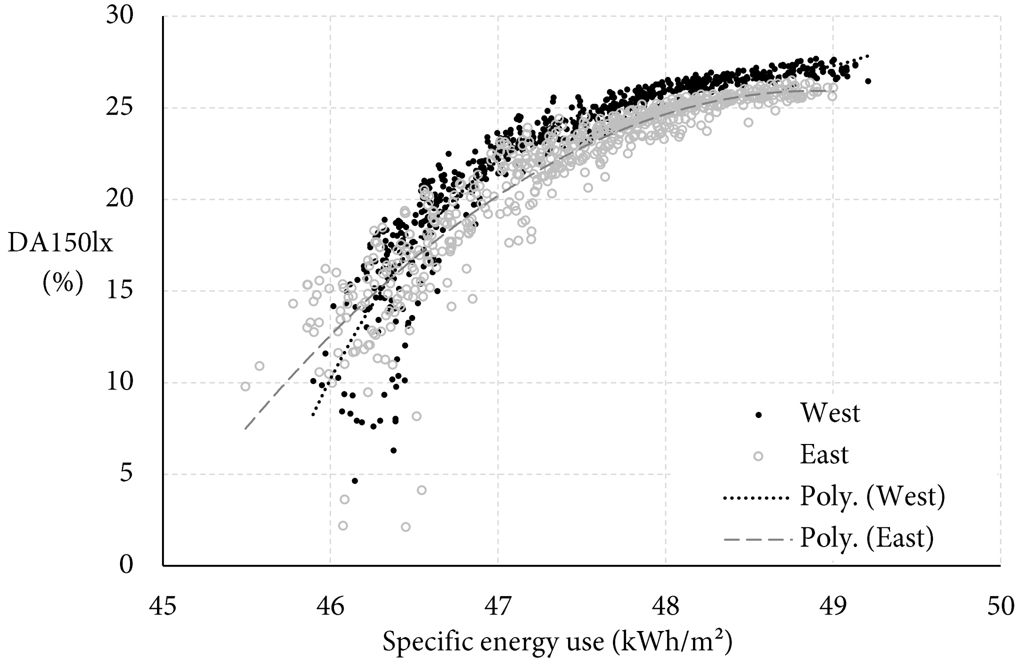

Figure 67: DA150lx and specific energy use for 600 fenestration designs on west and east orientations

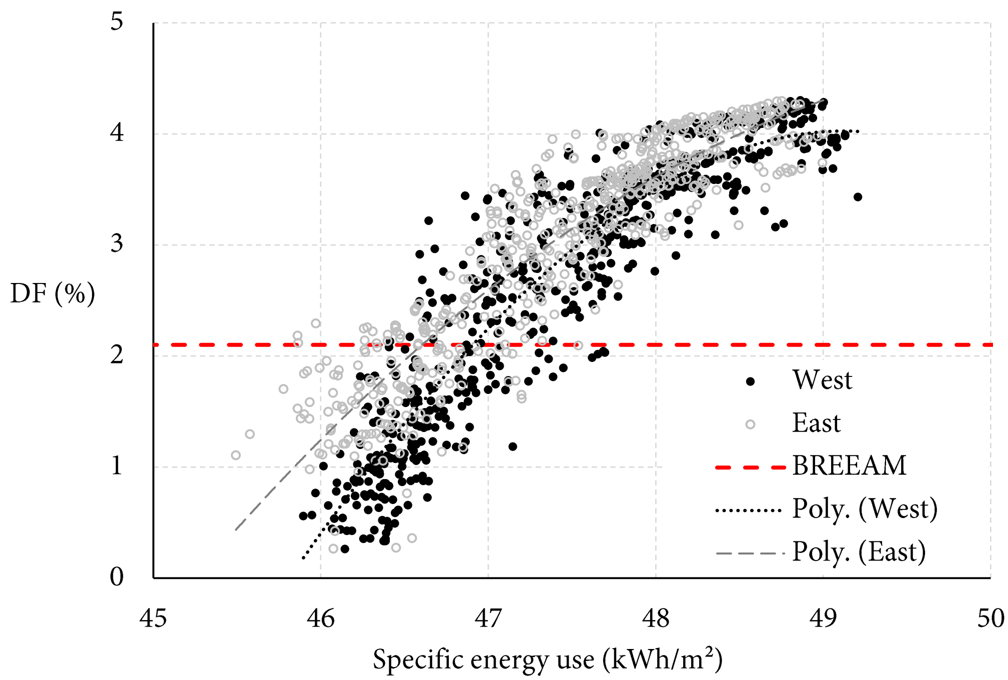

Figure 68: Average DF and specific energy use for 600 fenestration designs on west and east orientations.

Figure 69 shows the correlation of the overlit area with the DA150lx (left chart) and DF (right chart). The overlit area is the percentage of the area for which the illuminance is ten times higher than the 150 lx threshold, hence 1500 lx, for more than 5 % of the occupancy time. This amount of illuminance in reality is direct sun patches on the sensor points. For the west orientation, it is shown that a given overlit area percentage can correspond to a DA150lx range of 5 %, i.e. an overlit area of 50 % corresponds to a DA150lx between 20 % and 25 % (left chart). The same overlit area (50 %) corresponds to a DF ranging from 1,7 % to 3,6 %, which is a much higher range considering the lower and upper bounds of the two metrics. In brief, there is not as clear of a correlation between the average DF and the possibly overlit areas as there is with the DA150lx, which is normal, since DA150lx includes sunlighting, which is in direct correlation with overlit areas. Regarding the orientation, it is evident that more sunpatches can be found on the west orientation, due to the occupancy schedule of 18:00 to 21:00 hours.

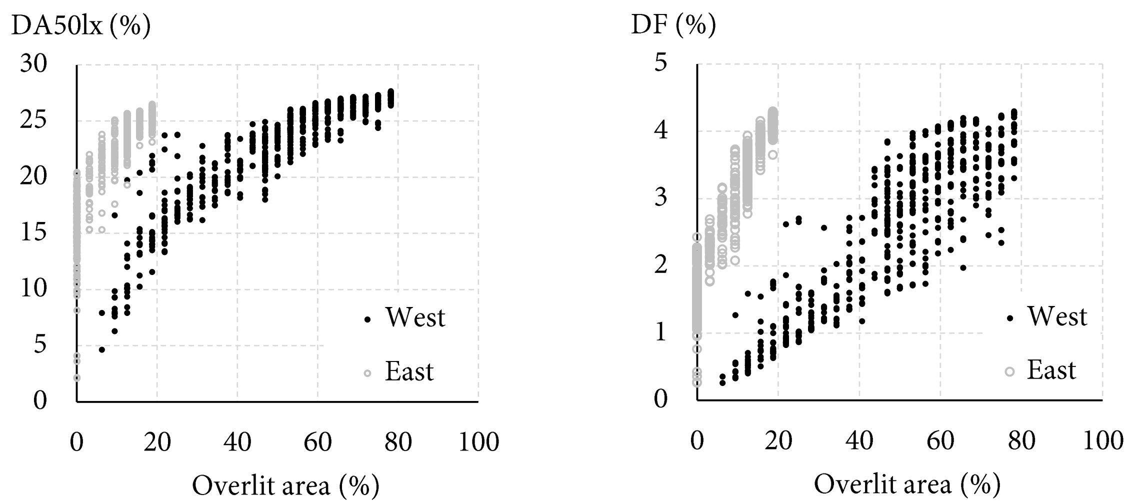

Figure 69: Correlation of the overlit area with the DA150lx (left chart) and DF (right chart).

If a clear correlation between DF and DA150lx could be established, then the DF could be used to define the daylight conditions better. Figure 70 shows the correlation between DA150lx and DF for different amount of windows used to fenestrate the west living room. The figure shows that the coefficient of determination for the trends of each dataset is increasing as the number of windows decreases. In other words, when less windows are utilized, the correlation between DA150lx and DF is lower. This variability is not necessarily a function of the number of windows, but of their position on the façade.

In the case of two windows (Figure 70), the variability is a result of the many options for window placement. The balcony area could have two windows or none, which is considerably different, due the shading of the balcony slabs. Figure 71 shows the correlation of DA150lx and DF for different placement of two and three windows on the living room zone. It is shown that for a given DA150lx, the DF can vary depending on whether or not the windows admit high amounts of irradiation on a specific area (green points) or low (blue points).

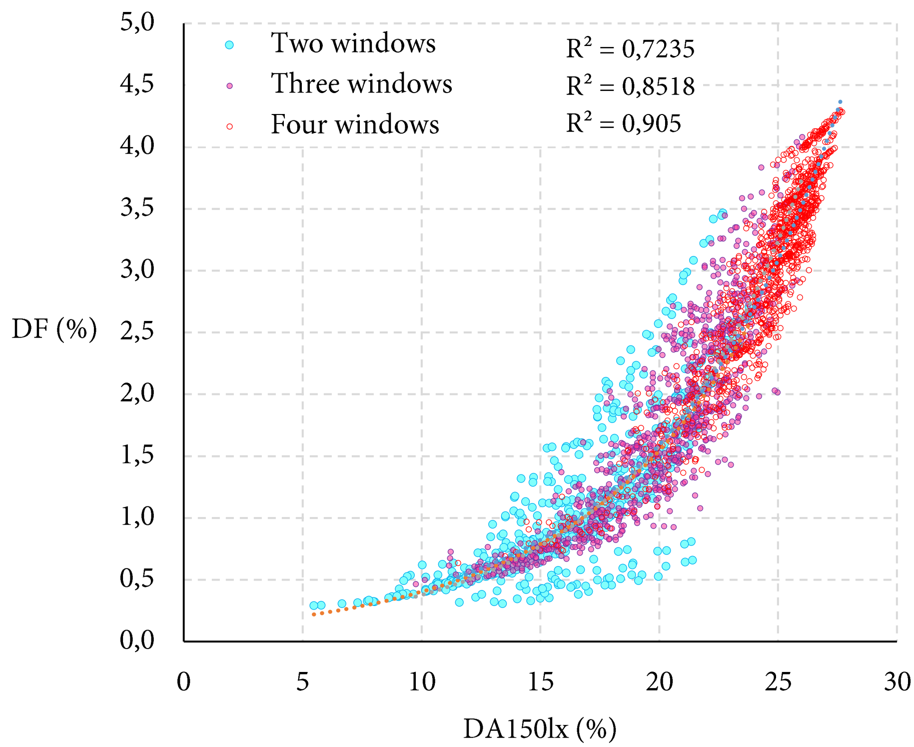

Figure 70: Correlation between DA150lx and DF for different number of windows used to fenestrate the west living room.

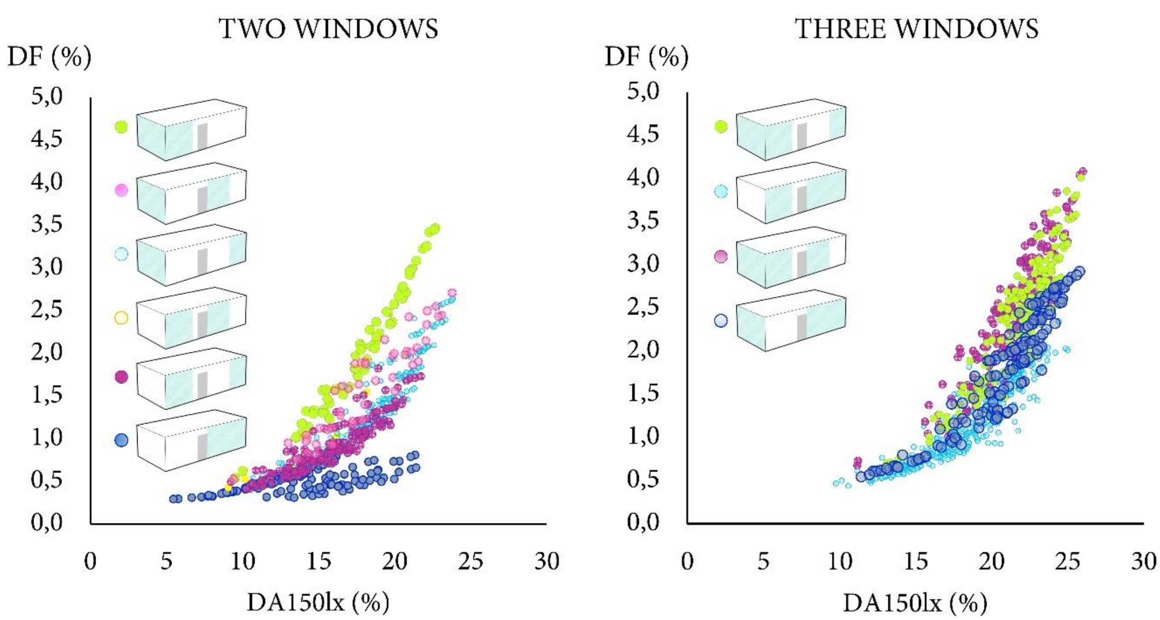

Figure 71: Correlation of DA150lx and DF for different placement of two and three windows on the living room zone.

Figure 72 and 73 show the DA150lx and DF distribution for two fenestration designs of an equal WWR: A case where the windows are placed behind the balcony area, shaded by the balcony slab of the upper floor, and a case where the windows are placed on fenestration zones F2 – F3, where there is no obstruction above the windows head. The results indicate that for both cases, the DA150lx distribution across space is more even than the DF distribution.

The median DA150lx is approximately equal to the average DA150lx. On the contrary, the DF reaches high values in front of the openings, and it rapidly decreases for sensors away from them. The result is that a large part of the living room area is illustrated as completely dark. In the case of the DA150lx, illuminated meshes are reported further away from the windows, as direct irradiation is modelled bouncing on interior surfaces. It is interesting that the average DA150lx between the two cases increases from 14,5 % to 17,1 % (18 % increase), while the corresponding DF values increases from 0,71 % to 2,02 % (185 % increase).

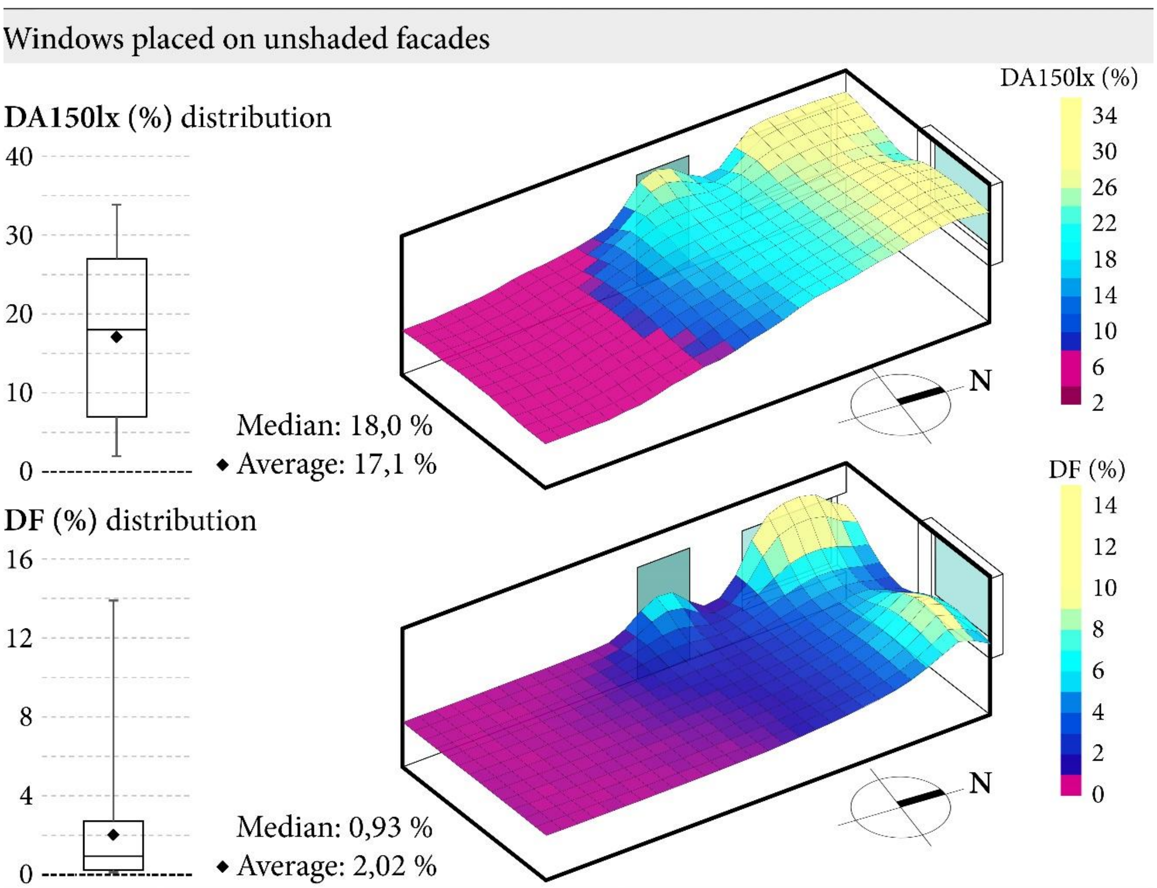

Figure 72: Comparison between the DA150lx and the DF distribution for the case of two unshaded (by the balcony) windows.

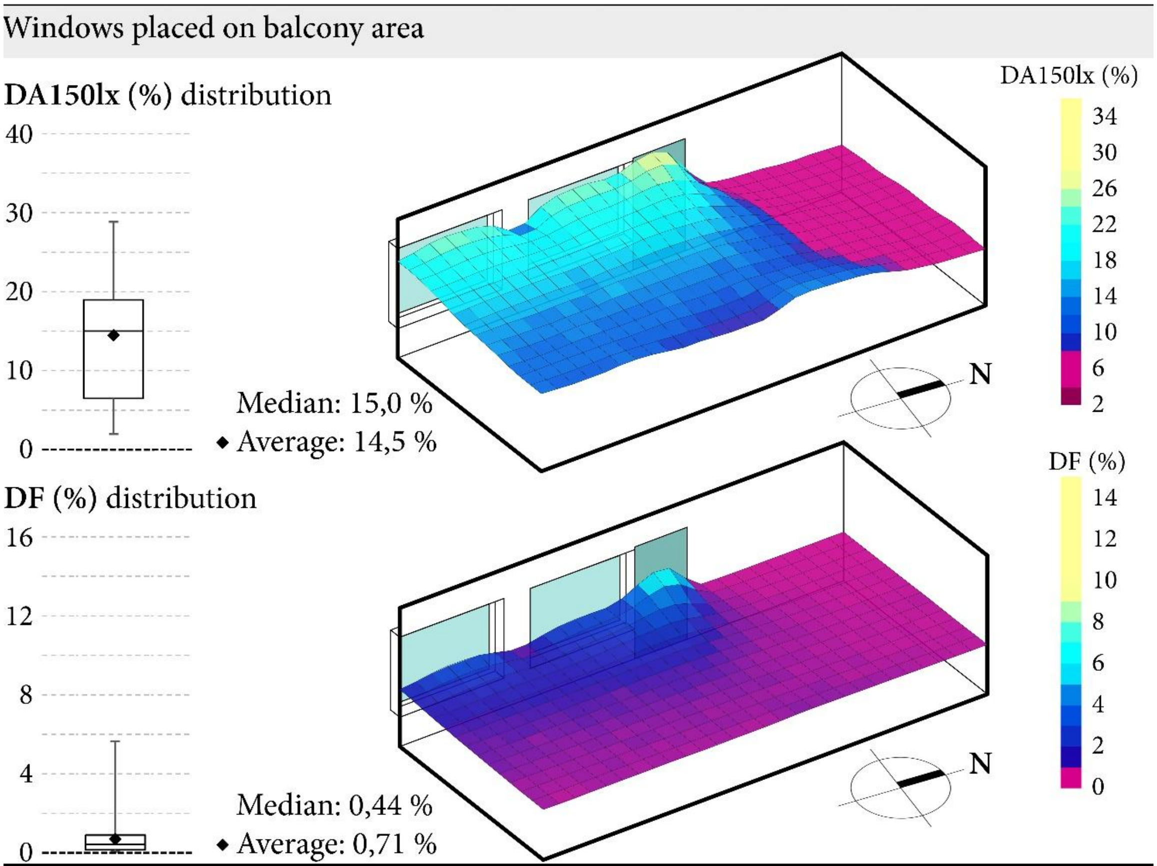

Figure 73: Comparison between the DA150lx and the DF distribution for the case of two shaded (by the balcony) windows.

3.2.6 Selection based on multiple objectives

This section only investigates the west apartment, and specifically the living room area. There were 51 Pareto optimal solutions for the optimization of heating and daylight, and 48 for the optimization of daylighting an overheating time. A choice of two or three best cases between these designs was made based on the following criteria: Number of windows, specific energy use, overheating time, DA150lx, DF and UR. The cases are shown below, for the possibilities of having two or three windows.

Daylighting and Heating optimization - Designs with two windows

Figure 74 shows the two-window solutions that achieve the highest possible uniformity ratio UR. It is shown that the windows in order to satisfy this objective are spread on the apartment envelope, in other words, there is a considerable distance between the two windows. What is interesting here, is that for a pareto optimal solution to have a high uniformity ratio, the average DF is below the BREEAM requirement of 2,1 %.

RENDERING	PHENOTYPE	WWR* (%)	SEU* (kWh/m²)	OT* (%)	DA150lx* (%)	DF* (%)	UR* (-)
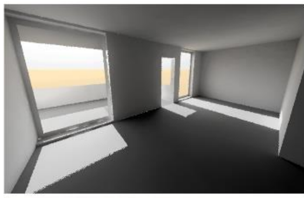	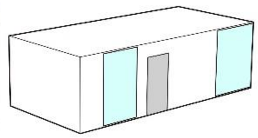	33,4	46,5	22,6	20,5	1,4	0,17
	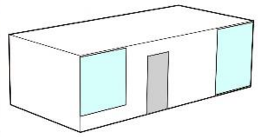	34,1	46,6	23,4	21,0	1,7	0,15

*WWR: Window-to-wall ratio, SEU: Specific energy use, OT: Overheating time, DA: Daylight autonomy, DF: Daylight factor, UR: DF uniformity ratio

Figure 74: Two-window Pareto optimal solutions that achieve the highest possible uniformity ratio UR.

Figure 75 shows the two-window solutions that achieve the BREEAM criterion for an average DF of 2,1 %. The figure shows that the windows are not placed on the balcony area, in order to capture a higher portion of the sky dome, thus, more diffuse irradiation. The achieved DF values are significantly higher than the BREEAM requirement (3,2 % and 4,5 %). The problem here is the low uniformity ratio, which is a result of placing both windows on the far north-west part of the living room. Compared to the previous figure (high uniformity), the overheating time is slightly higher in this case.

RENDERING	PHENOTYPE	WWR* (%)	SEU* (kWh/m²)	OT* (%)	DA150lx* (%)	DF* (%)	UR* (-)
	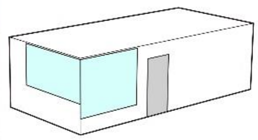	35,7	46,6	26,5	21,9	3,2	0,06
	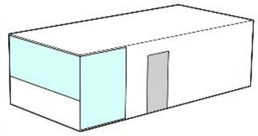	40,3	46,9	28,4	22,6	4,5	0,07

*WWR: Window-to-wall ratio, SEU: Specific energy use, OT: Overheating time, DA: Daylight autonomy, DF: Daylight factor, UR: DF uniformity ratio

Figure 75: Two-window solutions that achieve the BREEAM criterion for an average DF of 2,1 %.

Daylighting and Heating optimization - Designs with three windows

Figure 76 shows the three-window Pareto optimal designs that achieve the highest possible DF and UR simultaneously. These cases are approximately the same as in Figure 73, where UR was maximized for two windows, only with an additional window high up on the northern façade to improve the DF.

RENDERING	PHENOTYPE	WWR* (%)	SEU* (kWh/m²)	OT* (%)	DA150lx* (%)	DF* (%)	UR* (-)
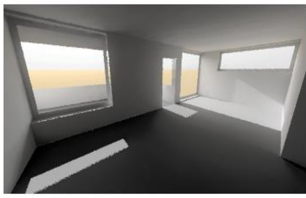	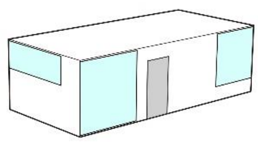	47,2	47,1	30,9	24,4	2,8	0,14
	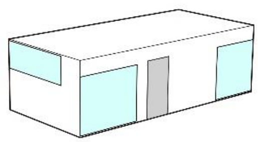	43,4	46,9	28,9	23,4	2,4	0,14
	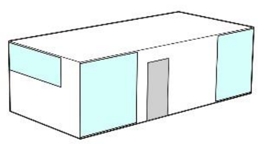	50,3	47,1	31,8	24,6	2,9	0,15

*WWR: Window-to-wall ratio, SEU: Specific energy use, OT: Overheating time, DA: Daylight autonomy, DF: Daylight factor, UR: DF uniformity ratio

Figure 76: Pareto optimal three-window designs that maximize DF and UR simultaneously.

Figure 77 shows the Pareto optimal three-window solutions that achieve the BREEAM criterion and have the lowest possible overheating time. It is evident that smaller WWR induces less overheating, as the difference between the two cases is considerable large. The small highly placed windows help achieve a high DF by letting light penetrate deeper in space. The problem is that they are not as spread on the available envelope area, leading to a very low uniformity ratio (second case).

RENDERING	PHENOTYPE	WWR* (%)	SEU* (kWh/m²)	OT* (%)	DA150lx* (%)	DF* (%)	UR* (-)
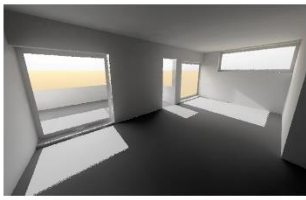	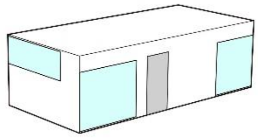	43,4	46,9	28,9	23,4	2,4	0,14
	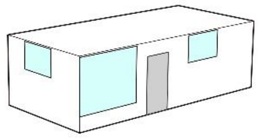	31,1	46,5	23,3	19,7	2,2	0,06

*WWR: Window-to-wall ratio, SEU: Specific energy use, OT: Overheating time, DA: Daylight autonomy, DF: Daylight factor, UR: DF uniformity ratio

Figure 77: Pareto optimal three-window solutions that achieve the BREEAM criterion and have the lowest possible overheating time.

Figure 78 shows the Pareto optimal three-window solutions that result in the lowest possible specific energy use and have the highest possible DA150lx simultaneously. The window-to-wall ratio can be 37 % when placing all windows on the west façade, and 31 % when placing one of the windows on the northern façade. The latter is achieving a higher DF but a lower UR.

RENDERING	PHENOTYPE	WWR* (%)	SEU* (kWh/m²)	OT* (%)	DA150lx* (%)	DF* (%)	UR* (-)
	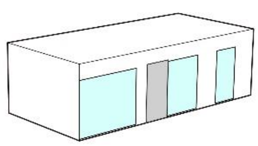	37,2	46,5	26,2	20,8	1,6	0,13
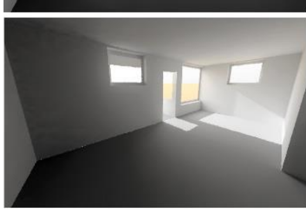	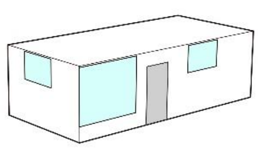	31,1	46,5	23,3	19,7	2,2	0,06

*WWR: Window-to-wall ratio, SEU: Specific energy use, OT: Overheating time, DA: Daylight autonomy, DF: Daylight factor, UR: DF uniformity ratio

Figure 78: Pareto optimal three-window solutions that yield the lowest possible specific energy use and have the highest possible DA150lx.

Daylighting and Overheating optimization - Designs with two windows

Figure 79 shows the Pareto optimal two-window solutions that yield the higher DA150lx levels and the least optimum overheating time. The WWR is 20 % - 23 %, and the windows are placed behind the balcony, to avoid solar irradiation that could overheat the living room. When optimizing this two parameters, the DF is at very low levels, and the uniformity is average.

RENDERING	PHENOTYPE	WWR* (%)	SEU* (kWh/m²)	OT* (%)	DA150lx* (%)	DF* (%)	UR* (-)
	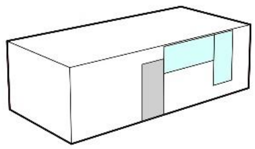	20,0	47,5	4,9	17,0	0,4	0,10
	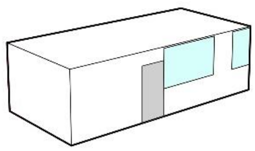	23,0	47,5	5,0	18,1	0,5	0,13

*WWR: Window-to-wall ratio, SEU: Specific energy use, OT: Overheating time, DA: Daylight autonomy, DF: Daylight factor, UR: DF uniformity ratio

Figure 79: Pareto optimal two-window solutions that yield the higher DA150lx levels and the least possible overheating time.

Figure 80 shows the two-window designs that yield the lowest possible specific energy use while keeping a low overheating time. In order to satisfy these two objectives, the algorithm converged to smaller WWRs (16 % - 17 %), with a negative impact on the daylight conditions.

RENDERING	PHENOTYPE	WWR* (%)	SEU* (kWh/m²)	OT* (%)	DA150lx* (%)	DF* (%)	UR* (-)
	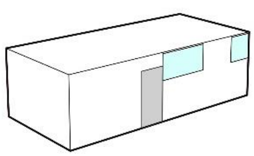	16,0	47,3	4,0	13,4	0,3	0,10
	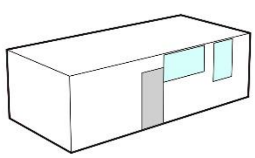	17,0	47,4	4,4	14,0	0,3	0,12

*WWR: Window-to-wall ratio, SEU: Specific energy use, OT: Overheating time, DA: Daylight autonomy, DF: Daylight factor, UR: DF uniformity ratio

Figure 80: Pareto optimal two-window designs that yield the lowest possible specific energy use while keeping a low overheating time.

Daylighting and Overheating optimization - Designs with three windows

Figure 81 shows the three-window designs that yield the highest possible uniformity ratio while keeping a low overheating time and achieving the BREEAM criteria of an average DF above 2,1 %. A third window is now placed on fenestration zone (F2), to illuminate the northern part of the living room and achieve both higher UR and DF values. In order for the DF to meet the BREEAM requirement, it is a necessity that the overheating time exceeds 10 % of the occupancy time. The WWR in both designs is 36 %.

RENDERING	PHENOTYPE	WWR* (%)	SEU* (kWh/m²)	OT* (%)	DA150lx* (%)	DF* (%)	UR* (-)
	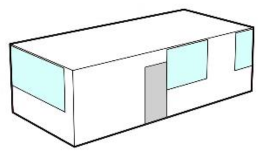	36,0	48,4	11,4	22,4	2,3	0,14
	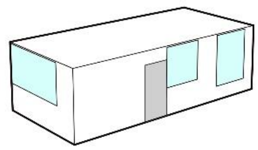	36,0	48,3	12,6	22,5	2,1	0,17

*WWR: Window-to-wall ratio, SEU: Specific energy use, OT: Overheating time, DA: Daylight autonomy, DF: Daylight factor, UR: DF uniformity ratio

Figure 81: Three-window designs that yield the highest possible uniformity ratio while keeping a low overheating time and achieving the BREEAM criteria of an average DF above 2,1 %.

Overall the results indicate that in order to reduce the overheating time, fenestration zone F3 should not be utilized. This is in conflict with the daylight and heating optimization goals, where fenestration zone F3 is needed in order to reduce the heating demand and the light dependency. Moreover, it was shown that for all cases, the average DF can achieve the highest values (over 3 %) when the windows are placed on the north-west corner of the living room, with a negative effect on the uniformity of daylight across the space.

4 Discussion

Multi-objective optimization of fenestration was investigated for a single apartment using climate-based daylight modelling (CBDM) simulations and dynamic thermal modelling (DTM) simulations. The results of the study indicate that the goals of daylight and heating are in conflict within the Swedish context, but not to a high extent when having highly insulated buildings. The issues covered in the body of this thesis are integrated below, divided in the methodology aspects and the results.

4.1 Methods

The methods used in this thesis provided the framework for the optimization process to be possible, given the relative time constraints. The long run times that the Radiance simulation engine yields, when climate-based metrics are assessed, led to the study of the daylight measurement grid in terms of the accuracy of the results and the required simulation time. The results of the study indicate that when changing the number of ambient bounces (ab) and the measurement grid size (m), the average DA150lx is not a sufficient figure to validate the model. The minimum DA150lx difference between the Reference case (6 ab and 0,25 m) and a random case (3 ab and 2,00 m) indicate that a study only on the average DA150lx fails to detect the deviations of values across space. The implementation of the ΔVol proved to be a good weighting factor, as it helped monitor the probable deviations in DA150lx, especially when changing the grid size. Overall, the results indicate that the existence of the balcony space (closed and open balcony) make it absolutely necessary to use a grid size of 1 m or less, and at least 4 ab. After a number of 3 ab, the simulation time was not really sensitive to the number of ambient bounces, as it was to the grid density, in other words, to the number of sensor points. The necessity for a high grid density indicates that the illuminance across space is highly uneven, mainly because of the shading of the balcony.

The results presented for the bedroom study showed that there is a clear correlation between DA50lx and DF for all orientations. This can be attributed to the fact that the bedroom has a simple geometrical shape, one window and is not shaded by obstructions. On the contrary, the living room study showed that it is difficult to correlate the two metrics, when there are windows receiving different amounts of irradiation. For that reason, the DA150lx was shown to express the daylight conditions more accurately in the living room area. The argument here is that although there is a high percentage of time with overcast sky conditions in Sweden, different geometries and obstructions make the climate-based metrics more precise in quantifying the daylight conditions.

A useful finding of this thesis was the correlation between the minimum point DF (as per the Miljöbyggnad requirement) and the median DF. The geometrical nature of the requirement is based on the lack of software in the past, or even in the present architecture offices. The fact is that a DF simulation across multiple sensor points can capture more effectively the probable perception of daylight in space than a single point measurement. It is therefore important to find the means to connect the older geometrical daylight rules with the state-of-the-art simulation capacities. The Miljöbyggnad minimum point DF of 1,2 % can be alternatively approximated to a median DF that is 1,5 times larger, thus DF_{median} = 1,5 · 1,2 % = 1,8 % in order to meet the current criteria. It must be noted that this correlation is only valid for simple geometries such as the bedroom, and that for more complicated plan layouts, more research has to be conducted.

When dealing with genetic optimization problems it can be difficult to conclude that any global optimum solution or set of solutions are found in the process. To a high extent, this depends on the interaction between the genes and the mathematical nature of the problem at hand. In this study roughly 0,04% of the total amount of possible window configurations were simulated. Due to the complexity of interdependent factors and size of the solution space, one can reasonably assume that given more time, the algorithm would have found additional undominated solutions. Since there are a lot more possibilities in placement for small windows it is probably in the low WWR-range that most of these solutions would have been found. Looking at Figure 4-1 it is evident that solutions are sparsely populated along the low WWR-bounds area, which indicates that convergence is yet to be reached.

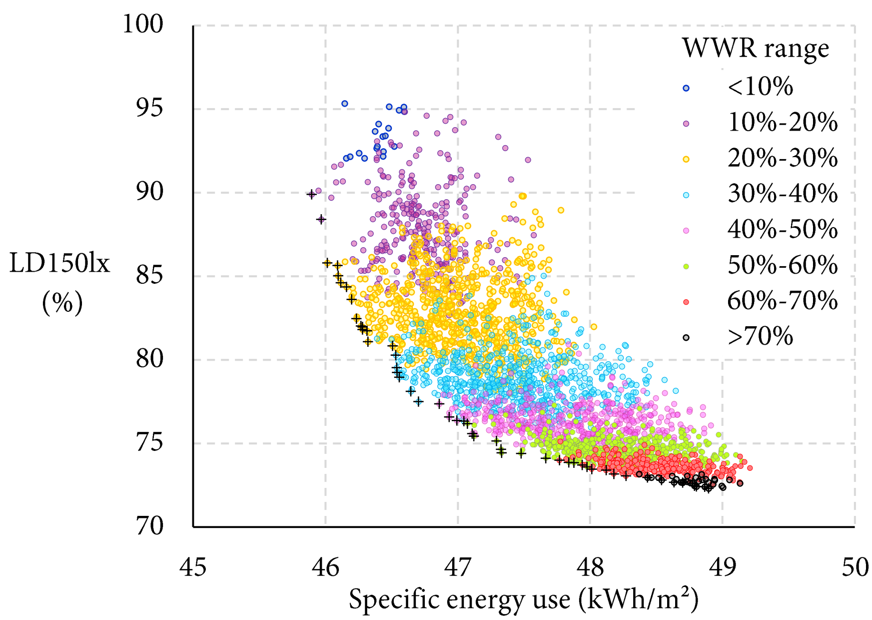

Figure 4-1: Distribution of solutions in terms of the optimization objectives of heating and daylighting, marked by their WWR ranges.

Interactive manipulation of the settings used to influence the optimization process are of paramount importance in advancing the Pareto front efficiently. Local optima can be time costly and difficult to both spot and evade. Having an informed visual overview of the qualities of phenotypes can help avoid this. In the first set of generations, as shown in Figure 4-2, one can see how the solutions were converging prematurely (already from the 5th generation). In this case, it was due to a limited set of initial solutions lacking genetic diversity, in conjunction with a relatively narrow WWR filter setting. This emphasizes the importance of correct settings, and of tools that allow user interaction to be made dynamically.

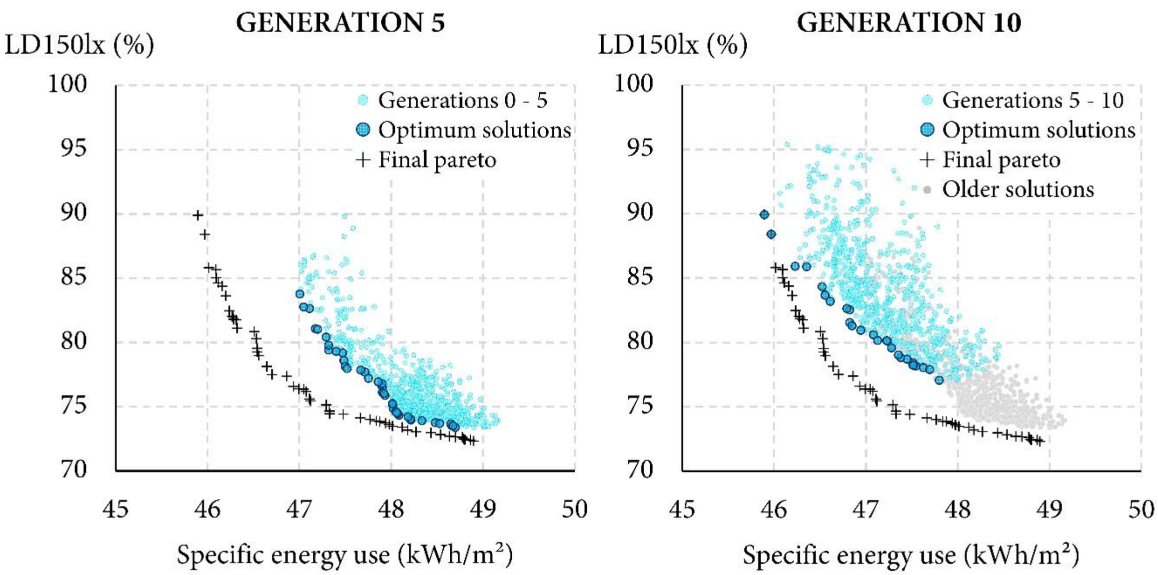

Figure 4-2: Evolution of the optimization process from the initial random generation 0 until the end of the 10th generation, for the optimization of heating and daylighting.

As geometrical filters and optimization objectives are added, the solution space shrinks. For instance, there can be limitation filters in order to maintain an equal head height and/or sill height of all windows. This can increase the chance of finding global optimum solutions faster. However, exploring only a subset of the solution space in this way comes at the risk of not finding larger trends in the dataset, which was a necessity in order to examine interdependencies in this thesis. In a practical design situation, the priorities chosen in this matter might differ from the methodology followed in this research.

4.2 Daylight and heating optimization

The study of the apartment bedroom showed that the orientation plays a major role in determining which fenestration design constitutes the optimum choice in order to satisfy both luminous and thermal needs for the occupants. The conventional rule of preferably placing windows on a south façade was validated, as for this orientation the increase of the WWR resulted in a reduction of annual heating demand, along with higher daylight levels. Nevertheless, due to the high insulation of the studied room, overheating was proven a higher issue, which is a strong argument on actually decreasing the WWR on the south façade. This argument has been stated by researchers in the past, especially for the Swedish context (Persson, et al., 2006). The north Pareto front was the most extended between all orientations, indicating that the objectives of heating and daylighting are in conflict for this orientation. An extended Pareto front actually indicates that there is a wide range of optimum solutions, from highly daylit to low-energy ones. A good practice could be to consider the actual efficiency of different energy types, and their corresponding market values. If, for example, saving 1 kWh on heating energy as opposed to saving electricity used for lighting is more beneficial in the Swedish context, then a fenestration choice should lean towards smaller WWRs for north, provided that the minimum daylight requirements are met. The opposite would be true if electricity was more expensive than heating energy. The east and west orientations presented similar performance in terms of the optimization objectives, with the west being slightly better on daylighting, due to the occupancy schedule that matched sunlighting. For these orientations, a WWR between 40 % and 50 % was shown to perform best. The low deviation between east and west on the daylight levels captured by DA50lx indicates that the low illuminance threshold of 50lx makes the choice of orientation less important in terms of DA50lx. On the other hand, the overlit area calculation where a threshold of 1500 lx was used showed a high deviation between east and west, where the overlit area plateau was 20 % for east, and 80 % for west. This indicates that the choice of orientation in terms of daylight levels is more important when the required illuminance threshold is high.

The results of the living room study indicate that it is possible to avoid simulating a large number of fenestration solutions by the use of genetic algorithms. The algorithm was proven to work as an evolutionary tool, that converges towards better performing solutions. In this case, a mere 0,04 % of all possible window configurations was simulated to reach to the Pareto front for the living room zone. The fact that it was possible to specify desired WWR ranges during the optimization process proved significantly important, as local optima of high WWRs were avoided, and the exploration of the solution space was more diverse. An inconsistency in the lower WWRs of the living room solutions can be attributed to the random initial solutions, upon which the final solutions are dependent, and on the low amount of generations. Nevertheless, these final solutions are not meant to be the global optimum solutions, but rather a good set of solutions for designers to work with in the initial design stage. Although conventional architectural wisdom is hard to be substituted by a genetic algorithm, this process can be implemented in order to acquire information about designs that will perform better in the future, and about designs that should better be avoided. The necessity here is for this approach to be followed in the initial design stage, which can shape the final building performance dramatically.

4.3 Effect of independent variables

Initially from the literature review, it was observed that the exact window placement has not been assessed as much as the impact of the WWR. The bedroom study showed that the WWR does not provide sufficient information on the building performance, in terms of daylighting. It was shown that WWRs ranging from 10 % to 20 % could actually admit more daylight than some cases ranging from 30 %-40 %. Highly placed windows resulted in higher illuminance levels, as daylight can penetrate deeper in space when it enters at a high level. From an energy perspective, it was shown that the heating demand is increasing for higher WWRs on the north, while it decreases on the south. For east and west, the heating demand was not a linear function of the WWR. Very small or very large windows yielded a higher heating demand. This indicates that the equilibrium between the building envelope losses and the solar gains is what defines the optimum WWR for these orientations. The results therefore depend on the insulation level of the windows and their placement, as well as on their g-value and their losses through radiation. The consistently optimum height-to-width ratio near 1,0 can be attributed to the lower frame area per overall window area when a shape is square rather than an elongated rectangle. This derives from the fact that the frame U-value was 1,10 W/m²K compared to the glazing U-Value of 0,6 W/m²K. Longer frames in elongated windows also yielded a higher thermal bridge between the frame and the glazing, which was set to 1,01 W/mK.

In the living room study, the optimum WWR was more dependent on the exact placement of the openings, due to the shading factor of the balcony. Several fenestration solutions of a WWR below 20 % resulted in the same specific energy use with solutions of 50 % WWR. Placing windows below the balcony proved to be costly in terms of energy use, due to the loss of passive solar gains. On the other hand, not placing any windows facing the balcony resulted in poor daylight uniformity across space, but more importantly, it resulted in overheating issues. The lack of daylight uniformity was captured by the electric lighting results, where it was shown that a more even distribution of windows throughout the envelope results in less electricity used for lighting. The dilemma is the same here: Visual comfort or energy efficiency? Nevertheless, it was consistently shown that in order to satisfy the objectives of heating and daylighting, more glazing should be placed on the unshaded western fenestration zone F3, and that placing windows only behind the balcony area is not a wise choice, unless overheating is the main priority.

The optimum number of windows for the living room area was defined to minimum two and maximum three. This was explained by the lack of daylight when using only one window, and by the extensive overheating issues when using four windows. Using four windows does not improve the daylight conditions significantly too, compared to using three.

4.4 Impact of solar gains

This thesis shows that passive solar gains are important even in the cloudy climate of Sweden and that they do contribute to reduce heating demand. It was shown that higher passive solar gains allow for larger glazing areas, when the heating demand is a priority. It should be noted here that this is true for highly insulated windows, as in this case. Increasing the WWR with poorly insulated windows would probably increase the heating demand despite the utilization of solar gains. In addition, larger glazing areas yield higher daylight levels. The outcome is that for both of the objectives, solar gains are beneficial. Future implementation of the optimization algorithm should therefore include a preliminary solar irradiation study that could define the optimum envelope areas for window implementation. On the other hand, for as highly insulated spaces as the Greenhouse apartments, the overheating time is proportional to the solar gains admitted.

The bedroom energy study showed that an increase of the window size would mostly be beneficial on the south orientation. East and west orientations can profit from passive solar heating only within specific bounds of WWR, specifically from 20 % to 40 %. The energy use outside these bounds is increased. The reason for this is that after a specific window U-value, the transmission losses become so high that the energy gained by solar radiation is not sufficient to compensate for the increase in heating demand. The low direct solar irradiation on the north on the other hand is the reason why decreasing the WWR is beneficial on this orientation, if the heating demand is to be minimized.

The living room study showed that the Pareto optimal solutions of heating and daylighting were consistently the ones with the highest possible solar gain, compared to designs of an equal WWR. This explains why the fenestration zones behind the balcony were not considered by the algorithm as much as the unshaded western zone F3. It is logical to assume, that the solar gains are a parameter to be maximized, with only the drawback of overheating. The latter could be controlled by providing windows with efficient exterior solar shading devices.

Overall, it should be noted that the solar gains of exterior surfaces, such as windows, is a combination of direct and diffuse solar radiation. The amount of this radiation that will be beneficial for a thermal zone is the part that will be transmitted through the windows and the absorbed part (by glass) that will be radiated inside the zone. The solar gain is therefore dependent on the glazing properties, which makes the presented results case specific.

4.5 Overheating time

The bedroom study showed that maximum daylight levels can be achieved with an overheating time (T_{op}>25 °C) below 10 % only on the north orientation. Although west is the orientation with the highest DA50lx for small (not overheating) WWRs, for peak DA50lx levels the required window area lead to an overheating time of 25 %. This can be attributed to the higher amount of solar gains admitted by windows facing west compared to north. In reality, the concept of measuring overheating hours is more developed for office spaces, where the occupants do not have the flexibility to use openings for natural ventilation. In the case of residential spaces, the fenestration choices have not been based on overheating time, although as it was shown, due to the highly insulated envelope of the apartment, there is a high risk of overheating. The argument here is that the occupant comfort should not depend on having windows opened, for various reasons. For instance, the ambient air is not always as healthy as it should be, and it might require filtering through the ventilation system prior to entering the interior zones.

The overheating time presented for the study of the living room zone was calculated as the number of hours during occupancy, for which the operative temperature exceeded a specific benchmark temperature. The optimum WWR to avoid overheating varies based on this temperature benchmark. For lower benchmarks (25 °C), it was shown that the overheating time increases rapidly as the WWR is increased, starting from the least amount of glazing. For higher benchmarks (28 °C), the overheating time was not increasing dramatically until a WWR of 50 % was reached. Considering that the overheating issue occurs during the summer months, when the ambient air temperature is higher, it is reasonable to assume that the occupants will have a higher tolerance for higher operative temperatures. Hence, it could be argued that it is more efficient to use a benchmark such as 28 °C, and select the glazing size based on this threshold. Overall, it was shown that overheating in conflict with the objectives of heating and daylighting, as the solar gains benefit both daylighting and heating, but increase the operative temperature.

If daylighting and overheating are the parameters to be optimized, the fenestration solutions follow a different pattern. The fenestration zones that need to be utilized are the ones that receive the least possible irradiation, hence the zones behind the balcony area, and the northern façade. If an average DF above 2,1 % is to be achieved, then placing three windows is the optimum choice, with a minimum overheating time of 10 % of the occupancy schedule. This can be considered satisfactory, considering that the occupants can also ventilate the space by opening the windows.

5 Conclusions

The main conclusions deducted from this study are stated below:

- A genetic algorithm can facilitate the exploration of different fenestration solutions, by tracking the most efficient designs and by bypassing the ones that are outperformed.
- A measurement grid size of 1,0 m and a number of 5 ambient bounces was the optimum selection for the deployment of daylight measurement sensors in the living room area. When examining different grid sizes and ambient bounces, the average DA150lx is not sufficient to validate the results, as it does not convey the information of positive or negative deviations. The proposed method of assessing the volumetric difference ΔVol proved to be a useful weighting factor for the selection of the most accurate and time-efficient settings.
- The objectives of heating and daylight are in conflict with each other on all orientations except for the south.
- Both daylighting and heating can be improved by the utilization of passive solar gains except for the north orientation. The result is an increase of the overheating time.
- The window-to-wall ratio does not provide sufficient information neither for the energy nor for the daylight performance. An energy assessment requires the height-to-width ratio and information on the window position is needed for a daylight analysis.
- The use of a balcony affects both heating and daylighting levels negatively, if the windows are placed beneath it, but it retains the operative temperature below extremes. It also improves daylight uniformity, which is connected with the electric lighting use.
- The heating demand is not dramatically affected by the WWR, as the studied apartment has a very high insulation level.
- Overheating due to the effect of solar gains is an issue for all orientations except for the north.

More specifically for the bedroom study:

- Windows on a south orientation should be maximized, if heating and daylighting are the objectives of optimization. The drawback is a high increase in the operative temperature, hence, exterior solar shading should be added to control overheating.
- The optimum WWR range on east and west orientations, for the optimization of heating and daylighting is in the range of 40 % to 50 %, more specifically 42 %.
- North windows should be square-shaped and placed high on the façade. A WWR of 34 % is adequate for satisfactory daylight levels, low heating demand and no overheating.
- The north orientation is preferable for a bedroom, as the necessary illuminance can be achieved by diffuse irradiation and the overheating time is the least possible. Alternatively,

the west orientation is a good choice due to the occupancy schedule.

- DA50lx is the highest possible when using windows with a high head height on the west.
- DA50lx stabilizes after a WWR in the range of 40 % - 50 %, more specifically 42 %.
- The Miljöbyggnad minimum point DF of 1,2 % can be alternatively approximated to a median DF of 1,5 · 1,2 % = 1,8 % for simple convex geometries with one opening. For different designs and shapes, more research should be conducted.

More specifically for the living room study:

- The optimization process can be facilitated by dynamic control over independent variables, as the window-to-wall ratio.
- Two or three windows is the optimum number of windows in order to optimize both heating and daylighting.
- It is impossible to have a Pareto optimal two-window design for heating and daylighting if a DF above 2,1 % and a high uniformity ratio are required simultaneously. The geometry of the living room area is such, that the DF and the UR are contradicting each other. Using three windows is a way to solve this issue, i.e. distributing window glazing across the building envelope.
- In order for a two-window solution to be Pareto optimal and have a high uniformity ratio simultaneously, the WWR must be 30 % - 35 % and the windows must be placed far from each other.
- In order for a two-window solution to achieve the BREEAM criterion of an average DF above 2,1 % there must be at least one window on the northern façade, placed high.
- High DF values (over 3 %) do not necessarily mean satisfactory daylight conditions for a two-window design. The results indicated that in order for the DF to exceed 3 %, the windows have to be placed on the unshaded fenestration zones F2 and F3, on the northwest corner of the living room. This results in poor daylight uniformity across space.
- If no window is placed on the unshaded (by the balcony) western fenestration zone F3, then a two-window solution cannot achieve an optimum trade-off between heating and daylighting.
- Three windows are necessary to design a Pareto optimal solution in terms of heating and daylighting, have an average DF above 2,1 % and have a high uniformity ratio simultaneously.
- When placing three windows, the unshaded (by the balcony) western fenestration zone F3 should be avoided if a DF above 2,1 % and a high uniformity ratio is to be achieved at the same time. It should also be avoided if solutions with low overheating time are sought for.
- The use of four windows does not yield significant daylighting improvement. However, it yields overheating issues.
- When using three windows, it is a necessity that the overheating time exceeds 10 % of the occupancy time, if the BREEAM DF requirement is to be met.

Future developments

The proposed optimization workflow of this thesis could be further developed in order to increase its efficiency and to decrease the computational time. A way of increasing the efficiency of convergence is by manually adding solutions that are derived based on designer intuition or geometrical rules set by a preluding study, i.e. a façade irradiation analysis. These can be input as the optimization is running and can be derived from inspiration gained from results therein, creating a feedback loop. This type of workflow can be made possible with an intuitive and data rich solution-space visualization environment, like the one created for the work with this thesis. It could be possible to divide the design process into two steps where the first step does an optimization run based on calculations with a low computational cost. Examples of this are a steady state heat transfer calculation and an estimate on solar heat gain depending on WWR distributions in different orientations. The output from this could then be used as part of an initial population in the optimization process. This has the potential of increasing the efficiency of the algorithm.

In an open scripting environment like Grasshopper that connects well with external calculation and simulation software it is possible to implement other optimization objectives that could increase relevance of the tool. Life cycle costing, moisture analysis and life cycle analysis are examples of potential additional objectives to implement in further studies.

Regarding the concept of façade optimization, future work could include shading elements and/or glazing properties (e.g. g-value). This way, the results could be altered, as higher WWRs could yield a lower overheating time, either with lower g-values or with rightly timed movable shading devices. The geometry of these devices could also be investigated in a dynamic form-generating workflow, as the one used for the generation of different window geometries for this study.

Summary

Multi-objective optimization of fenestration was investigated for a single apartment using climate-based daylight modelling (CBDM) simulations and dynamic thermal modelling (DTM) simulations. The results of the study indicate that the goals of daylight and heating are in conflict within the Swedish context, but not to a high extent when having highly insulated buildings. The latter leads to the overheating issues being a key parameter for designing.

A literature review was conducted to situate the thesis focus within the broader academic field of façade optimization. The analysis of related publications indicated that the use of a genetic algorithm could facilitate the optimization process, when multiple parameters are to be considered. Of all the parameters defining fenestration, the window position on the façade was the least investigated in past studies.

Genetic algorithms can accelerate the optimization process but they require a substantial amount of iterations to yield conclusive results. This leads to costly simulation run times, hence a parametric study was conducted to define the optimum measurement grid and the number of ambient bounces for the daylight model, in order to save time but ensure accuracy. The study showed that the optimum grid size was 1,0 m and the number of ambient bounces were 5,0.

The results included two different rooms of the apartment, the bedroom and the living room. The bedroom study focused more on the effect of different orientation and the windows head height and height-to-width ratio. The living room study examined more thoroughly the position of windows on different areas of the envelope. For both rooms, it was shown that the daylighting and heating objectives are conflicting, with the exception of the south orientation. The optimum amount of glazing area depends on the orientation and on the objective under consideration. If heating is to be optimized, south openings should be maximized, but if overheating is the defining parameter, then northern windows should be larger.

The results indicated that the window-to-wall ratio does not constitute sufficient information on the building performance, in terms of daylighting. It was shown that WWRs ranging from 10 % to 20 % could actually admit more daylight than some cases ranging from 30 %-40 %. Highly placed windows resulted in higher illuminance levels, as daylight can penetrate deeper in space when it enters at a high level. In addition, the annual heating demand can be improved by placing windows on surfaces with a high solar gain, while daylight uniformity and the electricity use for lighting can be more effectively improved when spreading the openings throughout the envelope.

Overall, the results indicate that the optimization process can lead to a good set of solutions for designers to work with in the initial design stage. Although conventional architectural wisdom is hard to be substituted by a genetic algorithm, this process can be implemented in order to acquire information about designs that will perform better in the future, and about designs that should better be avoided. The necessity here is for this approach to be followed in the initial design stage, which can shape the final building performance dramatically.

6 References

Acosta, I., Laborda, M. A. C. L. & Muñoz, C. M., 2013. *Daylight in window design: optimization of proportion and position under overcast sky conditions.* Lisbon, s.n., p. 45.

Aizlewood, M. et al., 1998. *Data Sets for the Validation of Daylighting Computer Programs.* Ottawa (Canada), Proceedings of the Daylighting '98 Conference: International Conference on Daylighting Technologies and Energy Efficiency in Buildings.

Anon., 2015. *Passive House Institute.* [Online]
Available at: http://www.passiv.de/en/01_passivehouseinstitute/01_passivehouseinstitute.htm
[Accessed 16 March 2016].

Aries, M., Aarts, M. & van Hoof, J., 2015. Daylight and health: A review of the evidence and consequences for the built environment. *Lighting Research & Technology*, Volume 47, pp. 6-27.

ASHRAE, 2013. *Handbook-Fundamentals.* s.l., American Society of Heating and Air-Conditioning Engineers.

Bader, J. & Zitzler, E., 2008. HypE: An Algorithm for Fast Hypervolume-Based Many-Objective Optimization. *Evolutionary Computation*, Volume 19, pp. 45-76.

BBR22, 2015. *Regelsamling för byggande,* Karlskrona (Sweden): Boverket. ISBN 978-91-7563-254-4.

BELOK, 2008. *Innemiljökrav,* Version 3: BELOK Effektiv energi i lokaler.

Bladh, M., 2008. *En lysande framtid? Om belysning i hemmen,* s.l.: ISSN 1101-1289 ISRN LiU TEMA-T-WP-XXX-SE.

BREEAM, 2014. *Code for sustainable built environment,* s.l.: Technical Manual SD5076:0.1. 61-63.

Bülow-Hübe, H., 2001. *Energy-Efficient Window Systems, Effects on Energy Use and Daylight in Buildings,* Lund: LTH, Lund University.

Burke, E. K. & Kendall, G., 2005. *Search Methodologies - Introductory Tutorials in Optimization and Decision Support Techniques.* 1st ed. New York: Springer Science+Business Media, LLC.

Caldas, L., 2008. Generation of energy-efficient architecture solutions applying GENE_ARCH: An evolution-based generative design system. *Advanced Engineering Informatics*, Volume 22, pp. 59-70.

Caldas, L. G. & Norford, L. K., 2002. A design optimization tool based on a genetic algorithm. *Automation in Construction*, Volume 11, pp. 173-184.

Chantrasrisalai, C., Ghatti, V., Fisher, D. & Scheatzle, D., 2003. *Experimental Validation of the EnergyPlus Low-Temperature Radiant Simulation,* s.l.: ASHRAE Transactions. 109(2):614-623.

Christoffersen, J., Johensen, K., Petersen, E. & Hygge, S., 1999. *Post-occupancy evaluation of danish office buildings.* s.l., CIE.

CORE studio , (. T., 2014. *AEC Techonlogy Symposium & Hackathon 2014 Hackathon Info.* [Online]
Available at: http://core.thorntontomasetti.com/aec-technology-symposium-2014/aec-technology-symposium-2014-hackathon/
[Accessed 4 May 2016].

Crhistoffersen, J., 1995. *Daylight Utilisation in Office Buildings. PhD thesis,* s.l.: Horsholm: SBI forlag. (SBI-report; No. 258).

Designbuilder, 2015. *Version 4.2.0.054.* Designbuilder Software Ltd, (UK).

Dubois, M.-C., 2001. *Impact of Shading Devices on Daylight Quality in Offices Simulations with Radiance,* Lund: Lund University.

Dubois, M.-C., 2001. *Impact of Shading Devices on Daylight Quality in Offices. Simulations with Radiance,* Lund (Sweden): PhD Thesis. Lund University, Lund Institute of Technology. Report No TABK--01/3062.

Du, J., Hellström, B. & Dubois, M.-C., 2014. *Daylighting utilization in the window energy balance metric: Development of a holistic method for early design decisions,* Lund: LTH, Lund University.

FEBY 12, 2012. *Kravspecifikation för nollenergihus, passivhus och minienergihus - Bostäder,* (SWEDEN): Sveriges Centrum för Nollenergihus. LTH rapport EBD-R-12/36.

FEBY12, 2012. *Kravspecifikation för nollenerfihus, passivhus och minienergihus, Bostäder,* s.l.: Sveriges Centrum för Nollenergihus. (Sweden).

Fritz, R. M. & McNeil, A., 2016. *RADSITE.* [Online]
Available at: http://www.radiance-online.org/about
[Accessed 20 March 2016].

Futrell, B. J., Ozelkan, E. C. & Brentrup, D., 2015. Bi-objective optimization of building enclosure design for thermal and lighting performance. *Building and Environment*, Volume 92, pp. 591-602.

Gagne, J. & Andersen, M., 2012. A generative facade design method based on daylighting performance goals. *Journal of Building Performance Simulation*, Volume 5, pp. 141-154.

Gago, E., Muneer, T., Knez, M. & Köster, H., 2015. Natural light controls and guides in buildings. Energy saving for electrical lighting, reduction of cooling load. *Renewable and Sustainable Energy Reviews*, Volume 41, pp. 1-13.

Ghisi, E. & Tinker, J. A., 2005. An Ideal Window Area concept for energy e cient integration of daylight and artifial light in buildings. *Building and Environment*, Volume 40, pp. 51-61.

Grasshopper, 2016. Seattle: Robert McNeel and Associates.

Grasshopper, 2016. *Algorithmic Modelling for Rhino.* Seattle: Robert McNeel and Associates.

Gunnlaug, C., Skanning, J., Anker Hviid, C. & Svendsen, S., 2016. Roadmap for improving roof and facade windows in nearly zero-energy houses in europe. *Energy and Buildings.*

Heschong Mahone Group, Inc., 2003. *Windows and Offices: A Study of Office Worker Performance and the Indoor Environment,* Fair Oaks: California Energy Commission.

Heschong Mahone Group, Inc., 2006. *Sidelighting Photocontrols Field Study,* Fair Oaks: Southern California Edison Co., Pacific Gas and Electric Company and Northwest Energy Efficiency Alliance.

Heuman, A., 2016. *Human.* [Online]
Available at: http://www.food4rhino.com/project/human
[Accessed 6 March 2016].

Hou, D., Liu, G. & Wang, L., 2014. *Evolutionary Algorithm Based Approach of Envelope Optimization for Large-scale Space.* Nogoya, IBPSA.

IESNA, 2000. *The Lighting Handbook: Reference and Application.* 9th ed. s.l.:Illuminating Engineering Society of North America.

IESNA, 2011. *The Lighting Handbook: Reference and Application.* 10th ed. s.l.:Illuminating Engineering Society.

IESNA, 2012. *IES LM-83-12. Approved Method: IES Spatial Daylight Autonomy (sDA) and Annual Sunlight Exposure,* New York (USA): Illuminating Engineering Society of North America.

ISO10077-1, 2006. *Thermal performance of windows, doors and shutters -- Calculation of thermal transmittance -- Part 1: General,* Vernier, Geneva (Switzerland): ISO, International Organization for Standardization.

ISO7730, 2015. *Ergonomics of the thermal environment - Analytical determination and interpretation of thermal comfort using calulation of the PMV and PPD indices and local thermal comfort criteria,* Vernier, Geneva (Switzerland): ISO, International Organization for Standardization.

Iversen, A. et al., 2013. *Daylight calculations in practice - An investigation of the ability of nine daylight simulation programs to calculate the daylight factor in five typical rooms. SBi 2013:26,* s.l.: Danish Building Research Institute, Allborg University (Denmark).

Jarvis, D. & Donn, M., 1997. *Comparison of Computer and Model Simulations of a Daylit Interior with Reality.* Prag (Czech Republic), Proceedings of Fifth International IBPSA Conference / Building Simulation 97.

Jia Hu, S. O., 2013. Simulation-Based Model for Integrated Daylighting System Design. *Journal of Computing in Civil Engineering.*

Konis, K., Gamas, A. & Kensek, K., 2016. Passive performance and building form: An optimization framework for early-stage design support. *Saler Energy*, Volume 125, pp. 161-179.

Kwan, C., 2009. *Towards Climate-based Metrics: A Simulation Study of Annual Daylight levels in 31 Gymnasia,* MDesS thesis. Massachusetts, Boston (USA): Harvard Graduate School of Design.

Larson, G. W. et al., 1998. *Rendering with radiance: The art and science of lighting visualization,* SanFrancisco: Morgan Kaufmann.

Lartigue, B., Lasternas, B. & Loftness, V., 2014. Multi-objective optimization of building envelope for energy consumption and daylight. *Indoor and Built Environment*, Volume 23, pp. 70-80.

Laumanns, M., Zitzler, E. & Thiele, L., 2001. On The Effects of Archiving, Elitism, And Density Based Selection in Evolutionary Multi-Objective Optimization. *Lecture Notes in Computer Science,* Volume 1993, pp. 181-196.

LEED, 2016. *Promoting LEED Certification and Green Building Technologies.* [Online]
Available at: http://www.leed.net/
[Accessed 19 February 2016].

Lund University, 2016. *LUBseach - The Libraries' Shared Search Engine.* [Online]
Available at: http://www.lub.lu.se/en/search-systems-and-tools/lubsearch
[Accessed 12 1 2016].

Mangkuto, R. A., Rohmah, M. & Asri, A. D., 2016. Design optimisation for window size, orientation, and wall reflectance with regard to various daylight metrics and lighting energy demand: A case study of buildings in the tropics. *Applied Energy*, Volume 164, pp. 211-219.

Mans, D., 2014. *Bumblebee: Grasshopper + Excel.* [Online]
Available at: http://www.food4rhino.com/project/bumblebee
[Accessed 28 4 2016].

Manzan, M. & Padovan, R., 2015. Multi-criteria energy and daylighting optimization for an office with fixed and moveable shading devices. *Advances in Building Energy Research*, Volume 9, pp. 238-252.

Mardaljevic, J., 1999. *Daylight Simulation: Validation, Sky Models and Daylight Coefficients,* De Montfort, Leicester (UK): PhD Thesis. De Montfort University, Institute of Energy and Sustainable Development.

Mardaljevic, J., Heschong, L. & Lee, E., 2009. Daylight metrics and energy savings. *Lighting Research & Technology*, Volume 41, pp. 261-283.

Miljöbyggnad, 2016. *Miljöbyggnad.* [Online]
Available at: https://www.sgbc.se/var-verksamhet/miljoebyggnad
[Accessed 15 February 2016].

Nabil, A. & Mardaljevic, J., 2006. Useful daylight illuminances: A replacement for daylight factors. *Energy and Buildings; Special Issue on Daylighting Buildings,* Volume 38, pp. 905-913.

NCC, 2014. *Preliminär bygghandling: Greenhouse, Malmö - Byggnad 1 Energiberäkning,* Malmö (Sweden): NCC Construction.

Ochoa, C. E., Aries, M. B., van Loenen, E. J. & Hensen, J. L., 2012. Considerations on design optimization criteria for windows providing low energy consumption and high visual comfort. *Applied Energy*, Volume 95, pp. 238-245.

Pereira, W., Bögl, A. & Natschläger, T., 2014. *Sensitivity analysios and validation of an EnergyPlus model of a house in Upper Austria,* Cardiff, Wales (UK): Energy Procedia: 6th International Conference on Sustainability in Energy and Buildings, SEB-14.

Perez, R., Seals, R. & Michalsky, J., 1993. An All-Weather Model for Sky Luminance Distribution -- A Preliminary Configuration and Validation. *Solar Energy,* Issue 50, pp. 235-245.

Persson, M.-L., Roos, A. & Wall, M., 2006. Influence of window size on the energy balance of low energy houses. *Energy and Buildings*, Volume 38, pp. 181-188.

Rakha, T. & Nassar, K., 2011. Genetic algorithms for ceiling form optimization in response to daylight levels. *Renewable Energy*, Volume 36, pp. 2348-2356.

Reeves, C. R. & Rowe, J. E., 2003. *Genetic algorithms - Principles nad Perspectives, a Guide to GA Theory.* 1st ed. Dordrecht: Kluwer Academic Publishers.

Reinhart, C., 2004. Lightswitch-2002: a model for manual and automated control of electric lighting and blinds. *Solar Energy,* Volume 77, pp. 15-28.

Reinhart, C. F., 2004. Lightswitch-2002: a model for manual and automated control of electric lighting and blinds. *Solar Energy,* Volume 77, pp. 15-28.

Reinhart, C. F., 2016. *Daysim - Advanced Daylight Simulation Software.* [Online]
Available at: http://daysim.ning.com/
[Accessed 13 March 2016].

Reinhart, C. F., 2016. *DAYSIM header File Deyword: Electric Lighting System.* [Online]
Available at: http://daysim.ning.com/page/header-file-keyword-electric-lighting-system
[Accessed 20 March 2016].

Reinhart, C. F. & Walkenhorst, O., 2001. Validation of dynamic RADIANCE-based daylight simulations for a test office with external blinds. *Energy and Buildings,* Volume 33, pp. 683-697.

Reinhart, C. F. & Weissman, D. A., 2012. The daylit area - Correlating architectural student assessments with current and emerging daylight availability metrics. *Building and Environment,* Volume 50, pp. 155-164.

Reinhart, C. F. & Wienold, J., 2011. The daylighting dashboard - A simulation-based design analysis for daylit spaces. *Building and Environment,* Volume 46, pp. 386-396.

Rhinoceros, 2016. Seattle: Robert McNeel and Associates.

Rogers, Z. & Goldman, D., 2006. *Daylight Metric Development Using Daylight Autonomy Calculations In the Sensor Placement Optimization Tool,* Boulder, Colorado (USA): Architectural Energy Corporation.

Roudsari, M. S., 2015. *Pollination.* [Online]
Available at: http://mostapharoudsari.github.io/Honeybee/Pollination
[Accessed 4 May 2016].

Sadeghipour Roudsari, M. & Pak, M., 2013. *Ladybug: a parametric environmental plugin for grasshopper to help designers create an environmentally-conscious design.* s.l., s.n., pp. 3128-3135.

Sandberg, E., 2011. *Energirelaterade godhetstal för flerbostadshus - Nyproduktion,* Sweden: ATON teknikkonsult AB .

Shan, R., 2013. Optimization for heating, cooling and lighting load in building façade design. *Energy Procedia*, Volume 57, pp. 1716-1725.

Shen, H. & Tzempelikos, A., 2012. Daylighting and energy analysis of private offices with automated interior roller shades. *Solar Energy*, Volume 86, pp. 681-704.

SS 914201, 1987. *Building Design - Daylighting - Simplified method for checking required windows glass area,* s.l.: s.n.

Swedish Energy Agency, 2009. *Measurements of Cold and Hot Water Usage in 44 Single-Family Houses in Sweden,* Stockholm (Sweden): Swedish Energy Agency.

Tabares-Velasco, P. C., Christensen, C., Bianchi, M. & Booten, C., 2012. *Verification and Validation of EnergyPlus Conduction Finite Difference and Phase Change Material Models for Opaque Wall Assemblies,* Colorado (USA): National Renewable Energy Laboratory. U.S. Department of Energy. Prepared under Task No. BE12.0103.

The U.S. Green Building Council, 2002. [Online]
Available at: http://www.usgbc.org/LEED
[Accessed 25 02 2016].

Torres, S. L. & Sakamoto, Y., 2007. *Facade design optimization for daylight with a simple genetic algorithm.* s.l., s.n., pp. 1162-1167.

Tregenza, P. & Wilson, M., 2011. *Daylighting: Architecture and Lighting Design.* 1st ed. New York (USA): Routledge.

Tuhus-Dubrow, D. & Krarti, M., 2010. Genetic-algorithm based approach to optimize building envelope design for residential buildings. *Building and Environment*, Volume 45, p. 1574–1581.

Turing, A. M., 1950. Computing Machinery and Intelligence. *Mind*, pp. 433-460.

U.S. Department of Energy, 2015. *energyplus.net.* [Online]
Available at: https://energyplus.net/sites/default/files/pdfs_v8.3.0/EngineeringReference.pdf
[Accessed 25 02 2016].

U.S. Department of Energy, 2016. *Energyplus.* [Online]
Available at: http://bigladdersoftware.com/epx/docs/8-3/getting-started/idf-editor-brief-introduction.html
[Accessed 16 March 2016].

Ubbelohde, M. S. & Humann, C., 1998. *Comparative Evaluation of Four Daylighting Software Programs.* Ottawa (Canada), Proceedings of the Daylighting '98 Conference: International Conference on Daylighting Technologies and Energy Efficiency in Buildings.

US Department of Energy, 2015. *energyplus.net.* [Online]
Available at: https://energyplus.net/sites/default/files/pdfs_v8.3.0/EngineeringReference.pdf
[Accessed 25 02 2016].

Vierlinger, R., Zimmel, C. & Grohmann, S., 2016. *Octopus Version 0.3.6.* [Online]
Available at: http://www.grasshopper3d.com/group/octopus
[Accessed 17 March 2016].

Wang, W., Zmeureanu, R. & Rivard, H., 2005. Applying multi-objective genetic algorithms in green building design optimization. *Building and Environment*, Volume 40, pp. 1512-1525.

Ward Larson, G., 1996. *Radiance: Reference Manual.*, s.l.: Adeline 2.0 Advanced Daylighting and Electric Lighting Integrated New Environment. International Energy Agency: Solar Heating and Cooling - Task 12: Building Energy Analysis and Design Tools for Solar Applications.

Ward Larson, G. & Shakespeare, R., 1998. *Rendering with Radiance: The Art and Science of Lighting Visualization.* San Francisco, California (USA): Morgan Kaufmann Publ..

Wienold, J. & Christoffersen, J., 2006. Evaluation methods and development of a new glare prediction model for daylight environments with the use of CCD cameras. *Energy and Buildings,* Issue 38, pp. 473-757.

Wikipedia, c., 2016. *Instructions per second.* [Online]
Available at:

https://en.wikipedia.org/w/index.php?title=Instructions_per_second&oldid=714478771
[Accessed 21 January 2016].

Wikipedia, c., 2016. *Non-uniform rational B-spline.* [Online]
Available at: https://en.wikipedia.org/w/index.php?title=Non-uniform_rational_B-spline&oldid=711673028
[Accessed 30 March 2016].

Wright, A. J., Loosemore, H. A. & Farmani, R., 2002. Optimization of building thermal design and control by multi-criterion genetic algorithm. *Energy and Buildings*, Volume 34, p. 959–972.

Wright, J. & Mourshed, M., 2009. *Geometric optimization of fenestration.* Glasgow, IBPSA, pp. 920-927.

Zemella, G., Davide, D. M., Matteo, B. & Irene, P., 2011. Optimised design of energy efficient building fac¸ades via Evolutionary Neural Networks. *Energy and Buildings*, Volume 43, pp. 3297-3302.

Zimmermann, J. P., 2009. *End-use metering campaign in 400 households In Sweden - Assessment of the Potential Electricity Savings,* s.l.: Swedish Enegy Agency.

Zitzler, E., Marco, L. & Lothar, T., 2001. *SPEA2: Improving the Strength Pareto Evolutionary Algorithm,* Zurich: Swiss Federal Institute of Technology.

Zitzler, E., Marco, L. & Lothar, T., 2001. *SPEA2: Improving the Strength Pareto Evolutionary Algorithm. Tecnickal report 108,* s.l.: Computer Engineering and Networks Laboratory, ETH Zurich (Switzerland).

Znouda, E., Ghrab-Morcos, N. & Hadj-Alouane, A., 2007. Optimization of Mediterranean building design using genetic algorithms. *Energy and Buildings*, Volume 39, pp. 148-153.

APPENDIX A
Daylight specific data

A1. Recommended task illuminance levels for residential spaces by IESNA

Ever since the 9th edition of the IESNA Lighting Handbook (IESNA, 2000), the recommended illuminance values are only provided with a reference to a specific application. These applications have been grouped into seven categories and have been organized in three sets of visual tasks, as shown in Table A1.

Table A1: Determination of IESNA Illuminance Categories and sets of visual tasks.

Categories	Determination	Recommended Illuminance	Visual Tasks
A	Public spaces	30 lx	Orientation and simple
B	Simple orientation for short visits	50 lx	
C	Working spaces where simple visual tasks are performed	100 lx	
D	Performance of visual task of high contrast and large size	300 lx	Common
E	Performance of visual tasks of high contrast and small size, or visual tasks of low contrast and large size	500 lx	
F	Performance of visual tasks of low contrast and small size	1000 lx	
G	Performance of visual tasks near threshold	3000 to 10000 lx	Special

For the *orientation and simple visual tasks*, the visual performance is unimportant. They are found in places where visual inspection or reading are only occasionally performed. Visual performance is important for *common visual tasks*. These are found in commercial, industrial and residential spaces. The *special visual tasks* are of critical importance.

Different tasks are performed in different rooms of a residence. IESNA has connected the aforementioned categories with different residential activities, which were assigned by the authors of this thesis to specific rooms of the studied apartments. Table A2 shows the different residential activities and their corresponding recommended illuminance, as per the 10th edition of the IESNA Lighting Handbook (IESNA, 2011).

Table A2: Recommended horizontal and vertical illuminance levels per residential task.

RESIDENTIAL Task	Horizontal Illuminance	Vertical Illuminance
General Lighting	50 lux (B)	
Conversation, relaxation, entertainment	30 lux (A)	
Circulation	30 lux (A)	
Specific Visual task		
Dining	50 lux (B)	
Handcrafts and Hobby		
Crafts	300 lux (D)	50 lux (B)
Sewing	500 lux (E)	100 lux (C)
Work bench	1000 lux (F)	300 lux (D)
Easel hobbies		300 lux (D)
Kitchen range		
Cooking	500 lux (E)	100 lux (C)
Kitchen Sink		
Difficult Seeing	500 lux (E)	100 lux (C)
Cleaning Up	300 lux (D)	50 lux (B)
Kitchen counter		
Cutting	500 lux (E)	100 lux (C)
General	300 lux (D)	50 lux (B)
Laundry	300 lux (D)	30 lux (A)
Music (Piano)	300 lux (D)	50 lux (B)
Reading		
In a chair (casual)	300 lux (D)	50 lux (B)
In a chair (serious)	500 lux (E)	100 lux (C)
In a bed (casual)	300 lux (D)	50 lux (B)
Reading at desk		
Casual	300 lux (D)	30 lux (A)
Serious	500 lux (E)	100 lux (C)
Table games	300 lux (D)	50 lux (B)

For this thesis, the two studied zones were assigned with different illuminance requirements, according to the tasks assumed in each one. The tasks assumed in the Living Room zone were *conversation, relaxation, entertainment, circulation, casual, table games and reading*. An average illuminance requirement of 150 lx was therefore assumed. For the Bedroom zone, it was assumed that only *conversation, entertainment and relaxation* is taking place, leading to an illuminance requirement of 50 lx.

APPENDIX B
Construction specifications

B1. Construction details

Table B1 shows the construction characteristics used for the energy model in EnergyPlus. The data were weighted in order to match the overall U-Values provided by the Jaenecke Arkitekter office.

Table B1: Construction details.

Construction	Material	d / m	λ /(W/m·K)	R / (m^2·K/W)
Exterior Wall	Rso	-	-	0,040
	Fiber cement board	0,025	0,600	0,042
	Wooden battens	0,028	0,130	0,215
	Gypsumboard	0,025	0,250	0,100
	Mineral wool	0,220	0,036	6,111
	Concrete	0,200	1,130	0,177
	Rsi	-	-	0,130
	Total	0,498		6,815
	Overall U-Value / (W/m^2·K)			**0,147**
Interior partitions	Gypsumboard	0,025	0,250	0,100
	Mineral wool	0,045	0,036	1,250
	Gypsumboard	0,025	0,250	0,100
	Total	0,095		1,450
	Overall U-Value / (W/m^2·K)			**0,690**
Ceiling/Floor Slab	Wood boards (oak)	0,015	0,170	0,088
	Rubber underlay	0,015	0,170	0,088
	Concrete	0,200	1,130	0,177
	Sound insulation	0,035	0,060	0,583
	Gypsumboard	0,025	0,250	0,100
	Total	0,290		1,037
	Overall U-Value / (W/m^2·K)			**0,965**
Balcony sills	Fiber cement board	0,025	0,600	0,042
	Total	0,025		0,042
	Overall U-Value / (W/m^2·K)			**24,000**

APPENDIX C
Domestic Hot Water (DHW) calculations

C1. Calculated annual DHW energy use

The specific energy use, stated in FEBY12 (FEBY12, 2012), is set in terms of space heating, DHW and property electricity. Space heating was simulated in EnergyPlus and property electricity was acquired from the preliminary documentation of the studied apartments' energy performance, conducted by NCC (2014). The DHW energy use was calculated using the assumptions shown in Table C1:

Table C1: DHW calculations input data.

Apartment area	68 m^2
Number of occupants	2
Hot water use*	42 liters/(person·day)
Cold tap water temperature	8 °C
Hot water outlet	60 °C
Water specific heat capacity c_p	4,186 KJ/(Kg·K)
Water density ρ_{water}	1000 Kg/m^3

* (Swedish Energy Agency, 2009)

The DHW energy use is calculated according to equation C1:

$$E = \rho_{water} \cdot \dot{V} \cdot c_{p\ water} \cdot \Delta T \cdot t_{hot\ water} \qquad [C1]$$

Where:

E is the annual energy use to heat the required DHW, in kWh/m^2

ρ_{water} is the water density, in Kg/m^3

$\dot{V}$ is the water volume flow rate, in m^3/s

c_p is the water specific heat capacity, in KJ/(Kg·K)

ΔT is the temperature difference between the cold tap water and the heated water, in K

$t_{hot\ water}$ is the annual duration of hot water use, in hours

The annual energy use was calculated according to equation *C1* to 27,26 kWh/m^2 annually. Possibly various water saving systems of these newly built apartments may result in a lower DHW use than the one retrieved here from literature (42 liters/person·day).

APPENDIX D
Energy model validation

D1. Validation input data

Table D1 shows the input data used for each step of the energy model validation.

Table D1: Energy validation input data per step.

STEPS	Input data	
1	**Heating**	
	Setpoint	21 °C
	Setback	19 °C
	Schedule	Always ON
	Cooling	No
	Constructions	
	External wall U-Value	0,15 W/m^2
	Roof U-Value	0,15 W/m^2
	Floor U-Value	0,15 W/m^2
	Electrical lighting	No
2	**Roof U-Value**	0 W/m^2
3	**Infiltration**	0,72 $l/(s \cdot m^2$ floor area)
4	**People**	0,14 $people/m^2$
	Occupancy schedule	*as shown in Table 9 of section 2.5.3*
	Metabolic rate	100 W/person
	Clothing	1 clo
5	**Equipment**	2 W/m^2
	Equipment schedule	*as shown in Table 10 of section 2.5.3*
	Radiant fraction	0,2
6	**Mechanical ventilation**	
	Fresh air per person	No
	Fresh air per m^2	0,7 l/s
	Heat recovery	80r%
	Schedule	Always ON
7 & 9	**Window 1,2**	
	Window pane	Single
	Glass U-value	3,08 W/m^2
	Frame U-Value	1,10 W/m^2
	Glass thermal bridge	1,01 $W/(m \cdot K)$
	Window light transmittance	82r%
	Window g value	74f%

D2. EnergyPlus Input Data Files (IDF)

The two software (Designbuilder and Honeybee) that were used in the validation process can export EnergyPlus *.idf files after each simulation. Using the Energyplus IDF Editor (U.S. Department of Energy, 2016), the user can monitor all model input data in different groups. This is the optimum way to evaluate an energy model, as it lists all input data used by the simulation engine. Figure D2 shows a screenshot of the IDF Editor window.

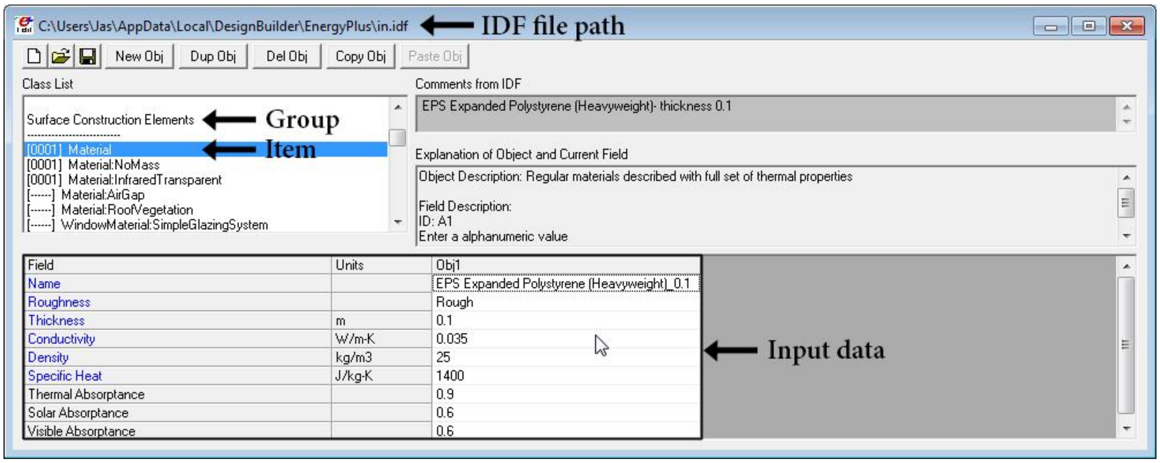

Figure D2: Screenshot of an *idf file opened using the IDF Editor.

APPENDIX E

Measurement grid study - details on computational power

E1. Computer specifications

The specifications of the computer used for the measurement grid study, where the simulation time was recorded, are shown in Table E1. Honeybee allows Radiance to run simultaneously on multiple processors, so three (3) cores were utilized during the study to reduce simulation time.

Table E1: Simulation computer system specifications.

OS Name	Microsoft Windows 7 Ultimate
OS Manufacturer	Microsoft Corporation
System Type	x64 based PC
Processor	Intel® Core™ i5 CPU 750 overclocked @ 3,2GHz, 4 cores
Total physical memory	8 GB
Storage	Samsung SSD 850 EVO 250 GB ATA Device
Display	2 x AMD Radeon HD5670 crossfire connected, 1+1 GB

APPENDIX F
Grasshopper related plugins

F1. Grasshopper plugins used in developing the optimization algorithm

HUMAN

"Extends Grasshopper's ability to create and reference geometry including lights, blocks, and text objects. Also enables access to information about the active Rhino document, pertaining to materials, layers, linetypes, and other settings." (Heuman, 2016). This plugin developed by Andrew Heuman allows grasshopper to assign information to Rhino geometry, in effect turning Rhino into a Building Information Model (BIM) or database of sorts. It was used in this thesis for data management, animations and visualizations.

BUMBLEBEE

Bumblebee is a Grasshopper plugin that provides a low latency link between Grasshopper and Microsoft Excel. It can be used to both write and read data in a variety of ways, and in this thesis it was used as a central part in the database management. It was developed by David Mans (2014).

APPENDIX G

Specific simulation results

G1. Simulation results of the bedroom study.

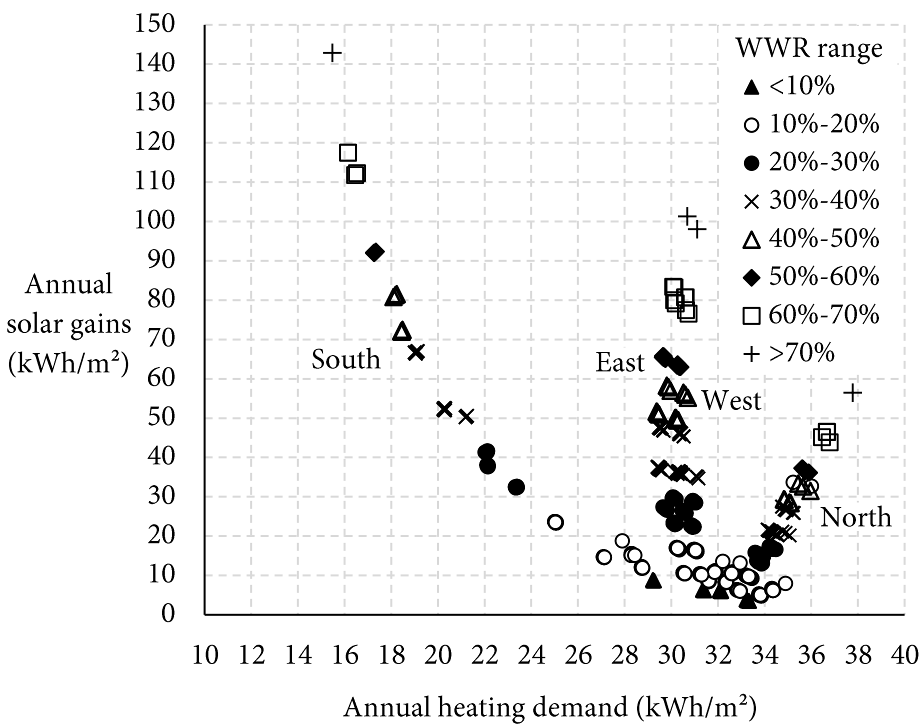

Figure G-1: Annual heating demand as a function of solar gains for all orientations of the bedroom.

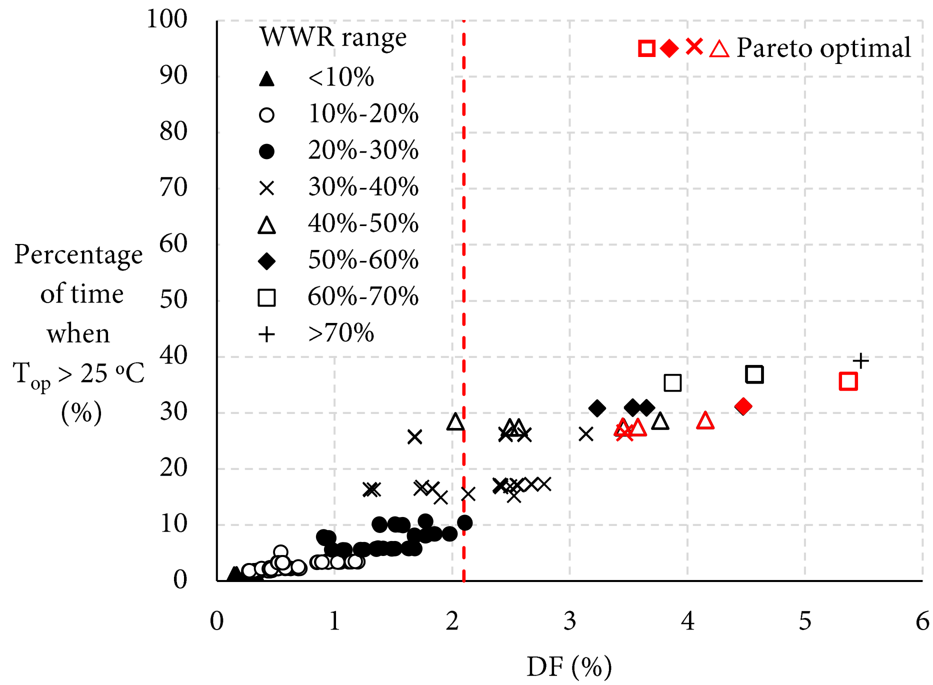

Figure G-2: Overheating time (Top>25 °C) as a function of the achieved DF levels for an east-facing bedroom.

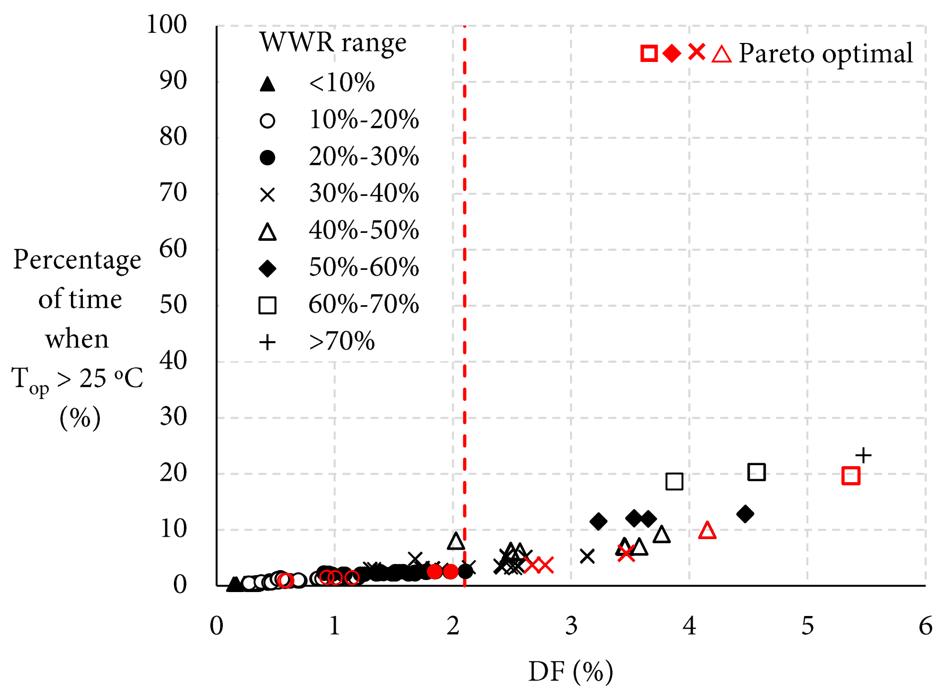

Figure G-3: Overheating time (Top>25 °C) as a function of the achieved DF levels for a north-facing bedroom.

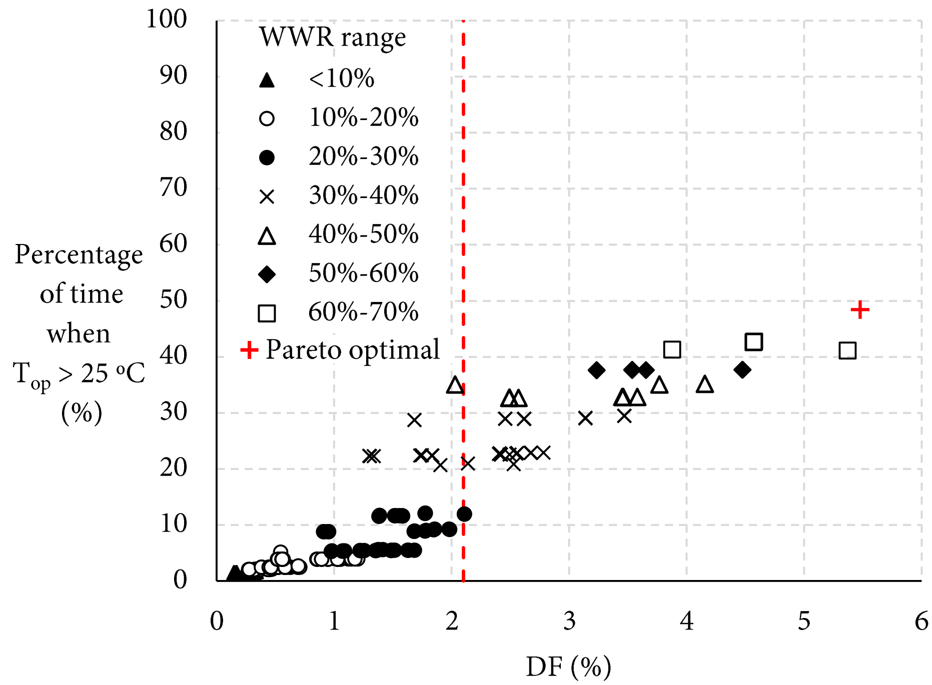

Figure G-4: Overheating time (Top>25 °C) as a function of the achieved DF levels for a south-facing bedroom.

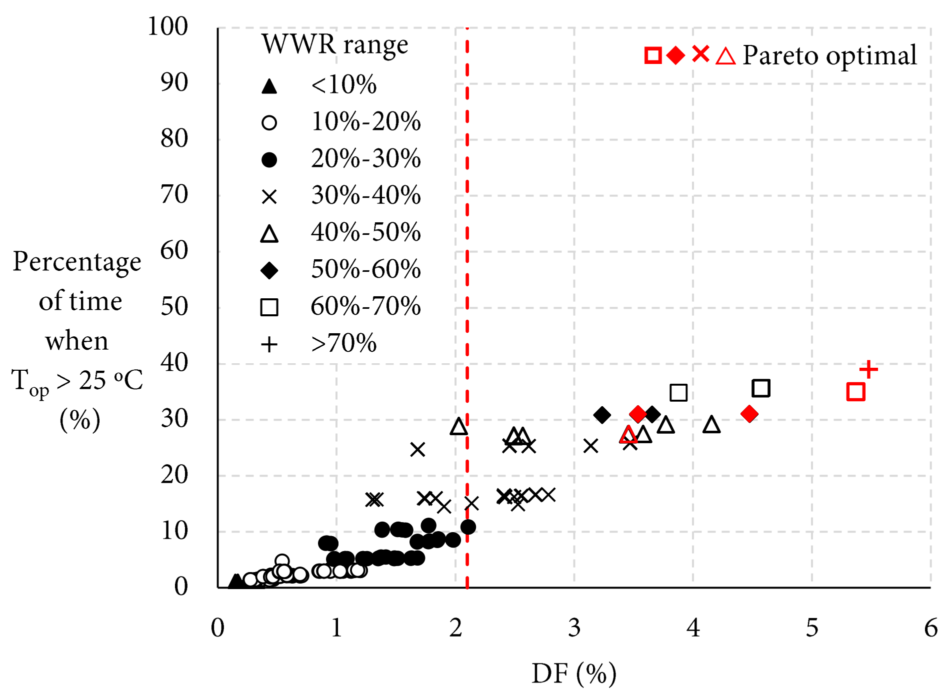

Figure G-5: Overheating time (Top>25 °C) as a function of the achieved DF levels for a west-facing bedroom.

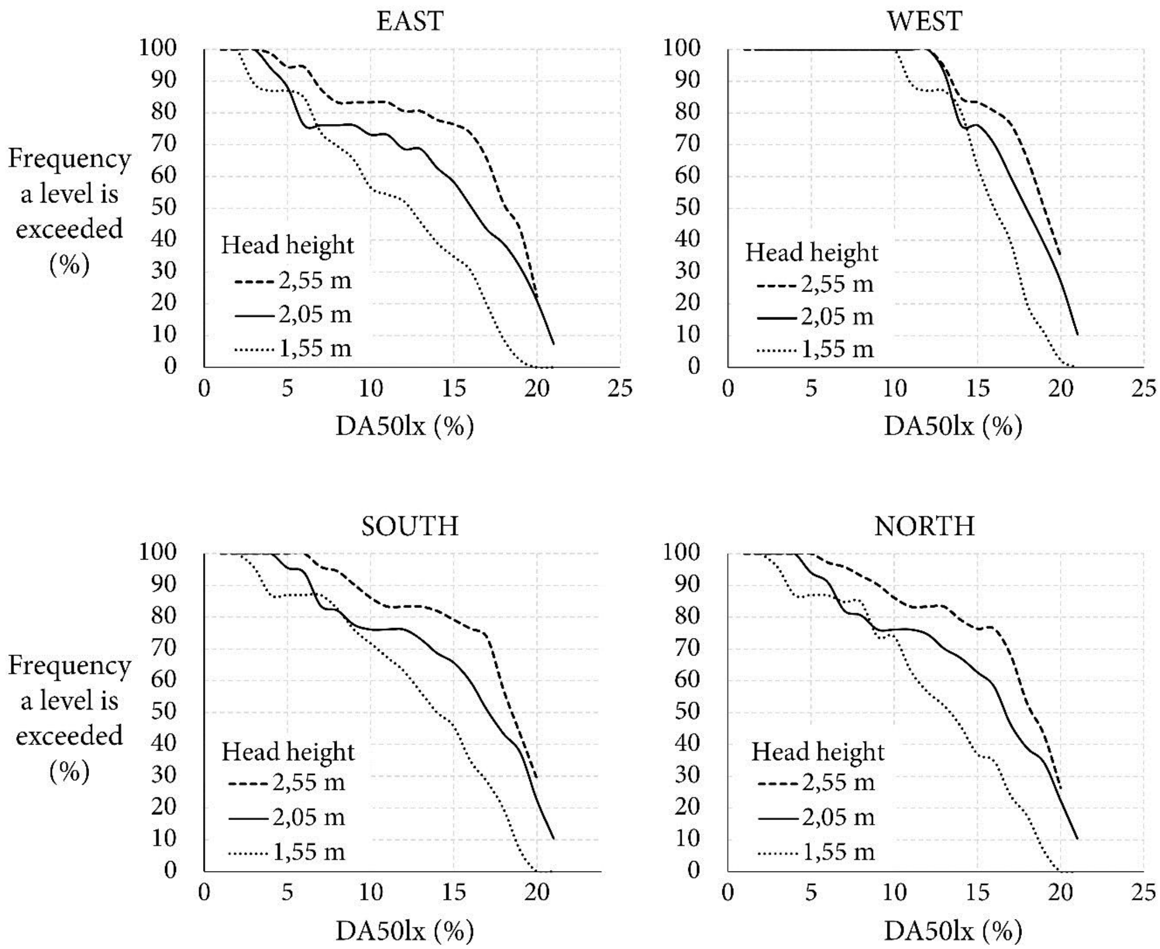

Figure G-6: Percentage of simulated designs for which the DA50lx exceeded a given value, for different window head heights (all orientations included).

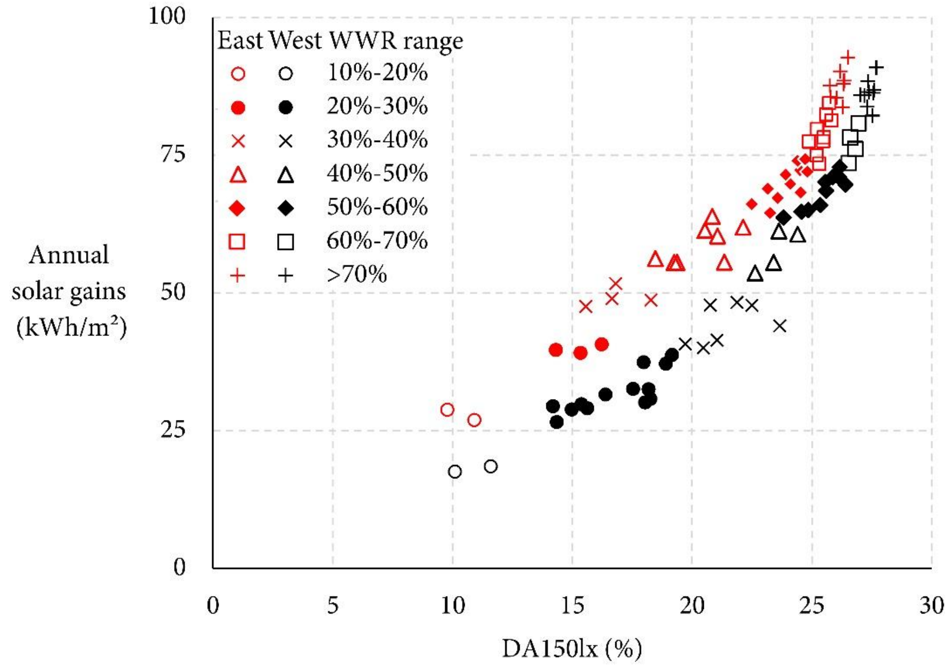

Figure G-7: DA150lx as a function of solar gains for different WWRs on the east and west orientations.

APPENDIX H

The following is the conference paper that was written during this thesis to be presented on the 32th PLEA conference, between the 11th and the 13th of July 2016. It includes the bedroom study, only with a different occupancy schedule.

Bi-objective optimization of fenestration using an evolutionary algorithm approach

Ludvig Haav[1], Iason Bournas[1], Stephanie Jenny Anjeraini[1]

[1]Division of Energy and Building Design, Department of Architecture and the Built Environment, Lund University, Lund, Sweden.

ABSTRACT: This study assesses the trade-offs between the conflicting objectives of reducing heating intensity and increasing daylight utilization in the context of Swedish residential spaces, specifically for a north oriented bedroom. The optimization process is conducted within the visual programming environment of Grasshopper, where the simulation engines of Energyplus, Radiance and Daysim are interconnected and combined with the Strength Pareto Evolutionary Algorithm 2 (SPEA2). A fenestration algorithm is proposed that generates conventional window geometries in differing size and placement while considering the view towards the exterior environment. Iterations are assessed for their influence on annual measures of heating energy intensity, daylight illuminance deficit (ADID), electrical lighting use. Results indicated that diverse and efficient solutions can be generated by this method, allowing the design team to select among them based on higher-level / unquantifiable information. It was proven that the commonly used WWR parameter is not sufficient to assess the thermal and luminous needs of space. Different window configurations can yield different results depending on the actual position of the opening.
Keywords: bi-objective optimization, heating energy, daylight autonomy

INTRODUCTION

This paper assesses the trade-offs between heating and daylighting when considering fenestration solutions for residential spaces. To facilitate this goal, a case study was chosen: the MKB Green House project in Augustenborg, Malmö (Fig. 1). In northern countries such as Sweden, with large seasonal variations in natural lighting, the ambient air temperature remains beneath the comfort zone for most of the year. It is therefore important to design fenestration with respect to both the daylight and heating needs of the occupants.

Researchers in the context of energy codes and certification system requirements have mentioned this conflict between the heating and daylight objectives. Mardaljevic et al. (2009) argued in a seminal paper that practitioners encounter recommendations for target daylight factor (DF) values that result in over-glazed buildings with excessive solar gain and/or heat loss. The Heschong Mahone Group (2006) monitored six building spaces that did not achieve the LEED criteria of an average daylight factor of 2 % (The U.S. Green Building Council, 2002). They found that even with high transmission glass, the window area would need to have been increased to such an extent that the spaces would not pass the energy code requirements.

Figure 1: MKB Greenhouse residential building in Malmö, Sweden (Image: Jaenecke Arkitekter AB)

Due to the geometrical complexity of the parameters involved in fenestration studies, some researchers have utilized evolutionary-based optimization algorithms to find a range of façade solutions that satisfy both energy and daylighting goals. The goal of this study is to simulate the effects of different fenestration alternatives on a single bedroom by means of generative design. The aim is not a single optimum window configuration for heating and daylight, but rather a diverse set of solutions.

METHODOLOGY

The MKB Greenhouse project includes three different apartment layouts of different orientations. For this paper, a north-facing bedroom of a mid-rise apartment was selected as the study object (Fig. 2). The north orientation was selected due to its lack of direct radiation, an attribute that highlights the conflict between the objectives of daylight and heating. The bedroom has an area of 14 m² and a volume of 36.56 m³. It is exposed on the north façade, and on part of the east façade as shown in Fig. 2. The area defined by the points ABCD represents the available surface for the allocation of one window opening. The exposed walls are shaded in grey in Fig. 2, other surfaces are considered adiabatic. The definition of the script that generates different window designs is explained under the "Fenestration Definition" section further below.

The simulation model was created in the Grasshopper environment, which is a visual programming language that is integrated in the Rhino3D modeller (Grasshopper, 2016; Rhinoceros, 2016)). The workflow included designing the geometry within Rhino 3D, importing it in Grasshopper and from there using Honeybee components to set the energy model, the daylight model and the electrical lighting model. Honeybee connects the visual programming environment of Grasshopper to the validated simulation engines - specifically, EnergyPlus, Radiance, Daysim and OpenStudio - which evaluate building energy consumption, comfort, and daylighting (Sadeghipour Roudsari M., Pak M., 2013). For every window alternative, Radiance calculates the average daylight autonomy with a benchmark of 150lx (DA150lx) for a nine-point grid, illustrated in Fig. 2. A Daysim simulation sums the hourly lighting energy use (kWh/m² annually) and finally Energyplus calculates the heating energy intensity of the bedroom (kWh/m² annually).

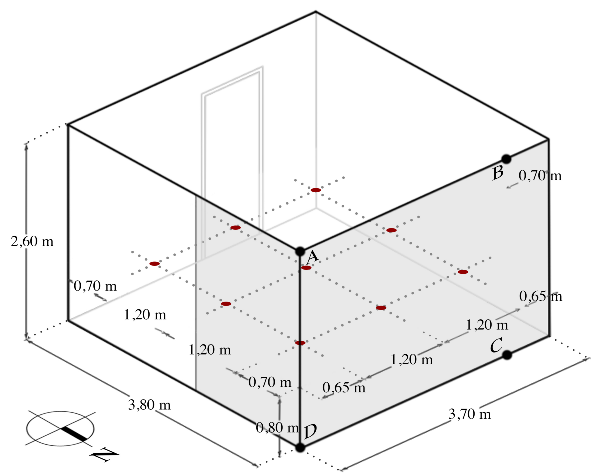

Figure 2: Overall bedroom dimensions, the daylight analysis grid and the fenestration definition area ABCD.

DAYLIGHT MODEL

The overall Radiance settings for the daylight simulation are shown in Table 1. The DA150lx was calculated for an occupancy schedule of 00:00 – 07:00 and 22:00 – 00:00 hours during weekdays and for 00:00 – 09:00 and 23:00 – 00:00 hours during weekends, throughout the year.

Table 1: Daylight model input data.

Radiance overall settings			
Ambient bounces	Ambient division	Ambient sampling	Ambient resolution
4	512	128	128

Radiance material properties			
	Material	Reflectance	Transmissivity
Walls	Plastic	0,80	-
Glass	Glass	0,14	0,86
Frame	Plastic	0,80	-
Floor	Plastic	0,40	-
Ceiling	Plastic	0,90	-

Relevant research has shown how time-intensive Radiance simulations are (Larson, et al., 1998). As the window iterations for this paper reached a number of 864, the Radiance overall settings were selected in order to provide a medium level of accuracy (Dubois, 2001). In addition, a transmissivity value of 0,86 was calculated for a triple glazed unit that is represented in the model by a single glass surface. The daylight result was fed in the optimization algorithm component in values of $f(d)_t = 100 - f(DA150lx)_t$, where $f(d)_t$ is the hourly daylight illuminance deficit. It is the percentage of time when the daylight illuminance is lower than 150 lx, which is the inverse of the daylight autonomy DA150lx. It was set this way because the evolutionary algorithm is optimizing by minimizing both objectives. This is due to the SPEA2 fitness assignment definition. The sum of all hourly deficits is the annual daylight illuminance deficit (ADID). The daylight simulation was connected to Daysim in order to generate the corresponding annual lighting energy intensity (kWh/m²) for every window alternative. The probability of the occupant to turn on or off the lighting was set according to the statistical analysis of the *Lightswitch* study (Reinhart, 2004).

ENERGY MODEL

After the electrical lighting calculation, the energy simulation is conducted automatically using the Energyplus simulation engine. Lighting is calculated upsteam in the algorithm because it must be used as an input in the energy simulation for the sensible heat gains of the lamps. Table 2 shows the energy model input data. Heating is provided by the *Ideal Air Loads System* of Energyplus (US Department of Energy, 2015). In brief, the system is a demand controlled all-air system, where space heating is provided by air supplied in the zone to meet set ventilation requirements by the user. The algorithm was instructed to monitor the heating energy alone and couple it to the daylight illuminance deficit.

Table 2: Energy model input data.

Heating	
Setpoint	21 °C
Setback	19 °C
Schedule	Always ON
Cooling	No
Mechanical ventilation	
Fresh air per person	7 l/s
Fresh air per m²	0,35 l/s
Heat recovery	80 %
Schedule	Always ON
Internal loads	
Schedule	Operational time
People	0,14 people/m²
Infiltration	3 l/(s·m²)
Equipment	0,65 W/m²
Lighting	4 W/m²
Target illuminance	150 lx
Lighting control	Manual
Constructions	
External wall U-Value	0,15 W/m²
Window pane	Triple
Glass U-value	0,60 W/m²
Frame U-Value	1,10 W/m²
Glass thermal bridge	1,01 W/(m·K)
Window light transmittance	74 %
Window g value	53 %

FENESTRATION DEFINITION

The geometry assigned to the aforementioned daylight and energy models consists of two parts: 1) a constant geometry that includes the floor, ceiling, door and all walls excluding the north-facing one and 2) the area of the north-facing wall within the boundary of ABCD of Fig. 2. The geometry of this wall alters, according to the window size and position that is generated by the algorithm. There are specific geometric constraints that define the window generation, as shown in Fig. 3.The area is subdivided in a 0,5 x 0,5 m² grid, which defines squares that a window area can populate. The window width, height and sill height have therefore dimensions in integers of 0,5 m. To reduce simulation time and to comply with realistic terms, the algorithm is ordered to bypass the cases where the window:

1. Has an area of 0,5 x 0,5 m² or 0,5 x 1,0 m²
2. Is a concave polygon

To account for the occupant view towards the exterior environment, a view-zone was set as shown in dashed lines in Fig. 3. Any generated window that does not intersect with this zone and lies altogether below or above is bypassed by the algorithm. In case a window design is a duplicate (one that was calculated in the past), the algorithm is instantly using the previous result.

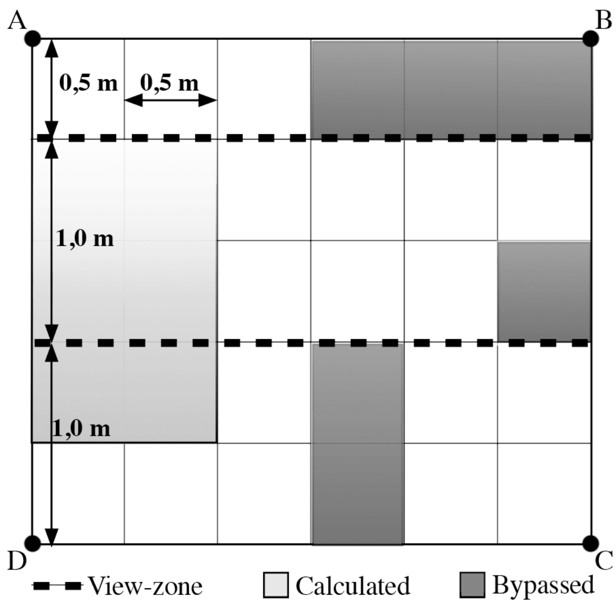

Figure 3: The window generation scheme in Area ABCD.

According to Equation 1 the window *U*-value, U_{win}, is dependent on the total window area A_1, areas of glazing A_g, and frame A_f. Other factors include U-value for frame U_f and glazing U_g, as well as the length L_g of the linear thermal bridge Ψ of the glazing perimeter. A constant frame width of 113 mm is adjusted parametrically for all window sizes. Calculating the *U*-value of the window according to this equation ensures that rectangular window geometries are given a lower *U*-value than square shaped windows.

$$U_{win} = A_1 \cdot \left(\frac{A_g \cdot U_g + A_f \cdot U_f + L_g \cdot \Psi}{A_g + A_f} \right) \quad [1]$$

To assess the trade-offs between the objectives of daylight and heating, results of DA150lx and heating energy intensity (kWh/m² annually) are supplied to the genetic algorithm for each valid window design. The genetic algorithm used is the Strength Pareto Evolutionary Algorithm, SPEA2 (Zitzler, et al., 2001) through the Octopus component in Grasshopper. Fig. 4 shows the overall scheme of the developed algorithm.

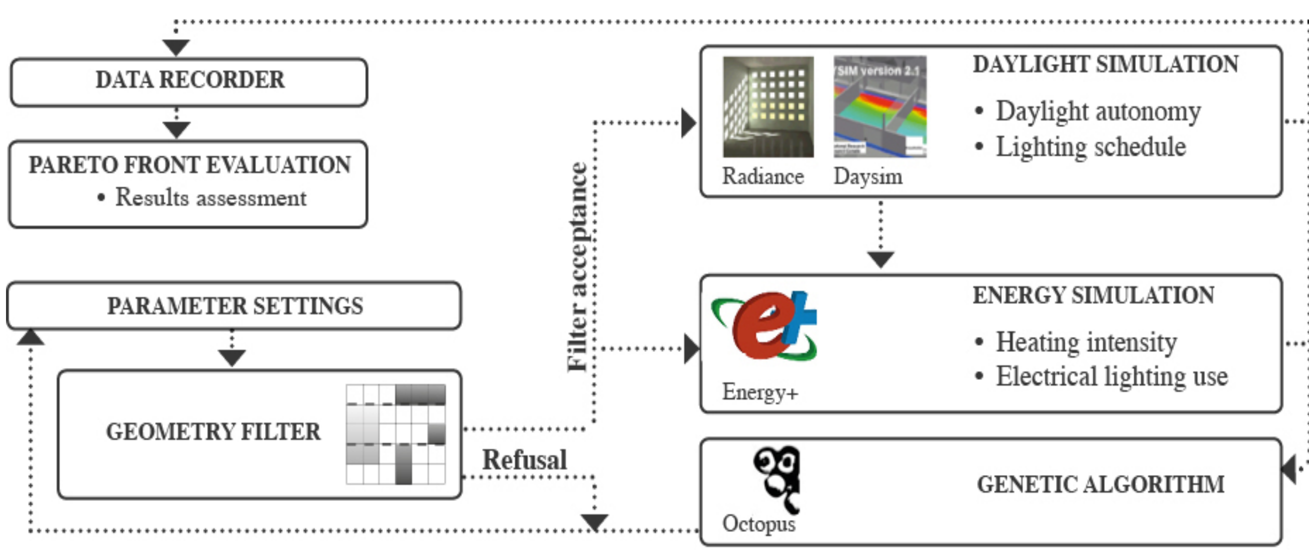

Figure 4: The scheme of the algorithm inside the visual programming environment of Grasshopper.

Table 3 shows the input data used for the optimization process. Mutation governs the search of the solution space as much as possible, whereas crossover controls the convergence of the objectives on the better solution. With a low mutation rate, different window iterations will not be generated to a full extent, posing a risk for the algorithm to converge to a local optimum solution. If the crossover rate is low, then designs will be generated but convergence towards optimum solutions will fail. The window design variables, that constitute the *genes* for the algorithm, were a) the sill height, b) the head height, c) the window width and d) the distance from the axis defined by points A, D in Fig. 3. Discrete values were used for all four genes, as shown in Table 4.

Table 3: Octopus settings for genetic algorithm.

Octopus overall settings				
Elitism	Mutation rate	Crossover rate	Population size	Mutation probability
0,70	0,60	0,70	462,00	0,01

Table 4: Octopus gene input variables.

Design variables			
Gene	Unit	Step	Range
Sill height	m	0,5	[0 - 1,5]
Window height	m	0,5	[0,5 - 2,5]
Window width	m	0,5	[0,5 - 2,5]
Distance from wall	m	0,5	[0 - 2]

RESULTS AND DISCUSSIONS

The Pareto front shown in black dots in Fig. 5 indicates that there is no single optimum solution for the efficient trade-off between daylight and heating. Different configurations can be used, according to the choice of the design team. The advantage is that a decision can be made between only 17 out of 864 solutions. The algorithm did not iterate between all these solutions, as the selection based on elitism decreased the necessary calculations. Fig. 5 shows that for smaller WWRs, the Pareto optimal solutions converge towards higher positions of the window. The window is placed more centrally to decrease ADID. It is also increased in size, always placed 1 m high above floor level, unless the WWR requires a lower sill height.

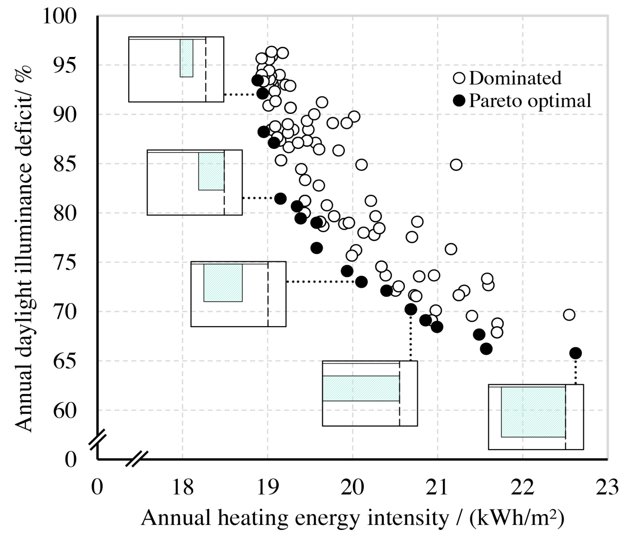

Figure 5: The Pareto front and dominated solutions.

Fig. 6 shows the electrical lighting use and the heating energy intensity for different ranges of WWRs. For WWRs between 10% - 40%, the electricity for lighting varies a lot, depending on the exact window position. The difference in the annual use for a WWR of 20-30% can reach 5 kWh/m², which is nearly 30% of the total use of the worst-case solution. It is also evident that a WWR of 10 – 20% can admit more daylight than a WWR of 30 – 40%.

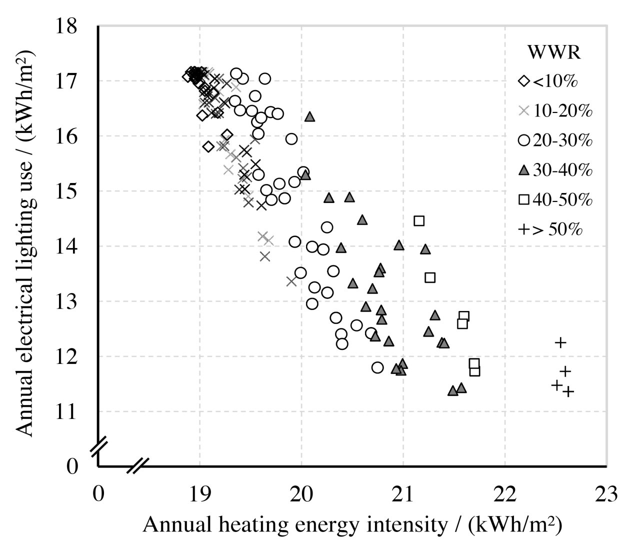

Figure 6: The electrical lighting use and heating energy intensity for different ranges of WWR.

The heating intensity on the other hand presents a more straightforward trend. There is a clear correlation between the amount of glazing and the heating energy use, due to the significantly lower U-Value of the window. Furthermore, the room is oriented towards north, and increasing the window area does not provide enough solar gains to compensate for the low U-Value. For a balanced trade-off between heating and daylight, a WWR of 10 – 30% is the optimum choice.

CONCLUSION

The optimization method presented in this paper generated a sufficient but at the same time limited amount of Pareto optimal solutions. All solutions complied to user defined requirements of view and window geometries. Simulation data from both Pareto optimal and non Pareto optimal window geometries was analysed and showed that WWR is an insufficient prediction of daylight utilization. Centrally and highly placed windows performed better in terms of the optimization objectives.

In order for this fenestration technique to be more useful for practitioners in the design field, a simultaneous optimization of multiple windows and extended capabilities of the geometric filter could be implemented. Such a filter could facilitate interactive reprogramming by the user to comply with new ideas and design requirements of the design team. The computational burden of a reliable Pareto front population is bound to increase exponentially as more parameters are included. Further studies could look into ways of decreasing computational cost in multi window configurations without adversely affecting the solution space. Possible ways would be to reduce gene range, and to limit the impact of solution duplication by use of a simulation results database.

REFERENCES

Dubois, M.-C., 2001. *Impact of Shading Devices on Daylight Quality in Offices Simulations with Radiance,* Lund: Lund University.

Grasshopper, 2016. Seattle: Robert McNeel and Associates.

Heschong Mahone Group, Inc., 2006. *Sidelighting Photocontrols Field Study,* Fair Oaks: Southern California Edison Co., Pacific Gas and Electric Company and Northwest Energy Efficiency Alliance.

Larson, G. W. et al., 1998. *Rendering with radiance: The art and science of lighting visualization,* SanFrancisco: Morgan Kaufmann.

Mardaljevic, J., Heschong, L. & Lee, E., 2009. Daylight metrics and energy savings. *Lighting Research & Technology*, Volume 41, pp. 261-283.

Reinhart, C., 2004. Lightswitch-2002: a model for manual and automated control of electric lighting and blinds. *Solar Energy,* Volume 77, pp. 15-28.

Rhinoceros, 2016. Seattle: Robert McNeel and Associates.

Sadeghipour Roudsari, M. & Pak, M., 2013. *Ladybug: a parametric environmental plugin for grasshopper to help designers create an environmentally-conscious design*. s.l., s.n., pp. 3128-3135.

The U.S. Green Building Council, 2002. [Online] Available at: http://www.usgbc.org/LEED [Accessed 25 02 2016].

US Department of Energy, 2015. *energyplus.net*. [Online] Available at: https://energyplus.net/sites/default/files/pdfs_v8.3.0/EngineeringReference.pdf [Accessed 25 02 2016].

Zitzler, E., Marco, L. & Lothar, T., 2001. *SPEA2: Improving the Strength Pareto Evolutionary Algorithm,* Zurich: Swiss Federal Institute of Technology.